Urban heat Island mitigation strategies in an arid climate. In outdoor thermal comfort reacheable

Suaad Ridha

Université Fédérale

Toulouse Midi-Pyrénées

THÈSE

En vue de l'obtention du

DOCTORAT DE L'UNIVERSITÉ DE TOULOUSE

Délivré par *INSA de Toulouse*
Discipline ou spécialité : *Génie Civil*

Présentée et soutenue par
Suaad RIDHA

Le *28 avril 2017*

Titre : *Urban Heat Island mitigation strategies in an arid climate. Is outdoor thermal comfort reacheable ?*

JURY

Mme Sylvie LORENTE, INSA Toulouse (Examinateur)
M. Walter BOSSCHAERTS, Ecole Royale Militaire de Bruxelles (Examinateur)
M. Stéphane GINESTET, INSA Toulouse (Examinateur)
M. Frédéric KUZNIK, INSA Lyon (Rapporteur)
M. Matthieu LABAT, INSA Toulouse (Examinateur)
M. Karim LIMAM, Université La Rochelle (Rapporteur)

Ecole doctorale : *Mécanique, Energétique, Génie Civil et Procédés (MEGeP)*
Unité de recherche : *Laboratoire Matériaux et Durabilité des Constructions (LMDC)*
Directeur(s) de Thèse : *Sylvie LORENTE et Stéphane GINESTET*

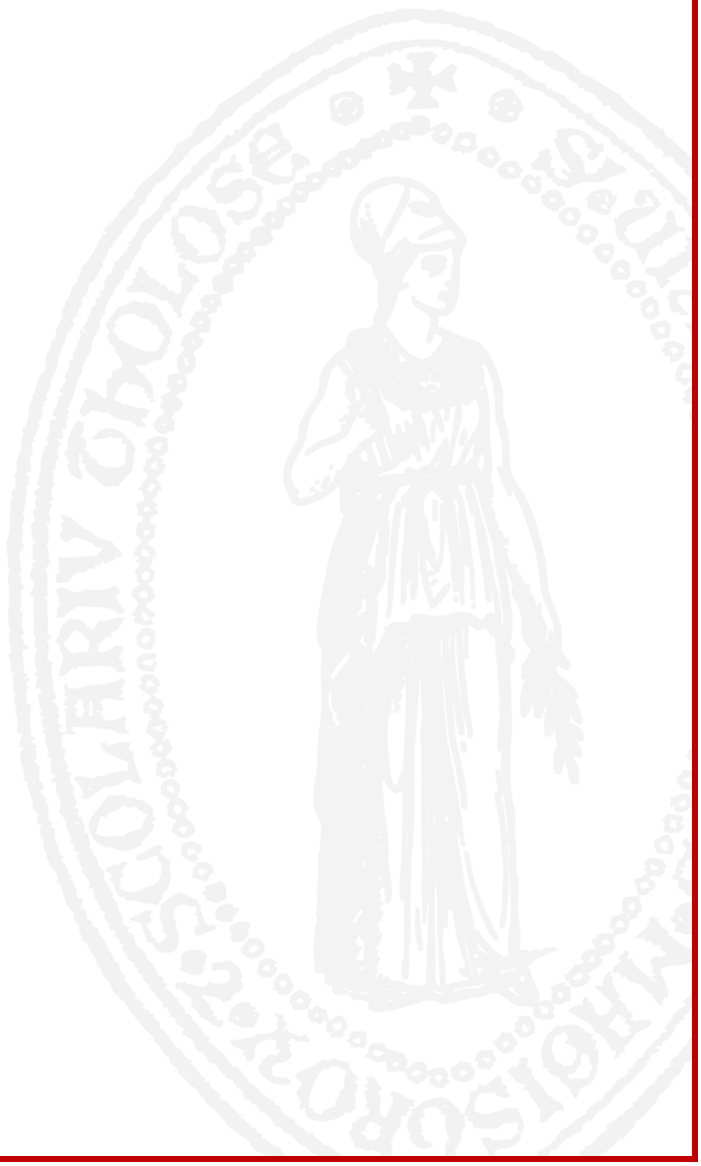

ACKNOWLEDGEMENTS

First and foremost I would like to express my gratitude and appreciation to my supervisor Professors Sylvie LORENTE and Stéphane GINESTET for their enthusiasm, encouragement, guidance and advice over the past four years.

This PhD. thesis was sponsored by the Ministry of Higher Education of Iraq and CAMPUS FRANCE. I am grateful so much for them help and support.

Sincere thanks are also due to the members of the committee for accepting to discuss my thesis: Professor Walter BOSSCHAERTS (Royal Military School of Brussels), Professor Matthieu LABAT (INSA Toulouse), Professor Frédéric KUZNIK (INSA Lyon), and Professor Karim LIMAM (University of La Rochelle).

I would also like to thank the laboratory LMDC where I spent four years. I could feel the spirit of cooperation and friendship within this laboratory with all the teams. Thanks also to all my colleagues in the ECC group (Energy Comfort Construction).

I want, particularly, to acknowledge Ayad May Asad engineer in Mayoralty of Baghdad, for providing the information for Baghdad city. Also, thanks to, Professor Ausama Tariq from Al-Mustansiriya University, Department of Geography /Astronomy.

I am immensely grateful to my family members for their continued love and encouragement throughout my life.

ABSTRACT

Numerous studies over the past several decades focused on the Urban Heat Island. Initial efforts on understanding the factors affecting UHI contributed to propose solutions and mitigation strategies. Mitigation strategies comprise to increase both the urban albedo (reflectivity to solar radiation), and evapotranspiration. Albedo increases are obtained through high albedo roofing and paving technologies. An increase in evapotranspiration is achieved through a combination of decreasing the fraction of impervious surfaces and planting vegetation in urban areas. The notion of outdoor thermal comfort depends on the perception and satisfaction of the pedestrians, especially in hot and arid climates. Consequently, this work focuses on the appropriate methods for reducing the Urban Heat Island and to enhance the pedestrian outdoor thermal comfort. There is limited research conducted on the outdoor thermal comfort in hot and arid climate. The studies on the mitigation the Urban Heat Island and the outdoor thermal comfort are almost non-existent for places like Baghdad city. Baghdad has a complex urban fabric with modern design buildings, traditional and heritage houses. The climate in summer is hot, and summer months are considered the longest season with nearly 7 months of the year. This study focuses on investigating possible mitigation strategies to determine how pedestrian comfort is affected by the constructions design choices, comparing a traditional district to a modern one. We are also interested on how vegetation and shading patterns contribute to reducing the effect of UHI and improving the outdoor thermal comfort. Four different scenarios are designed to assess the role of vegetation elements such as trees, grass, and different shading patterns. The evaluation was performed on the hottest day in summer. The mean radiant temperature, specific humidity, air temperature, and wind speed distributions have been analyzed using the software ENVI-met. A design is proposed to increase the thermal comfort on the hottest day and a typical day in summer. The study shows how the urban factors such as the aspect ratio, vegetation cover, shadings, and geometry of the canyon are crucial elements that urban planners and municipalities may take into account, especially for new urban developments in a hot, arid climate.

RÉSUMÉ

De nombreuses études au cours des dernières décennies ont porté sur l'effet l'îlot de chaleur urbain (ICU). Les efforts initiaux visant à comprendre les facteurs qui influent sur l'ICU ont contribué à la mise en place de solutions et de stratégies d'atténuation adaptées. Les stratégies d'atténuation comprennent généralement l'augmentation de l'albédo urbain (réflectivité au rayonnement solaire) et l'évapotranspiration. Les augmentations d'albedo sont obtenues grâce à des technologies de toiture et de pavage ayant un albédo élevé. Une augmentation de l'évapotranspiration est obtenue par une combinaison de la diminution de la fraction de surfaces imperméables et la plantation de végétation dans les zones urbaines. Le confort thermique extérieur est défini à partir d'indices prenant en compte différents paramètres physiques et traduit la perception et la satisfaction des piétons. Ce confort est très difficile à obtenir en climat chaud et aride. Par conséquent, le travail présenté dans ce document met l'accent sur les méthodes appropriées pour réduire l'ICU et ainsi améliorer le confort thermique en plein air des piétons. Jusqu'à présent, peu de recherches ont été menées sur le confort thermique extérieur dans un climat chaud et aride. Les études sur l'atténuation de l'ICU et le confort thermique extérieur sont pratiquement inexistantes pour la ville de Bagdad. Bagdad a un tissu urbain complexe avec des constructions modernes, des maisons traditionnelles et des éléments caractéristiques du patrimoine local. Le climat en été est chaud, et les mois d'été sont considérés comme la plus longue saison avec près de 7 mois de l'année. Dans un premier temps, cette étude se concentre sur l'étude des stratégies d'atténuation à envisager afin d'évaluer comment le confort des piétons est affecté par les choix de conception des constructions, en comparant un quartier traditionnel à un quartier moderne. L'étude envisage ensuite la façon dont la végétation et les ombrages contribuent à réduire l'effet de l'ICU et à améliorer le confort thermique extérieur. Quatre scénarios différents sont élaborés pour évaluer le rôle d'éléments végétaux tels que les arbres, l'herbe et les différents modèles d'ombrage. L'évaluation a été effectuée le jour le plus chaud de l'été, la température radiante moyenne, l'humidité spécifique, la température de l'air et les distributions de la vitesse du vent ont été analysées à l'aide du logiciel ENVI-met. Le confort thermique est ensuite évalué à l'aide des indices thermiques de la température équivalente physiologique PET et du PMV étendu aux ambiances extérieures. En outre,

une proposition de solution est abordée afin d'étudier son impact sur le confort thermique pour la journée la plus chaude (situation extrême) et une journée typique d'été. Les résultats ont révélé une amélioration du confort thermique dans la journée typique d'été. L'étude montre comment les facteurs urbains tels que le rapport d'aspect, la couverture végétale, les ombres et la géométrie du quartier sont des éléments cruciaux que les urbanistes et les municipalités doivent prendre en compte, en particulier pour les nouveaux aménagements urbains dans un climat chaud et aride. Une proposition d'aménagement global pour atténuer les ICU dans le cas d'un nouveau quartier sous climat aride, est détaillée en fin de mémoire.

Contents

List of Figures

List of Tables

Nomenclature

Symbol	Description	Unit
k_s	thermal diffusivity	m^2/sec
K	turbulent kinetic energy	$m^2 s^{-2}$
fvf	facade view factor	-
$J_{f,evap}$	evaporation flux at surface of foliage	ms^{-1}
$J_{f,trans}$	transpiration flux at surface of foliage	ms^{-1}
$J_{f,h}$	direct heat flux at surface of foliage	Kms^{-1}
K_Φ	turbulent exchange coefficient of Φ	$m^2 s^{-1}$
K_h^w	heat exchange coefficient at facade surface	$m^2 s^{-1}$
LAD	leaf area density	$m^2 m^{-3}$
x, y, z	cartesic coordinates	m
p	air pressure	P_a
p'	local pressure perturbation	P_a
q	specific air humidity	$kgkg^{-1}$
Q_{lw}	long wave radiation	Wm^{-2}
Q_{sw}	short wave radiation	Wm^{-2}
Q_Φ	local source of Φ	$\|\Phi\|s^{-1}$
S_u, S_v and S_w	local source or sink terms for impulse	ms^{-2}
t	time	s
T_a	air temperature	K
T_f	surface temperature of foliage	K
T_a	soil temperature	K

T_w	temperature of facade	K
u	three dimensional wind vector	ms^{-1}
u, v, w	wind speed in x, y and z direction	ms^{-1}
u_g, v_g	geostrophic wind speed in x and y direction	ms^{-1}
V	air volume	m^3
v_f	view factor	-
Greek letters		
Δx, Δy, Δz	dimension of the grid cells	m
ϵ	dissipation of kinetic energy	$m^2 s^{-3}$
ε_f	emissivity	-
η	volumetric water content of the soil	$m^3 m^{-3}$
λ_w	heat transfer coefficient of facade	$W(m^2 K)^{-1}$
ρ	air density	kgm^{-3}
σ_{svf}	sky view factor	-
θ	potential temperature	K

CHAPTER ONE

INTRODUCTION

1.1 General background

The Urban Heat Island (UHI) is a broadly investigated phenomenon in urban climate research, which characterizes the warming of cities comparing to their surrounding neighborhoods. Strategies to mitigate the Urban Heat Island represent an important objective in design and urban planning, especially in cities in hot climates. Lack of UHI studies, especially long-term in developing countries makes it difficult to hypothesize the mechanisms of UHI. Consequently, there is a growing interest in studies focusing the simultaneous analyses of UHI and trends throughout the world (Varquez, 2017). A significant increase in ambient temperatures is being found in urban and suburban places after the sun sets down, due to the heat release from buildings, streets, and other constructions, which was absorbed during daytime. UHI is indirectly connected to climate change due to its contribution to the greenhouse impact, and consequently, to global warming (Mobaraki, 2012). Many countries and regions have performed mandatory adaptation strategies reduce the effects of the Urban Heat Island and the change in urban climate. Change in urban climate depends on the interactions between the urban structure (dimensions of buildings, aspect ratio), ground cover (built-up, pavement, vegetation, soil, water), urban fabric (construction and natural materials) and the urban metabolism (heat, water, and pollutants due to human activity) (Simon, 2016). Consequently, the effects of mitigation measures cannot be easily assessed (Oke, 2006).

Climate change in the Arab regions creates severe impacts on natural and human systems; these regions are characterized by hot and an arid climate (desert climate). Only modest efforts were adopted in scientific research to propose mitigation strategies of Urban Heat Island effects and improve the outdoor thermal comfort of pedestrians (Medany, 2008). Arab world countries have endeavored to mitigate the effects of climate change, but there are numerous of challenges that they must overcome to keep up (Al-Mebayedh, 2013). This work tries to find keys on how to improve pedestrian comfort while reducing the UHI in the context of the city of Baghdad (Iraq).

1.2 Significance of the Study

Firstly, Iraq faces a unique set of environmental challenges as one of the most arid zone vulnerable to climate change. In recent years the change in climate patterns induced higher frequency and intensity of extreme weather events, rising environmental degradation throughout the country, more frequent and severe dust storms, droughts, and extremely high temperatures. Secondly, the diversity of the urban fabric in Baghdad and the different styles of construction where high-rise buildings are located in the vicinity of the old traditional constructions and urgent need to confront climate fluctuations over time. Up to the mid-1950 the urban housing stock in Baghdad consisted mainly of traditional courtyard houses. Since then the trend began to change and now modern buildings built on the outskirts of the city, form the majority. The term 'traditional' and 'modern' do not refer merely to the age of the building fabric, but denote buildings of fundamentally different design concept and characteristics (Al-Azzawi, 1984). The traditional courtyard house is characterized by its internal courtyard around which all rooms and spaces are grouped and look inwards for their daylight and natural ventilation. Such houses seem to have fulfilled the needs and aspirations of their inhabitants for yet to day decades modern neighborhoods resembles the one of West-Europe or North America. Such choices have impact not only on the pedestrian comfort but also on the energy consumption and the Urban Heat Island features.

1.3 The objective of the Study

In this work, we are looking for a better understanding on how pedestrian comfort is affected by the constructions design choices, comparing an old district to a new one and on how vegetation and shading patterns contribute to reducing the effect of UHI and improving the pedestrians outdoor thermal comfort. The usual approach consists of increasing the city permeability to facilitate heat exchanges and therefore the cooling of a city. How does it work in an arid climate? What lessons could we acquire from choices consisting in importing Western cities practices to such environment? We aspire to examine the impact of architectural choices on the main outdoor comfort indicators. We compare an old district built according to ancestral customs to a typical Western-type

neighborhood made of several high-rise buildings. Not only is the urban fabric different but also are the material choices. Next, we investigate mitigation strategies to provide more outdoor thermal comfort to pedestrians. This work is to our knowledge the first investigation on mitigation strategies of the Urban Heat Island and the prediction on the outdoor thermal comfort in a hot and arid climate (Baghdad). The results of this work will be discussed in the form of design recommendations intended to help improving UHI mitigation strategies and enhancing pedestrian comfort. Finally, we focus on possible procedures that could be taken to treat the problems of outdoor thermal comfort in hot, arid climate.

1.4 Methodology

Urban microclimate models vary substantially in many aspects: physical basis, temporal and spatial resolution, and input- output quantities. ENVI-met is a tool for representing the major processes in the atmosphere including wind flow, radiation fluxes, temperature, and humidity. ENVI-met simulates integrally all the microclimate factors influencing thermal comfort like air temperature, relative humidity, wind speed, solar radiation and mean radiant temperature (Ali-Toudert, 2005). This software was chosen because it can represent three-dimensional buildings and calculate the effect of the vegetation and its relation to the outdoor thermal comfort. We adopted PET (Physiological Equivalent Temperature) and PMV (Predicted Mean Vot**e)** indices to evaluate the outdoor thermal comfort at pedestrian level.

1.5 Structure of the Study

The thesis is organized into six chapters: chapter two gives a brief overview of definitions and the most significant findings related to the phenomena of Urban Heat Island and mitigation strategies, and explains the outdoor thermal comfort indices. Furthermore, it focuses on investigation researches on UHI and outdoor thermal comfort in hot and arid climates. Chapter three describes the background for the numerical modeling of the urban microclimate. It also focuses on significance and characteristics of ENVI-met. The results of the numerical simulations for the study case in Baghdad are presented, analyzed, and

discussed comprehensively in chapter four. Chapter five presents a proposal district design in an arid climate based on the architectural and implementation criteria to improve the climate and the pedestrians thermal comfort conditions. Chapter six involves the meaningful conclusions that are extracted from the simulation models for the two districts in Haifa Street (modern Western design) and the traditional houses in Al-Rasheed Street. Furthermore, it encompasses recommendations and suggestions of perspectives for further research in the future.

CHAPTER TWO

LITERATURE REVIEW

2.1 Introduction

2.1.1 Urban Heat Island definitions

Energy transfer within the earth-atmosphere system can occur in three modes (conduction, convection, and radiation). In the relationship between the atmosphere and the earth surface, the troposphere is the most influenced layer by the earth surface. The urbanization process produces a radical change in the nature of the earth surface and the atmospheric properties in an urban area. It relates to the transformation of the radiative, thermal, moisture and aerodynamic characteristics and thereby rarefies the natural heat and hydrologic balances. The features of the urban boundary layer are dominated by the nature of the surface of an urban area. The urban canopy layer, at the roof level, is produced by the operation in the streets (canyon) between the buildings. Figure (2-1) represents the classification of urban area layers. The air in the urban canopy layer is ordinarily warmer than the air in the vicinity. This could be lead to the appearance of the Urban Heat Island.

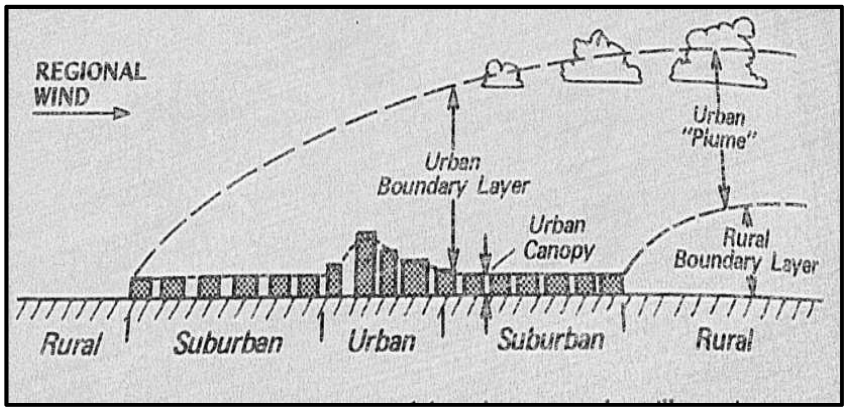

Figure (2-1): Classification of the urban atmosphere layer (Oke, 1976).

The urban Heat Island (UHI) may be defined as a phenomenon where surface and atmospheric modifications due to urbanization generally lead to modifying the urban climate that becomes warmer than the surrounding areas (Voogt, 2003, Coseo et al., 2014). Urban Heat Island describes a characteristic of the urban area in which the nocturnal temperatures are warmer than the surroundings landscape. Warmer urban air temperatures are a result of some interrelated causes associated with the urban modification to the natural surface, such the heat and the pollution released from the anthropogenic activities in the urban environment (Morris and Simmonds, 2000).

The Urban Heat Island is associated with the development of the cities and the urban expansion (Taleb et al., 2013). It has a direct effect on the energy efficiency, the environment, and ultimately human comfort and health. The urban environment is characterized by some features like the high density of population and buildings, high energy consumption and the shortage of the green areas (Busato et al., 2014). According to an investigation by Hathway et al., (2012) the absorption of the heat from surfaces of the buildings and the ground, the loss of moisture in the air due to the reducing of vegetation and a wide area of traffic and pavement, could contribute to the occurrence of Urban Heat Island.

Figure (2-2) explains the UHI phenomena in which the air temperature of an urban area is higher than the surrounding rural area. The first investigation of this phenomenon was conducted in 1833 by Luke Howard. He concluded from his findings that London was 1.48 ℃ warmer than the countryside. He based his study on the average of the monthly mean temperature during the period (1807-1816).

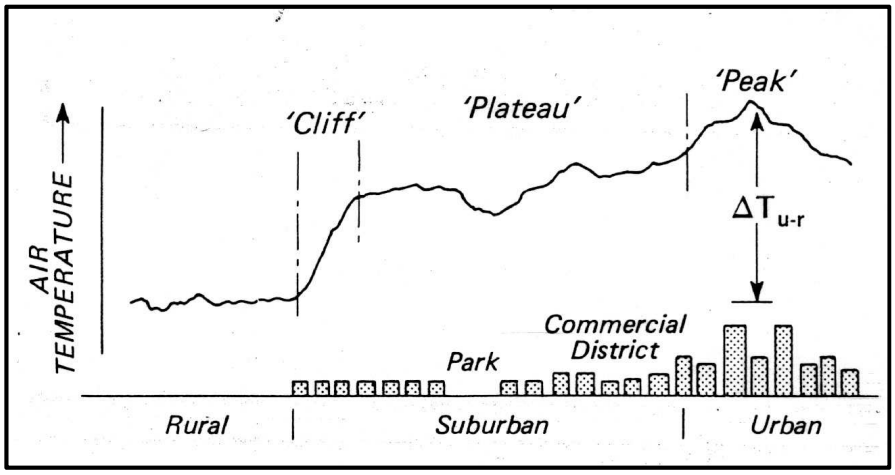

Figure (2-2): Generalized cross- section of a typical Urban Heat Island (Oke, 1987).

Oke (1976) mentioned that there are two types of Urban Heat Island layers, the first layer is the urban boundary layer, and the second one is the canopy. The research study presented by Erell et al., (2011) indicates that the urban boundary layer could be defined as the entire volume of air above the city that is impacted by the features of the surface and with the activities, as can be seen in Fig. (2-3). The urban boundary layer extends upward to about ten times the height of the buildings in the urban area.

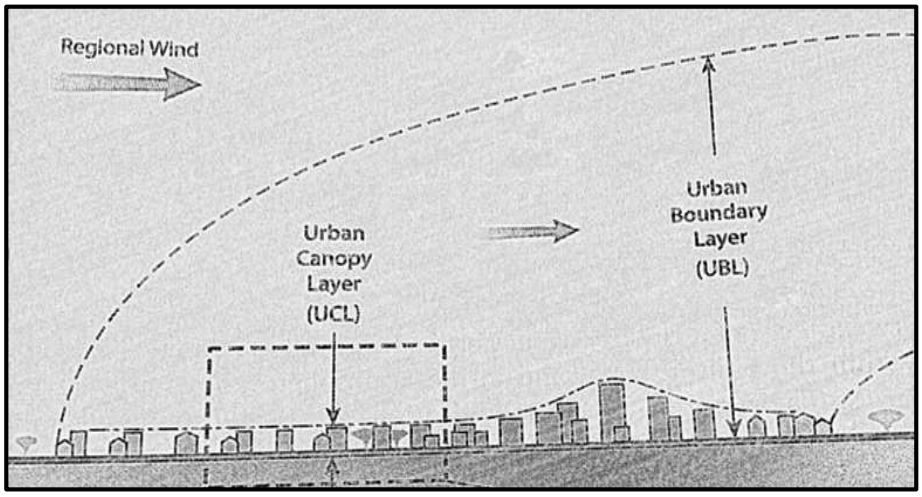

Figure (2-3): Urban boundary layer relative to the urban boundary layer (Erell et al., 2011).

Figure (2-4) shows the mixed layer which is defined as the layer of the atmosphere influenced by the presence of the urban surface. The Surface layer is to be up to a height of about four to five times for the average of the buildings. When the air passes over the ground, the surface layer forms. The properties of this layer are not affected by the urban elements such as the buildings and the streets.

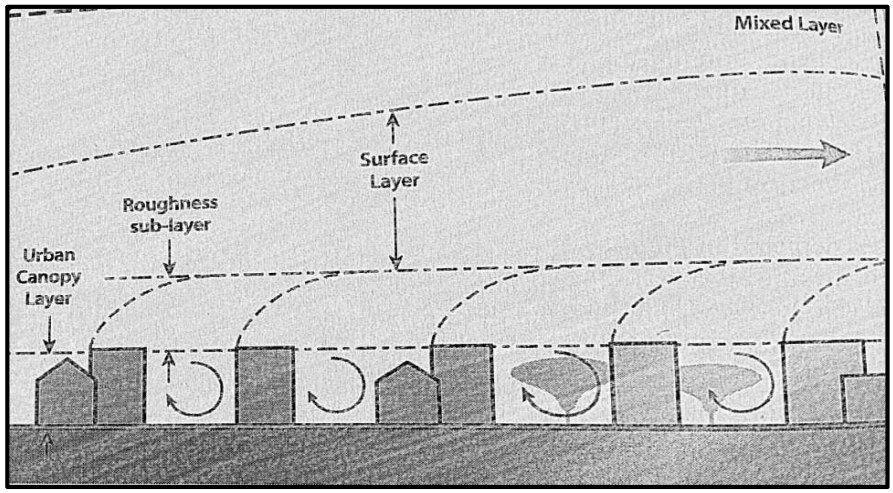

Figure (2-4): Description of the mixed layer, roughness sub-layer, and transition zones above and below the surface layer (Erell et al., 2011).

2.1.2 Researches on the Urban Heat Island (UHI)

The researches on the UHI focused on the urban effects, describing initially how the UHI has an effect on air pollution (Oke, 1982). However, the focus of UHI research has since moved to understanding the UHI process.

Many attempts were made to create a model of the urban area concerning with the effect of UHI (Arthur et al., 2003). Oke (1982) summarized the knowledge about the intensity, spatial and vertical structure, dynamics, and determinants of the UHI. He also reviewed the temperature patterns near the surface.

Attempts were made to simulate the dependence of the UHI on the urban geometry and the differences in thermal admittance (Arnfield, 2003, Johnson et al., 1991). Oke et al. (1991) indicated that the higher urban temperatures are due to the positive thermal balance of the urban areas caused by a significant release of anthropogenic heat. The excess storage of the solar radiation is affected by several factors, including the city structures, the lack of green spaces and cold sinks, the non-circulation of air in the urban canyons, and the reduce ability of the emitted infrared radiation to escape into the atmosphere. According to Radhi et al. (2013) the development of UHI influences the microclimate, thermal conditions and the quality of human life as can be seen in the increased the energy demand for cooling buildings, elevated greenhouse gas emissions and compromised human comfort. Remotely-sensed data from satellites represents a further potential for UHI researches (Carlson et al., 1981, Nichol, 1996). Carlson and Arthur (2000) used multiple linear regression models to reveal the impact of the urban development on the surface temperatures from multispectral satellite data. They explained how the surfaces of the urban area could affect the parameters derived from Landsat data, such as the fractional vegetation cover and the surface temperature. In this research, the fractional vegetation is considered as the most important variable, and a Normalized Difference Vegetation Index is used to estimate the fractional vegetation.

The intensity of the UHI effect is increased by the addition of pollution and anthropogenic heat to the air (Taha, 1997). As highlighted by Landsberg (1981) the high population density in the city centers has a tendency for consumption of a higher energy amount than the surroundings. The need for the air-conditioning during the summer months and the reduction of the need for heating in winter are the results of the Urban Heat Island. For these reasons, the UHI effect on the human life is necessary for the future investigation.

2.1.3 Factors affecting the intensity of UHI

The Urban Heat Island Intensity depends on the number of people living in the area, the morphology and the size of the urban area. The changes in the maximum city temperature and the suburban contextual temperature are presented as Urban Heat Island Intensity (UHII) (Oke,

1982). According to Shahmohamadi et al. (2010) the Urban Heat Island could be caused by different factors that can be divided into two types:

1. Meteorological factors, such as clouds cover, wind speed and humidity.
2. City parameters, such as the city and the population size, the anthropogenic heat and the urban canyon.

The Urban Heat Island occurs as a result of several reasons which could be categorized as controllable and uncontrollable factors as shown in Fig. (2-5). The controlled and uncontrolled factors could be classified as the temporary effect variables, such as air speed and cloud cover, and the permanent effect variables such as green area, building material, the sky view factor and cyclic effect variables such as solar radiations and anthropogenic heat sources.

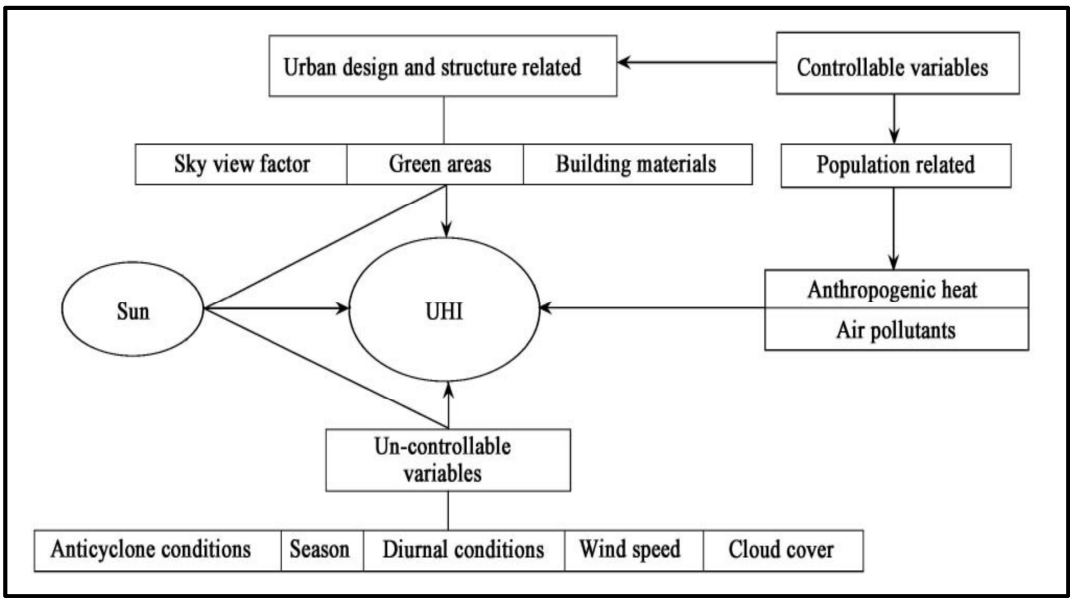

Figure (2-5): Generation of Urban Heat Island (Rizwan et al., 2008).

Based on an investigation study by Ratti et al. (2003) the significant variable includes:

1. Surface to volume ratio.
2. Shadow densities.
3. Daylight accessibility.
4. Sky- view factors.

Figuerola et al. (1998) carried out a research to investigate how the Urban Heat Islands in Buenos Aires city is affected by the factors such as cloud cover, wind speed and direction, the day of the week, and different seasons. It was observed in winter that the average value of the maximum urban heat island is 1°C lower on the windy and cloudy days than with weak winds and little sky coverage. The winds were blowing from the rural area towards the city when the maximum differences of temperatures occurred. The UHI creates heat stress such as tropospheric ozone formation and resulting health problems. Higher temperatures lead to increased electricity demand for the air conditioning, which, in turn, raises power plant pollution and greenhouse gas emissions. Also, UHI may increase water temperatures, resulting in water ecosystems impairment (Chun et al., 2014).

2.1.4 Impact of urbanization on UHI

The Urban Heat Island is one of the largest problems correlated with the urbanization and industrialization of human civilization. Many studies have analyzed urban activities that contribute to the development of UHI. According to an investigation research by Giannopoulou et al. (2011) on the statistical analysis of UHI features in Athens, the occurrence of high air temperatures depends on increased urbanization and industrialization coupled with the increased anthropogenic heat flows and the lack of vegetation. As highlighted by Guneralp and Seto (2008) the rapid urbanization means that the already significant environmental challenges present in urban areas will rise even further. The consequences of increased urbanization are reduced biodiversity, growing amounts of traffic, higher demand for energy-intensive indoor cooling systems. The UHI directly affects the well-being of inhabitants and health as they are exposed to higher rates of air pollution and more intense heat waves.

The UHI effect on the energy consumption for heating and cooling of buildings was investigated by Kolokotroni (2012). It is clear that increased temperatures in the urban centers have a significant influence on the energy demand for the heating and the cooling of the buildings. Therefore it was concluded that the site location should be taken into consideration by designers when estimating the energy consumption both in commercial and domestic buildings.

Poumanyvong et al. (2010) mentioned that most previous studies have implicitly assumed that the impact of urbanization on energy use and emissions is homogenous for all countries. Such an assumption can be questionable as there are many notable differences (e.g., energy structure and levels of urban public service provision) among countries of different levels of wealth. It is also in conflict with the arguments of ecological modernization and urban environmental transition

theories that urbanization pressure on the environmental may vary across the different levels of development. According to an investigation study conducted by Charabi et al. (2011) the preliminary investigations show the complex nature of assessing the impact of the urbanization in an arid tropical coastal environment. The results illustrate the meso and micro-level variability of the temperature due to several competing factors in this region-topography, mesoscale circulation, urban form, and landscape variability. Based on what was concluded by Borbora (2014) the replacement of natural vegetation areas with dry impervious surfaces, the use of building materials with high heat capacity and low surface reflectivity and the increase in anthropogenic heat emission into the urban atmosphere are likely to modify the thermal regime for Guwahati City in India.

2.1.5 Factors affecting the intensity of the Urban Heat Island

In spite of the efforts to realize the impacts of multiple urbanization factors on the Urban Heat Island, there is a lack for the knowledge of the effective role of urbanization on Urban Heat Island Intensity in different locations (Cui et al., 2016).

2.1.5.1 City size

For mid-latitude cities, Oke (1973) stated that there is a relationship between UHI (max) and logarithm of population (log (p)) of urban areas under the restriction of calm and clear (cloudless) weather conditions, for the West European cities and North America from years (1954-1972), the relationship as shown below:

$$\Delta T_{u-r(max)} = 2.96 \log p - 6.41 \quad (2.1)$$
$$\text{with } r^2 = 0.96$$

Europe from years (1929-1973)

$$\Delta T_{u-r(max)} = 2.01 \log p - 4.06 \quad (2.2)$$
$$\text{with } r^2 = 0.74$$

where $\Delta T_{u-r(\max)}$: maximum urban heat island intensity (℃)

2.1.5.2 Urban geometry

Researches on The UHI usually focus on the urban canyons, which can be illustrated by a narrow street lined by high buildings. During daytime, there are real effects for urban canyons. When sunlight reaches the surfaces of buildings and grounds in the canyon, the sun energy is reflected and absorbed by the building walls, which further lowers the overall city albedo. The reflectance from surface albedo plus urban geometry can increase temperatures. At night, urban canyons impede cooling the buildings and the structures can obstruct the heat transfer that is released from the surfaces of buildings and grounds.

Most researchers focused on the relationship between building height and density of buildings distribution. A measure for the geometry of the urban canyon is the height to width (H/W) ratio. This ratio describes how densely buildings are spaced on their heights. According to Gago et al. (2013) the geometry of urban canyons has an impact on the total energy consumption of up to 30% in commercial buildings and 19% in residential buildings. In deep canyons, wind speed variations can be substantial, resulting in significant temperature differences (approximately 5℃ higher) over the canyon than at street level. Also, the optimization of urban design/ planning concerning the energy consumption of buildings allows savings of up to 30%. As highlighted by Olàh (2012) the open space design and even the (building) architecture could have such new priorities which can eventuate the minimizing and prevent the development of the Urban Heat Island both locally and on the scale of the whole city.

Oke (1981) tried to find a relationship between the maximum intensity of the UHI and the height/width ratio of the street canyons (H/W). He observed these associations in 31 cities located in North America, Europe, and Australia. As shown in Fig (2-6), the relationships between the maximum intensity of the UHI ($T_{u-r(max)}$) and H/W can be summarized as follows.

$$\Delta T_{u-r(\max)} = 7.45 + 3.97\ ln\ (H/W) \tag{2.3}$$

where $\Delta T_{u-r(\max)}$: maximum urban heat island intensity (℃).

Height and Width were based on the ground-level and aerial photos, as well as on data sets from the buildings and streets dimensions. A more appropriate measure of radiation of a given site is the sky view factor which is the fraction of the overlying hemisphere occupied by the sky. It is a dimensionless (SVF) measure between 0 and 1, representing the openness of the sky to radiated transport. For all outdoor environments in urban areas, SVF at any point is less than one because of the obstacles in the urban sky (Yuan et al., 2011).

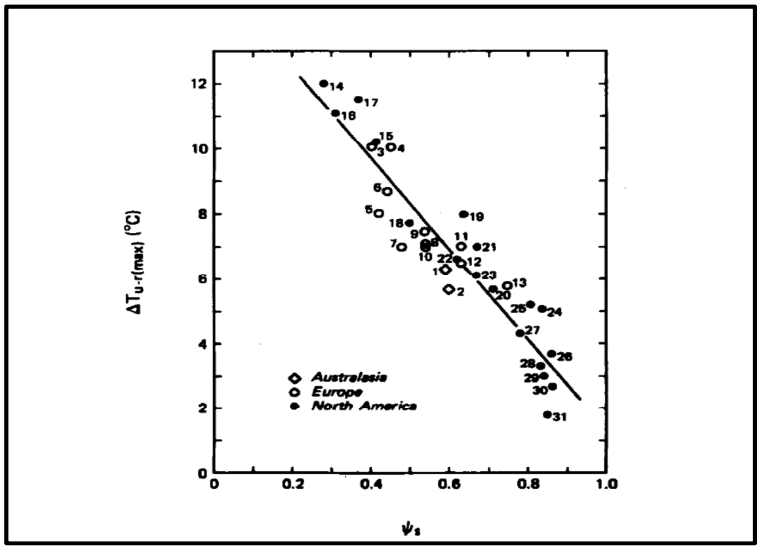

Figure (2-6): The relationship between maximum heat island intensity observed in a settlement ($\Delta T_{u-r\,(\max)}$) and the canyon sky view factor in its central area (Oke, 1981).

2.1.5.3 Properties of urban materials

Radiation and thermal properties of the materials influence the Urban Heat Island development: they determine how the sun energy is reflected, emitted, and absorbed. Furthermore, most materials used in the construction buildings and paving roads and walkways are impermeable to moisture. Consequently, more energy is available for long-wave emission, sensible heat flux and conduction to the surface.

According to an investigation by Hove (2011) the thermal emissivity ε is a measure of a surface ability to lose heat or emit long-wave (infrared) radiation. It is the ratio of energy radiated by the particular material to the energy radiated by a blackbody at the same temperature. An actual black body would have ε=1, while any real object would have ε<1.

Most building materials show an emissivity of 0.85 and higher. Building brick, metals, and some concrete mixes have relatively low values. Extensive use of these materials can reduce the overall urban emissivity which tends to increase the net radiation levels in urban areas.

Several studies investigated the ability to increase the albedo to mitigate the Urban Heat Island and decrease the cooling energy use. The albedo of a city depends on surfaces, the material used for roofs, and the solar position (site latitude, date and hour) (Bouyer et al., 2009).

Albedo is measured on a scale of 0 to 1. A surface with a relatively high albedo, 0.75 or greater, is light in color and reflects most of the sun rays. A surface a low albedo, 0.25 or less, is usually dark in color and will absorb most of the incoming solar energy (Gray and Finster, 1999).

According to an investigation study carried out in Los Angeles by Sailor (1995), the increase in the albedo in Los Angeles decreased the peak summertime temperatures by as much as 1.5 K. According to Taha et al. (1999) the large scale increases in surface albedo for ten cities in the U.S. reduced the air temperature by 0.5 to 1.5K in summer in the daytime and decreased the peak electricity demand by up to 10%.

There are other properties which can be considered more efficient on the properties of the urban material such as the thermal behavior of urban surfaces. The density material largely determines this behavior, specific heat capacity, thermal conductivity, and thermal admittance coefficients of the materials used. Urban building materials, such as steel and stone, have higher heat capacities than rural materials, such as dry soil and sand. As a result, cities are typically more efficient at storing the sun energy as heat within their infrastructure. Downtown areas can absorb and store twice the amount of heat compared to their rural surroundings during daytime (Hove, 2011).

Simulations carried out by Montavez et al. (2008) show that the most desirable combination of geometry and thermal properties can produce a UHI intensity of 10 K. According to a simulation model developed by Oke et al. (1991) the thermal properties have a significant influence. Differences in thermal admittance between rural and urban areas alone can produce heat (or cold) island. In contrast to differences in geometry, differences in thermal admittance are less clear and visible. Thermal admittance is the rate of flow of heat between the internal surfaces of the structure and the environmental temperature in the space. As highlighted by Elsayed (2012) the effect of the thermal admittance on the surface of the material is one of the most significant thermal properties in causing the Urban Heat Island. Temperature variation depends inversely on the thermal admittance. While urban materials have low thermal admittance, moist soils and vegetation have higher thermal admittance. In accordance to what has been mentioned by Oke et al. (1991) the cities whose environs are characterized by high admittances (wetlands, irrigated soils, paddy fields or rock) could only support a small Heat Island.

2.1.6 Descriptions of the geometry of the urban canyon

Erell et al., (2011) proposed three principle descriptors for the geometry of the urban canyon:

1. The height –width ratio, also known as the aspect ratio. It is defined as the ratio between the average height of adjacent vertical elements (such as building facades) and the average width of the space. As shown in Fig. (2-7).

2. The canyon axis orientation (θ) represents the direction of the elongated space. (in degree) as the angle between a line running north-south and the main axis running the length of the street or other linear space, measured in the clockwise direction.

3. The sky view factor (SVF) of an urban canyon is closely related to its aspect ratio (H /W), also describes the cross - sectional proportions of the canyon. Figure (2-8) shows the sky view factor as a function of canyon aspect ratio (H/W). Figure (2-9) depicts the emission of long-wave radiation (L↑).

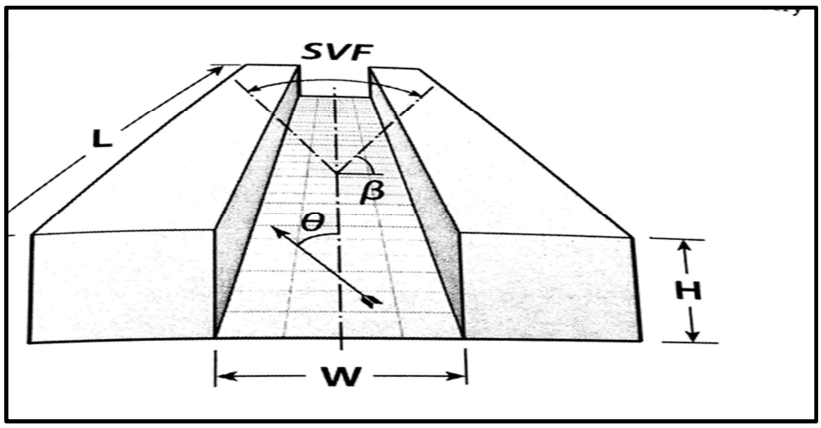

Figure (2-7): The view of a symmetrical urban canyon (Erell et al., 2011).

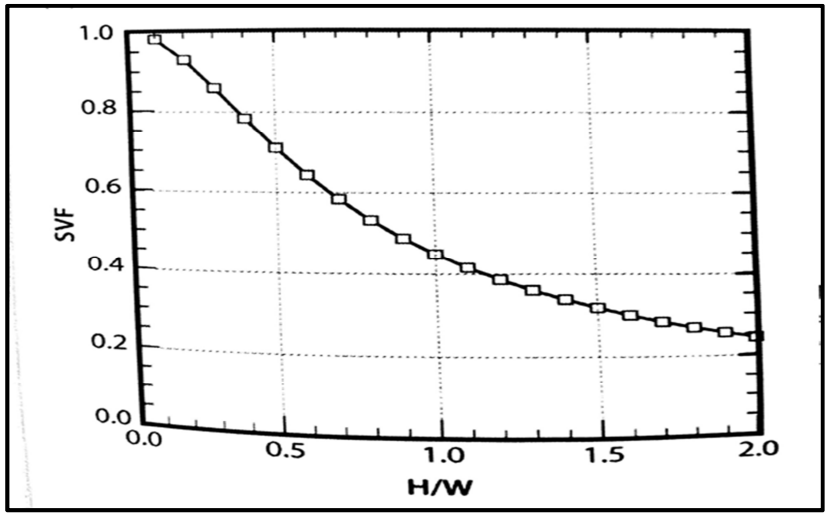

Figure (2-8): The sky view factor as a function of canyon aspect ratio (H/W) (Erell et al., 2011).

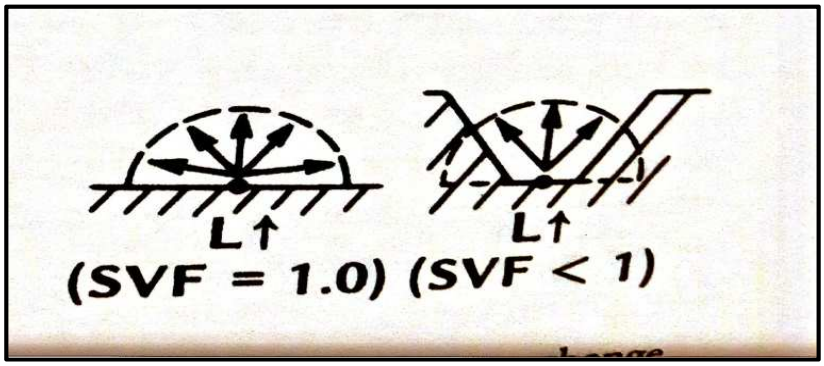

Figure (2-9): Emission of long-wave radiation ($L\uparrow$) (Oke, 1987).

2.1.6.1 The Impact of sky view factor on UHI

Oke (1981) developed a formula to correlate the maximum Urban Heat Island and the sky view factor (SVF) in the middle of an urban canyon floor:

$$\Delta T_{u-r\,(\max)} = 15.27 - 13.88 \times SVF \qquad (2.4)$$

When the Urban Heat Island occurs after sunset, this formula reveals that the Urban Heat Island is strongly related to the reduced long-wave heat loss by the restricted view of the sky. Oke (1987) stated that SVF is a measure of the percentage of radiation penetrating the urban canopy layer (UCL). Yamashita et al. (1986) concluded that the sky view factor has to be taken into consideration to explain the Heat Island intensities. They mentioned that the sky view factor is well correlated with Heat Island intensity, and moreover is easy to obtain from the photograph of the whole sky. Figure (2-10) shows the relationship between the Heat Island intensity and the maximum sky view factor of each city. In this figure, the white circles are daytime and the black circles are the night time observations. Temperature data was observed in February 1983. The (d, n, and t) represent the regression lines adjusted for the day- time, night- time and total values.

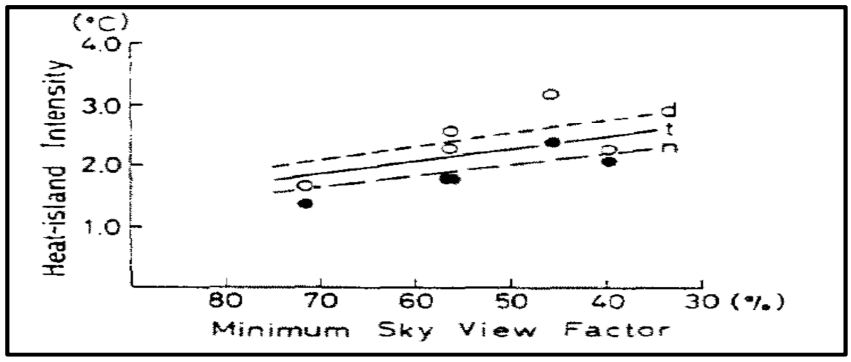

Figure (2-10) : The relationship between the minimum sky view factor and heat intensity on the cities along the Tama River Basin, Japan, in (February) 1983 (Yamashita et al., 1986).

Figure (2-11) shows the case observed on the cities along the Tama River Basin, Japan in May 1983. It is characteristic that daytime values of Heat Island Intensity are more related to minimum sky view factor than night time ones. Nevertheless, the sky view factor may be correlated with the Heat Island Intensity (Yamashita et al., 1986).

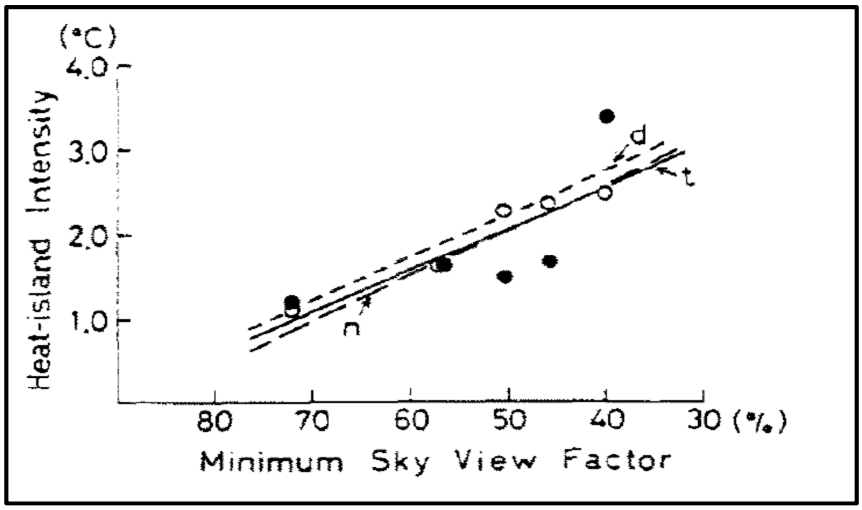

Figure (2-11): The relationship between the minimum sky view factor and heat intensity on the cities along the Tama River Basin, Japan, in (May) 1983 (Yamashita et al., 1986).

Based on what was mentioned by the Chen and Ng (2009) the first investigation on the sky view factor was proposed by Lindquist (1970) who showed that the differences of intra-urban surface air temperatures were strongly dependent on SVF. Also, they explained that the sky view factor values of the urban areas in Hong Kong were smaller than 0.5. These values indicated the reasonable agreement with temperature variations along the urban canyon. According to a study conducted by Oke (1981) a hardware simulation model showed that the sky view factor can produce nocturnal Urban Heat Island Intensity up to 7℃. He reported that the sky view factors for downtown sites ranged from 0.25 to 0.84. As highlighted by Brown et al. (2001), for the case where buildings cover 50% of the area of the sky, the sky view factor would be greater than 5% because sky view factor is weight by the spread of the radiation over the surface of the area. Referring to the definitions given by Yang et al. (2010), the tree view factor is defined as the fraction of the overlying hemisphere as shown in a sky view image that is occupied by the vegetation canopy. They also explained that the total site factor is developed to quantify the site solar access in an integrative manner. It is a function of the vegetation in the surrounding canopy geometry (buildings and tree), sun track, solar radiation intensity, and time. Paramita and Fukuda (2014) mentioned that the Urban Island could be the main reason for increasing the surface roughness, which in turn devotes the effect to mean radiant temperature with sky view factor. This effect occurs in heat intensity of the urban built environment, especially in a hot-humid

climate region. According to Yang et al. (2015), there is a relationship between the effective emissivity and the sky view factor. They clarified that the high density of the buildings in the urban area means that there is a small sky view factor and enhanced trapping of radiance. They confirmed that the method proposed could be used for a further study on improving the accuracy of urban surface temperature retrieval and emissivity modulation.

2.1.6.2 Determination of view-factors in urban canyons

The influence of view factors on the radiation exchange is not a new concept; we could find that the first investigations began in 1964 by Anderson and in 1967 by Reifsnyder. They described the effect of the view factors upon radiation exchange in a forest environment. According to Reifsnyder (1967) the view factor is defined as the geometric factor describing the ratio of radiation received by the radiometer emanating from a particular source to the total received from all sources. Furthermore, Giguère (2009) defined the sky view factor as a measure of the openness of the urban area texture to the sky, and linked it to climatological phenomena such as urban heat island, day lighting and heat absorption. A clear explanation on view factor was presented by Oke (1987) who indicated that view factor is a concept as a geometric ratio that explains the portion of the radiation output from one surface that intercepted by the another surface.

2.1.7 Mitigation strategies of UHI

UHI represents to the tendency for a city to remain warmer than its surroundings. Mitigation of UHI technique aims to balance the warmth of the cities by increasing thermal losses and reducing the corresponding gains. Several field studies investigated the measure of energy savings that result from the increasing of roof solar reflectance. Solar-reflective roofs remain cooler in the sun than the solar-absorptive roofs (Akbari et al., 2005). According to Oke et al. (1991) light color of many tropical building could be decreased the absorption of heat due to a higher albedo. As highlighted by Norton et al. (2015), increasing the vegetation cover in cities is one of the key approaches to lower both air and radiative temperatures and improve thermal comfort through shading and transpiration.

A recent mitigation strategy in the UK has demonstrated that even a small urban river can result in cooling effect during temperatures higher than 20℃. The cooling effects can be greatly enhanced by careful consideration of urban design. The researchers confirmed that the amount of cooling was significantly affected by the form of the urban areas. Streets and roads which were

opened to the river, combined with the river banks with more vegetation, led to more efficient cooling, which was sustained over a greater distance (Hathway and Sharples, 2012). Nuruzzaman (2015) proposed a diagram as shown in Fig. (2-12) to illustrate precisely the UHI mitigation strategies and how these strategies could be work to minimize the effect of Urban Heat Island.

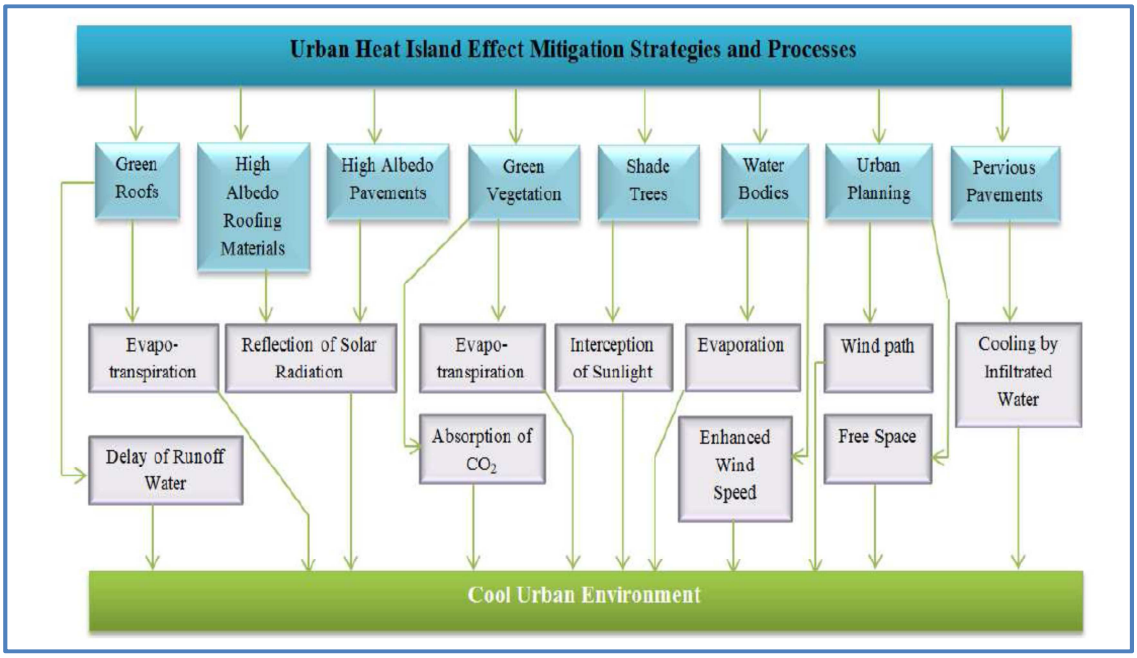

Figure (2-12): Urban Heat Island effect mitigation strategies and processes (Nuruzzaman, 2015).

The Urban Heat Island mitigation strategies for using the cool roofs are represented a low-cost strategy to reduce the cooling energy demand of the buildings and structures. According to Pisello et al. (2013), the coupled passive-active effect proposed a case study industrial office building located in Rome, Italy. This technology is the effective cool roof to decrease the suction air temperature of the heat pumps external units, when these units are located on the roof, and then to reduce also the temperature lift between the source and the output air of the heat pump in cooling mode. One of the first evaluations of the climates impact of the reflective surface was published by Sailor (1995), who simulated three- dimensional meteorological models to investigate the potential impact of urban surface appropriate modifications on local climate. The results of a base case simulation for the Los Angeles basin are compared to results from cases in which the urban albedo or the vegetative covers are increased. The results from these simulations indicate a potential to reduce urban energy demand and atmospheric pollution by 5%-10% through application of the surface modification strategies. According to Taha (1997) the use of high-albedo materials decreased the solar radiation absorbed by building and urban structures by keeping the surfaces cooler, the intensity of long wave radiation was reduced. A recent study

presented by Simon (2016) illustrated that vegetation is considered as a vital role in urban environments. Trees and other vegetation help to mitigate the effects of the urban heat island (UHI) by increasing the latent heat flux through evapotranspiration, which leads to reducing the air temperatures. According to an investigation by Santamouris (2012) only a few studies interested to evaluate the heat island mitigation potential of green roofs on a city scale are available. Most of the studies are using simulation techniques based mainly on mesoscale models. Studies are available for New York and Chicago in the US as well as for Hong Kong and Tokyo. Relevant information is also by an experimental study in Singapore. A simulation study aiming to evaluate the mitigation potential of green roofs in Chicago, US, is described by Smith and Rober (2011). Chicago had more than 50000 m^2 installed vegetative roofs in 2008. Yuan et al. (2011) presented a planning strategy based on the sky view factor and the urban morphology to mitigate the intensity of UHI. The study explained that the average air temperature is well related to sky view factor. 10% increase in sky view factor could decrease air temperature by about 0.4℃. This study also indicated that, for the areas with extremely high land use density, the sensitivity of sky view factor to change in site coverage and building height is very low. Urban planners must consider decreasing the land use density. As highlighted by Akbari et al. (2012) using cool roofs and cool pavements in the urban areas, could increase on average the mean albedo of the urban area by about 0.1. They estimated that the increase of the albedo of the urban roofs and paved surfaces worldwide would induce a negative radiative forcing equivalent to offsetting at least 40-160 Gt of emitted CO_2.

2.2 Thermal Performance of the Urban Area

A steady state heat transfer cycle begins by reflection and absorbance at canyon surfaces and including vegetation. The amount of absorbed heat is eventually radiated as long wave radiation from walls, ground and also from vegetation (Oke, 1987). After sunset, all canyons start to release absorbed heat by convection and radiation. In the dry air, the heat exchange depends on the human body temperature Tsk and air temperature Ta. Air is responsible for the convective transfer due to the difference in the temperature between the body and the surrounding air, and the convective exchange is directly propertied to the square root of air speed (Givoni, 1998). According to an investigation study by Ali-Toudert and Mayer (2006) the environmental thermal assessment and distinctions between different urban forms regarding pedestrian comfort and radiant exchanges are a complex interaction in the built environments. The pedestrian energy balance is the sum of the exchanges between the human body and the surrounding of the urban environment. The internal generation of heat by metabolism, as well as evaporative heat loss due

to sweating, are usually considered constant for all street configurations (Pearlmutter et al., 2006). Figure (2-13) shows the schematic depiction of the pedestrian energy exchange model.

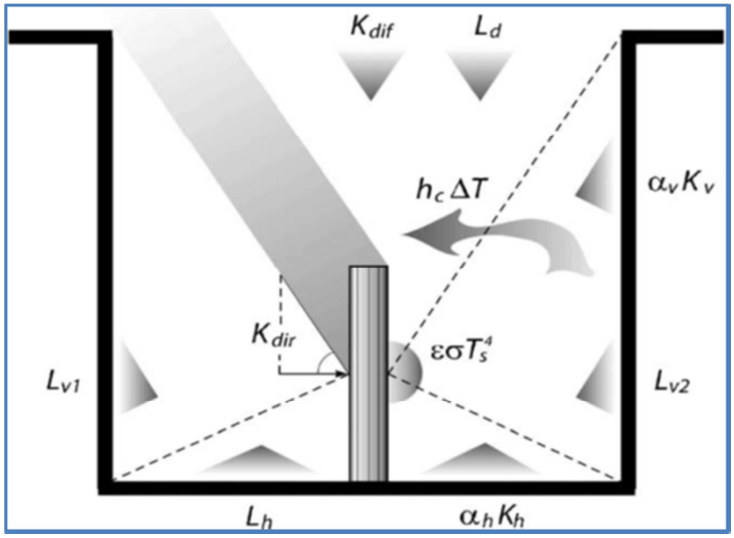

Figure (2-13): Schematic depiction of the pedestrian energy exchange model adapted from (Pearlmutter et al., 2006).

As explained by Fahmy (2010) the absorbed heat could be re-radiated as long wave radiation after certain time. The amount of the absorption and reflection depends on the physical properties of the ground surfaces and building facades and roofs. Furthermore, vegetation has a supporting role for ameliorating the radiation effect on the environment by receiving it as a direct radiation. Murakami (2006) explained the interaction of thermal performance in different scales. Figure (2-14) depicts the interaction of the thermal performance including the human scales and the urban scale.

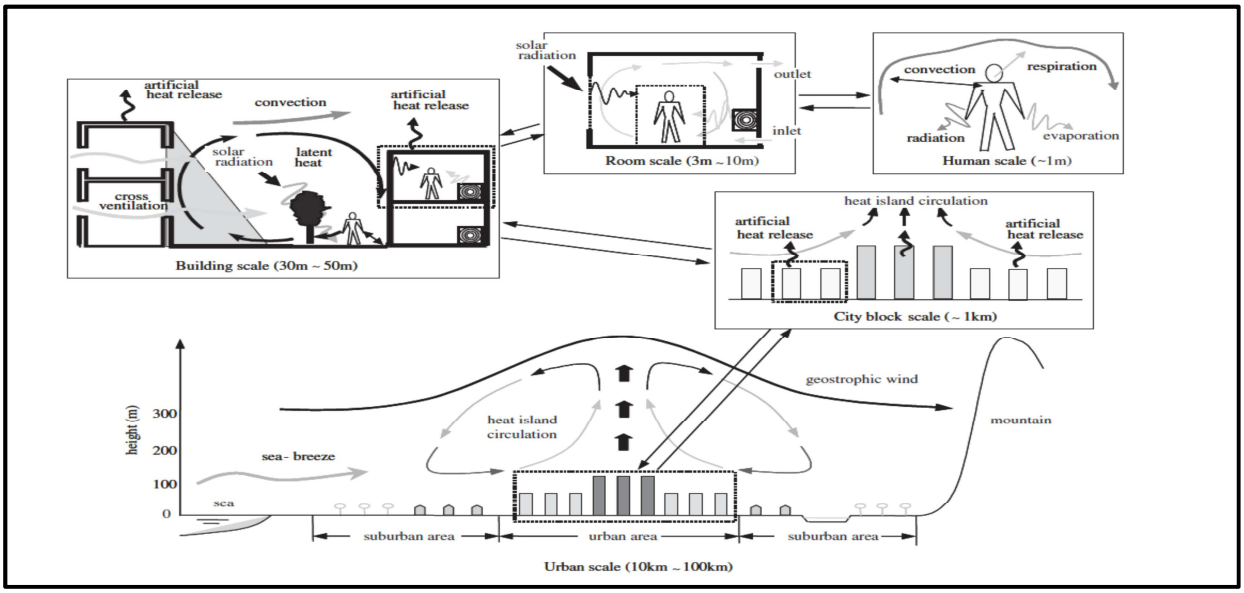

Figure (2-14): Interaction of thermal performance for different scales in an urban area (Murakami, 2006).

Many investigate involves urban climate studies, nevertheless there is a lack of connection between these studies and design solutions of the urban fabric and the link with the neighborhood climate scale (Landsberg, 1973, Arnfield, 2003, Ali-Toudert, 2005, Oke, 2006). In another study, Fahmy (2010) demonstrated that the deficiency in connection between the urban studies and the climate prevents from understanding the transient characteristics of outdoor thermal climates regarding pedestrian thermal sensation. There is also a difficulty to find a method for assessment of all urban details and the radiant exchanges.

2.3 Effect of Solar Access on Buildings and Pedestrians

The amount of the solar radiation that reaches the canopy layer is affected by several factors: the location, sky cover, and the urban structure. In arid climates, three main parameters affect the canopy layer climate: cooling techniques; ventilation evaporation and solar sheltering. In humid regions, evaporation required for cooling depends on the maximum evaporation capacity of air, which is a function of air humidity (Fahmy, 2010). The exposure of solar radiation access is one of the basic control factors which effects microclimate condition in urban design. Open spaces such as parks are usually more exposed to the solar radiation than the streets and semi-enclosed spaces. Controlling on solar access could be clarified briefly in two different parts as, solar access for buildings and solar access for pedestrians. Solar access is a fundamental requirement for the effect of solar heating of the buildings. Erell et al. (2011) defined the concept of solar light as a guarantee of exposure to direct sunlight for a predetermined period, typically several

hours each day. Controlling solar access for buildings includes the limits on the height or the volume of the buildings that are located from the visible position of the sun. The criteria for solar access rights of buildings are interpreted accurately by Erell et al. (2011). They explained that the criteria are based on defining an obstruction angle, which is based on the sun altitude at a given time on a specific date. The rules of solar access design could be presented as the following three questions:

1. What are the critical time and the date? Full exposure for several hours a daytime. Selecting a different time at noon means that the sunlight might be obstructed at all other times on the day.
2. Where should the obstruction angle be measured from? The effect of the obstruction such as the fences and single story buildings will be magnified when the ground level is taken to the base of the solar façade. Also, the results are unnecessarily stringent limits on the actual collector surfaces.
3. Which façade orientations warrant guaranteed solar exposure? Equator-facing surfaces of buildings gain the most insolation. The loss of potential solar gains is not substantial for the orientation about of 25 to 30 degrees away from due to South (or North).

The amount of solar radiation could directly affect the solar access. Hence, have an impact on the pedestrians outdoor thermal comfort. Therefore, the effect of solar access in urban design canyon is essential to improving urban microclimate (Shishegar, 2013). Pedestrians protected from the direct effect of sunlight by buildings elements such as colonnades, overhangs, awnings or trellises, and also by trees and other vegetation. Strategies of providing shade by restricting the width of the street are somewhat crude tools; shade may also be provided using trees along the pavements or using pedestrians arcades integrated at the street level of the adjacent buildings (Erell et al., 2011).

2.4 Background on the Outdoor Thermal Comfort

Human thermal comfort can be defined as the condition of the mind in which satisfaction as a thermal comfort. Taeghani et al. (2013) stated that thermal comfort had been discussed since 1930. Also, they indicated that there are two approaches to thermal comfort: the steady state model and the adaptive model. The adaptive model is based on the theory of the human body adapting to the outdoor and indoor climate. Fabbri (2015) defined comfort as the result of the interaction of many parameters of physical, physiological, psychological, social and culture rights. Thermal comfort depends on the architecture, clothing, the habits of eating and the

climate. Discomfort is caused by a vertical air temperature difference between the feet and the head, by an asymmetric radiant field, by local convection cooling or by contact with a hot or cold floor (ASHRAE Standard, 55-2012).

Indoor thermal climate concerns the hygrometric and indoor air quality aspects which influence the well-being inside buildings. The prediction of indoor climate plays a significant role in the evaluation of the buildings energy quality (Corgnati et al., 2011). As highlighted by Kalz and Pfafferott (2014) indoor air quality has a substantial impact on the overall satisfaction of the thermal environment. The indoor thermal environment has a considerable effect on the outdoor thermal comfort.

The history of thermal comfort came from the military scope, from the necessity to ensure that the military could continue the work on the ship and airplanes even in the environment with high temperatures (Fabbri, 2015). Recently, researchers began to take an interest in the effect of the outdoor thermal comfort, whereas most of them regarded thermal comfort as mainly concerning the interior space. The study of thermal comfort is to be conducted by considering various physical, physiological and psychological aspects, accounting for the interrelationships between the thermal conditions of the environment, physiological responses and psychological phenomena. Many factors effect on the thermal comfort, these factors could classify into three categories (Auliciem and Szokolay, 2007):

1. Climatic factors such as the effect of air temperature, relative humidity, the radiation, and the velocity.
2. Personal factors which belong to the metabolism and the clothing.
3. Contributing factors like the influence of the acclimation with the environment, age.

The mean radiant temperature (Tmrt) indicates the level of radiant temperature received by the human body, Fig. (2-15). The radiation includes all the radiative fluxes (direct, diffuse, reflected solar radiation and long-wave emissions from the surfaces (Jamei and Rajagopalan, 2015). The mean radiant temperature is considered as the most important factor affecting the human thermal comfort in an outdoor urban area (Landsberg, 1981). The value of Tmrt is the sum of all short-wave and long-wave radiation fluxes absorbed by the human body that affects its energy balance and human thermal comfort (Wang and Akbari, 2014). Peng et al. (2011) confirmed that the mean radiant temperature is a more accurate indicator than air temperature to evaluate thermal comfort. Thorsson et al. (2014) came to the same conclusion, stating that the mean radiant

temperature is the most important meteorological parameter governing the human energy balance and thermal comfort.

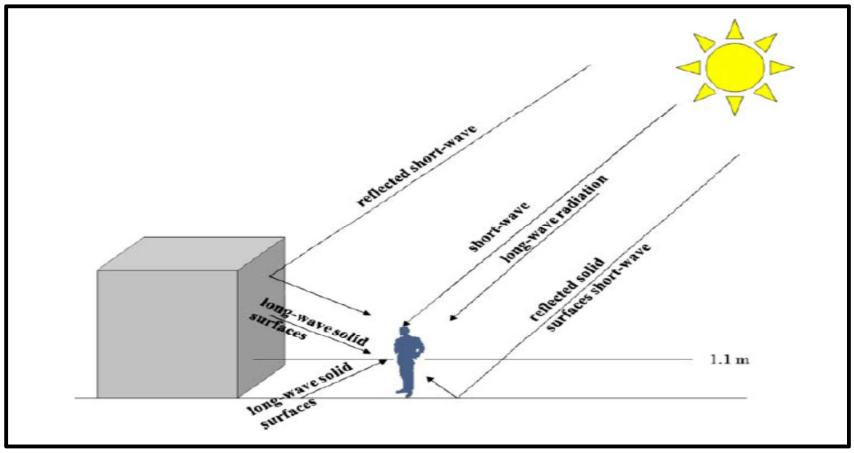

Figure (2-15): The radiation flux densities are important for the determination of the mean radiant temperature (Matzarakis et al., 2010).

The increase in incoming radiation leads to a high capacity of heat storage which contributes to intensifying the Urban Heat Island. The Physiological Equivalent Temperature (PET) is considered to be a good parameter for understanding the effect of radiation and wind velocity on the thermal comfort and the heat storage in an urban area (Kutscher et al., 2012). Note that the mean radiant temperature is considered to have the strongest influence on the physiologically significant thermal indexes like the Physiological Equivalent Temperature (PET) or the Predicted Mean Vote (PMV) which are derived from the models of human energy balance. According to Ali-Toudert and Mayer (2006) many studies showed that the outdoor thermal comfort is strongly dependent on the short wave and long wave radiation fluxes surrounding human activity. They confirmed that shading plays an important role in the strategy for heat mitigation in summer, together with the orientation of the street. Figure (2-16) depicts the parameters of the outdoor thermal comfort.

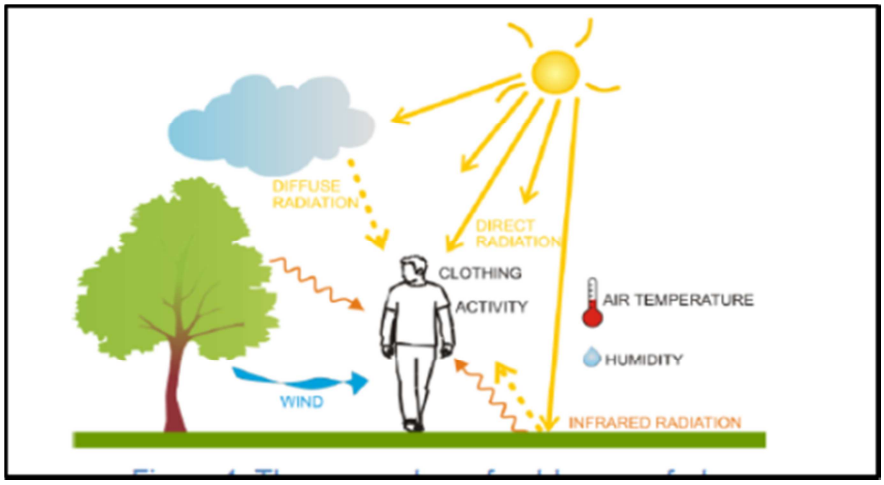

Figure (2-16): The parameters of outdoor thermal comfort (Perrineau, 2013).

Recent investigations indicated that the PET is the index that could be used to assess the thermal comfort conditions of outdoor environments rather than the indoor based thermal indices. Makaremi et al. (2012) concluded from their results that the human thermal comfort in outdoor spaces of the hot and humid climate of Malaysia could be integrated into the design guidelines to enhance the outdoor human comfort in tropical areas. The PET index is utilized to assess the thermal comfort conditions. Table (2-1) explains the ranges of the physiological equivalent temperature (PET) for different grades of thermal perception by human beings and physiological stress on human beings. Internal heat production is 80 W, heat transfer resistance of the clothing is 0.9 clothing.

Table (2-1): Classification of PET values in terms of the thermal perception and heat stress (Matzarakis and Amelung, 2008).

PET	Thermal perception	Grade of physiological stress
4°C	Very cold	Extreme cold stress
8°C	Cold	Strong cold stress
13°C	Cool	Moderate cold stress
18°C	Slightly cool	Slight cold stress
23°C	Comfortable	No thermal stress
29°C	Slightly warm	Slight heat stress
35°C	Warm	Moderate heat stress
41°C	Hot	Strong heat stress
	Very hot	Extreme heat stress

The Predicted Mean Vote (PMV) is the index evaluating the outdoor thermal comfort based on the heat balance and the perceived temperature. Table (2-2) shows the PMV index predicted as

the mean response of a large group of people according to the ASHARE 55-2004 thermal sensation scale. PMV assesses the mean thermal perception of a group of persons in the environment (Perrineau, 2013). Salata et al. (2015) indicated that the magnitude of the multiple reflections inside the buildings could decrease the index PMV of about 0.5 units, because of the presences of the lawn, trees and shrubs in the urban area.

Table (2-2): PMV index (ASHRAE Standard, 55-2004).

Cold	-3
Cool	-2
Slightly cool	-1
Neutral	0
Slightly warm	+1
Warm	+2
Hot	+3

More recently, Younsi and Kharrat (2016) mentioned that in addition to the Predicted Mean Vote (PMV) and the Physiological equivalent temperature (PET), they added the Universal Thermal Climate Index (UTCI). According to an investigation study by Monam and Ruckert (2013) four environmental factors affect thermal comfort: air temperature, mean radiant temperature, humidity, and wind speed. Also, they clarified that the most important personal variables that influence thermal comfort are clothing and the level of activity. According to Fanger (1973) a person could not be in thermal comfort if one part of his body is warm and another one is cold. He expressed it as an asymmetric radiant field or a local convective cooling of the body or by the contact between the warm and the cool floor. Rocheidat (2014) focused on person factors like clothing, activity level, and psychological factor. The heat balance of a person with the environment is explained clearly by Perrineau (2013). She showed that a person releases energy in a function of his activity. Energy is dissipated by the respiration and perspiration through the skin by convection process to the air and on the clothes after conduction through them, by long-wave radiation with the surrounding surfaces and by evaporation of the sweat. So, the air temperature of the ambient environment, the humidity and the temperature of the surrounding surfaces affect the outdoor thermal comfort. Ali-Toudert and Mayer (2007) stated that although the details of the outdoor thermal comfort factors are different, all these factors depend on the human energy balance and the applicable outdoors.

The Universal Thermal Climate Index (UTCI) represents the specific climates weather and locations comfort. The UTCI is very sensitive to the changes in the ambient (temperature, solar radiation, wind speed and humidity) better than the other indices. The UTCI scale can express even the slight differences in the humidity of the climatic (Blazejczyk and Epstein, 2012). Figure (2-17) depicts the UTCI equivalent temperature of actual thermal conditions which represent the air temperature of the reference condition causing the dynamic physiological response (Brode et al., 2009).

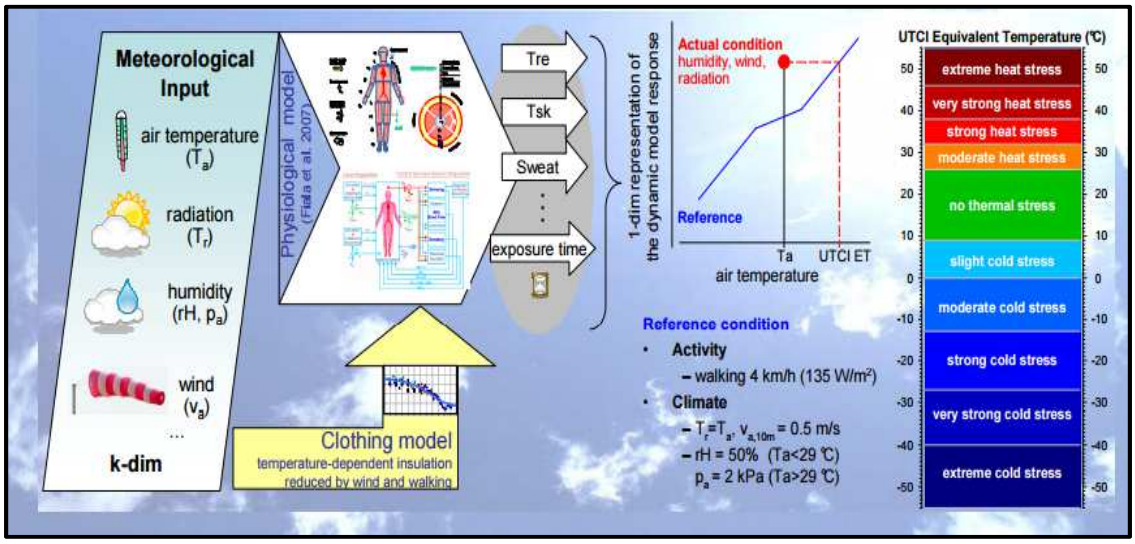

Figure (2-17): Response index (Brode et al., 2009).

2.4.1 Effect of the outdoor thermal comfort indices in the mitigation strategies of UHI

Makaremi et al. (2012) demonstrated from their conclusions that the use of trees and vegetation leads to the reduction in the PET index values by protection from the direct solar radiation. Shading is the significant characteristic of the vegetation that leads to moderate in the air temperature, while the value of mean radiant temperature is strongly reduced. They also concluded that a high shading level in outdoor environments increases thermal comfort and distends the continuity of the agreeable thermal conditions during the day. According to Jamei and Rajagopalan (2015) there is an improvement in the thermal conditions at the pedestrian level with the lower level of PMV and the mean radiant temperature. They noted that evident reduction is reported in the average of daytime in mean radiant temperature, air temperature, and PMV values after they had to implement a new plan strategy in Melbourne. Salata et al. (2015) compared the present configuration of the Cloister which is part of the Faculty of Engineering of Sapienza University of Rome with other configurations characterized by adding some vegetation and using materials with a high albedo, by taking into account the PMV (Predicted Mean Vote) model. The mitigation strategy with best results was used with adding some vegetation, whereas

using materials with a high albedo improved the microclimate if applied on surfaces characterized by a high sky view factor. According to a study focuses on human thermal comfort based on the physiologically equivalent temperature (PET) presented by Areu-Harbich et al. (2015) the shading of trees can influence significantly human thermal comfort. An analysis study presented by Panariti et al. (2014) focused on the impact of urban texture on the outdoor thermal comfort in the city of Durres in Albania. The study utilized different materials, green areas, and water reduces. The results showed that the urban texture in the case study influenced the outdoor thermal comfort. Referring to what came by Martinelli et al. (2015) there is a relationship between the hourly shading patterns and thermal comfort which could be represented by the hourly trend of the index PET for the shaded and unshaded locations as shown in Fig. (2-18). The difference in the direct solar radiation between shaded and unshaded areas could be indicated by a particular change in the PET values.

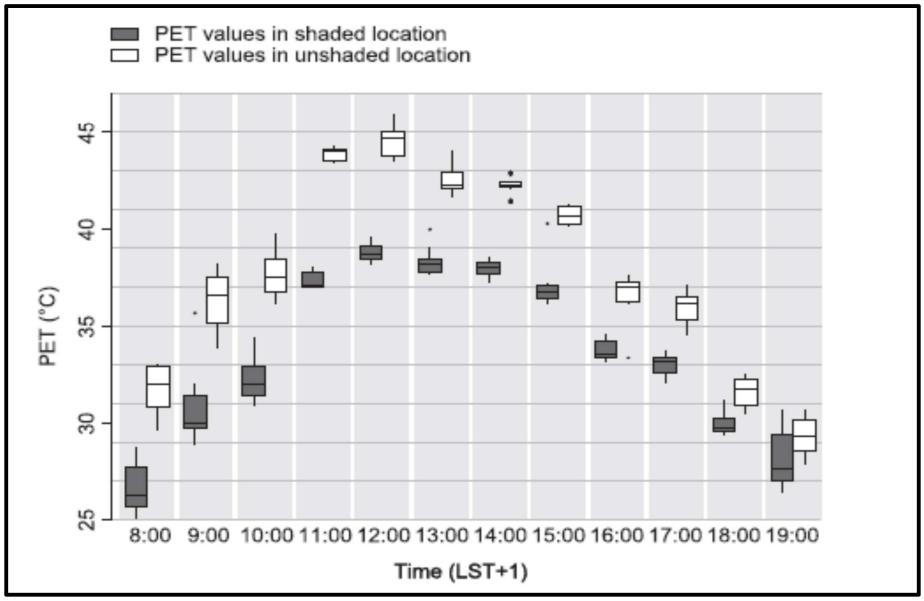

Figure (2-18): Hourly values of PET for shaded and unshaded locations from 8:00 to 20:00 (Martinelli et al., 2015).

According to an investigation by Ketterer and Matzarakis (2015) a comparison method had been adopted to assess the traditional ways of Urban Heat Island studies. Air temperature and PET were applied to indicate the impact of the thermal atmosphere in the city. As highlighted by Ali-Toudert and Mayer (2007) the effect of asymmetry galleries overhanging façade and vegetation on the thermal comfort that the PET gives a good indicator on the corrective measures for improving the climate quality of an urban street. The comfort is the most difficult to be ensured when the orientation of road is East-West. Planting and vegetation in East-West streets are

sensible since the duration and area of the discomfort will be critical. The results showed that the canyons, with a smaller sky view factor, with the orientation East-West canyons are the most stressful and deviating for improving the thermal comfort.

2.4.2 Counterbalance on effect of the Urban Heat Island and the thermal comfort

The strategies for mitigation the Urban Heat Island and improving human thermal comfort are not always matching. The Urban Heat Island occurs at night; outdoor human thermal comfort deals with daytime. Outdoor comfort strategies recommended implementing horizontal shade structures over pedestrian spaces. The same structure reduces the sky view factor and thereby trapped some of the heat that can be discharged to the sky at night (Rosheidat, 2014).

The strategy of mitigating the Urban Heat Island contributes to reducing the energy demand during summer and also provides health and environmental benefits such as reduced CO_2 emission, air pollution; is will lead to increased thermal comfort. Based on what came by Radhi et al. (2015) many investigations had been used to verify the impact of the Urban Heat Island on the thermal performance of an urban area, like field measurements, numerical modelling, and empirical models. Based on what was concluded by Rosheidat (2014), it is necessary to provide shading and to decrease the temperature of the surfaces that emit long wave radiations. The surface temperature of urban facades is the primary factor that could contribute to reducing thermal comfort.

2.5 Investigation on the Urban Heat Island and the Outdoor Thermal Comfort in Hot and Arid Climate

The outdoor thermal comfort is influenced by the perception and satisfaction of the pedestrians, especially in hot and arid climates. Accordingly, the researchers look for the appropriate methods to reduce the Urban Heat Island and thus to enhance the outdoor thermal comfort level of pedestrians. However, there is limited research conducted on the outdoor thermal comfort in hot and arid climate.

In a study on the role of greenery strategies Rajabi and Hijleh (2014) revealed that green roofs proved to perform poorly in reducing the surface temperatures in urban areas; this is because the cooling effects of green roofs reduce by distance and therefore this effect is negligible on the overall temperature reduction in urban areas. Also, regarding the composition of greenery, trees have the best contribution to the reduction of surface temperatures in the urban areas of Dubai.

Regarding the investigation study conducted in Iran (Tehran city) presented by Shahmohamadia et al. (2011) on the strategies to reduce the impact of the Urban Heat Island on human health, the results showed that the amount of vegetation placed on a building and its position (roofs, walls or both) is a more dominant factor than the orientation of the urban canyon. The canyon geometry with green roofs and walls that had a low thermal impact could play a more important role than the street orientation. Also, the study revealed that the heat sensation zones "hot" and "warm" are not achieved when urban roofs and walls are covered with vegetation, leading to more pleasant and comfort environments for the city residents. An investigation study was conducted of the warm core of the Urban Heat Island in the highland zone of Muscat, Oman. The valley is surrounded by mountains formed of dark colored rocks that can absorb the short wave radiation and contribute to the existence of the warmth in the core of the urban area. The study emphasized the importance of the nature of the rural baseline when assessing the urban effect on an urban area climate (Charabi and Bakhit, 2011). A study was conducted in Bahrain City to analyze the impact of the urbanization on the thermal behaviour of newly built environments. The results revealed that the recent process of the urbanization leads to an increase in the urban temperature by 2-5 ℃. The increase in temperature is enhanced by the urban activity such as on-going construction processes, shrinkage of green areas and sea reclamation (Radhi et al., 2013). Several studies indicate how the green effects have a crucial role in the process of sustainable cooling of the urban planning and in saving energy and improving human thermal comfort. A study was carried out in Cairo. There were acceptable comfort levels and cooling possible for some orientations for the urban area due to the clustered form with cool green islands and wind flow through the main canyons (Fahmy and Sharples, 2009).

The cooling effect of the green parks is remarkable not only locally in vegetated areas, but it can also be extended to the surrounding built environment (Shashua-Bar and Hoffman, 2000). An analysis study of the Urban Heat Island for Kuwait city was carried out by Nasrallah (1990). The temperatures values indicates that the urban warming influence in Kuwait city is lower than the values of temperatures measured for the dry land in cities of North America. The reason is that the city is located along moderate wind flows, lower buildings heights throughout the residential buildings and the city center, and the use of locally derived buildings materials with similar thermal properties then the surrounding desert terrain.

An investigation study was conducted in Phoenix (Arizona). Phoenix has a hot arid climate characterized by extreme summer temperatures. The results show that merely recommending massive tree planting in the urban areas may not abate the UHI effect as much as addressing the

combination of shading using trees and architectural shading structures. The properties of the materials for buildings and the surfaces, the density of construction of the urban area have a primary role in the increased temperature of cities. Additionally, irrigation enhances the cooling effect by adding latent heat exchange. However, the scarcity of water resources in an already dry climate dictates a careful balance between using water extensively for reducing urban surface temperatures. The appropriate solution is the shading surfaces to reduce the temperature and mean radiant temperature that are affecting the pedestrians thermal comfort at any given moment in time. The shading surfaces are able to discharge the stored energy at night so that could be contributing to providing thermal comfort to the pedestrians in the next day (Rosheidat, 2014).

CHAPTER THREE

URBAN ENVIRONMENTAL SIMULATION WITH ENVI-MET

3.1 Background for the Numerical Modeling of the Urban Microclimate

Simulation modeling plays a fundamental role for understanding and solving problems in complex environmental designs. The dynamic variability of weather conditions, complex geometry of urban design and different configurations of cities all over the world imposes limitations on the empirical study of urban microclimate. Thus, numerical modeling is expanding increasingly to involve the changing of urban microclimates. Urban climate models had been classified according to their scale, which can ranges from kilometers to a few centimeters. Usually, models developed for the urban climate are designed to imitate the effects of environments like the Urban Heat Island. Methods are required to link small-scale and meso-scale the urban climate design. Masson (2000) explained in details the concepts of the canyon geometry to calculate the urban surface energy budgets in meso-scale models. He indicated that a simplification of the real city geometry was necessary, and the canyon geometry is used to represent a city as part of the surface of an atmospheric model. An additional hypothesis of isotropy for the street directions has been added, to be representative of a city district, which allows the use of the scheme at horizontal scales larger than the road width, for local to regional impact studies. Urban microclimate models differ significantly according to their physical basis as well as their temporal and the spatial resolution. At the micro-scale, three-dimensional wind circulation versions are one of the most well started Johnsson and Hunter (1995) simulated a model to investigate the three-dimensional characteristics of the concentration field established for the flow perpendicular to the canyons with emissions released near the floor of the canyon by the motor vehicles. This investigation confined to the dispersion of passive pollutants. They concluded that the model could be used effectively in conjunction with existing experimental and field techniques. According to Herbert et al., (1998) a numerical modeling of the wind and thermal climates energy was simulated, the model tested the characteristic for the city canyons in Columbus Ohio and Los Angeles. The researchers concluded that the model had been used to investigate with reducing temperatures in built-up areas where the summertime that Urban Heat Island can pose a problem.

Regarding Bouyer et al. (2009) they proposed the solutions to reduce the energy consumption of the buildings by modifying the local climate. They used CFD tool (Fluent) and a thermo-radiative model (SOLENE). They concluded that the parameters concerned with the urban design that plays a role in microclimate and energy consumption are numerous: urban forms, surface materials, vegetation, and water presence, also the effect of geometry is taken into account by the sky view factor. Figure (3-1) shows the 3D simulation model and the surface mesh.

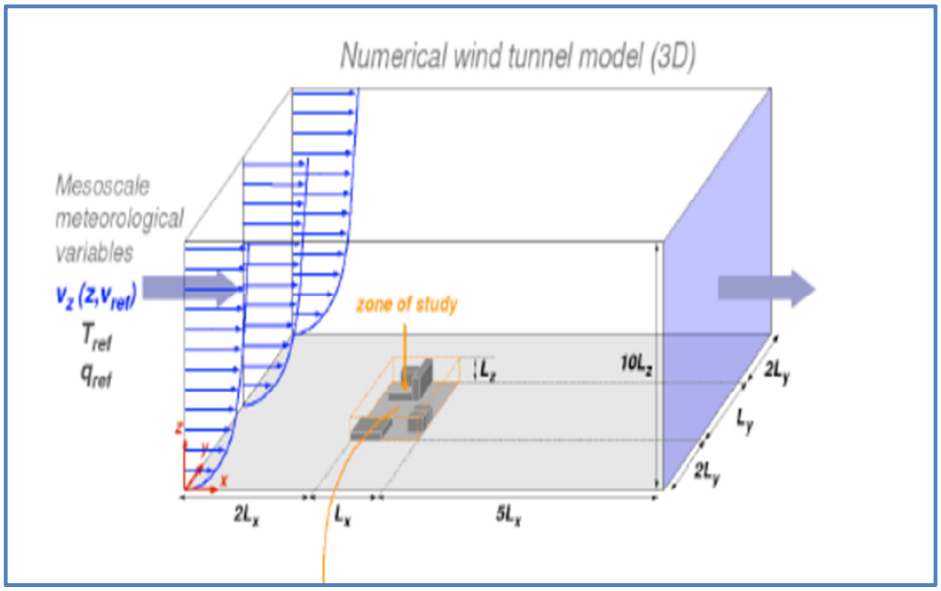

Figure (3-1): Simulation 3D model and surface meshing (Bouyer et al., 2009).

A study was conducted by Allegrini et al. in 2013 to investigate the urban microclimate and its potential influence on the energy demand of the buildings in an urban context. CFD (computational fluid dynamics) and BES (building energy simulations) had been used to simulate the model. Results revealed that the parameters that influence the local microclimate leading to local heat islands and complex wind flow structures. According to Dorer et al. (2013) the impact of the UMC (urban microclimate) on the space heating and the cooling energy demand was investigated for the typical office buildings in the street canyon configurations. Figure (3-2) depicts the multi- scale approach for the urban microclimate modeling. The researchers used BES for their simulation works. The results of the simulation work showed that the urban microclimate can have a significant

influence on the heat exchange and the energy demand of the buildings, depending on the geometries and the construction of the buildings.

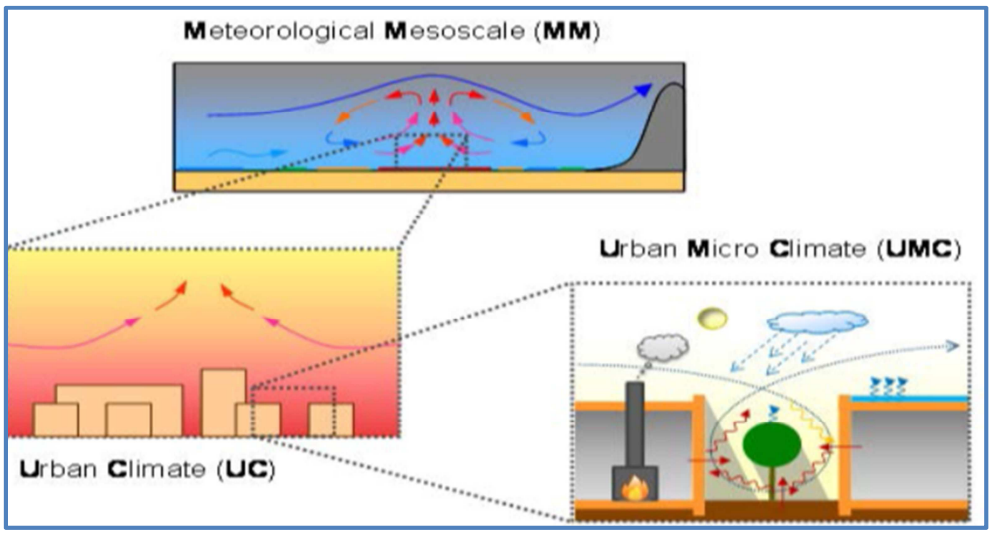

Figure (3-2): Multi-scale approach for urban microclimate modeling (Dorer et al., 2013).

An investigation study was conducted by Idczak et al., in 2010 for the validation of the thermo-radiative model (SOLENE) and its application for analyzing the street canyon energy balance. The results showed that the sensible heat was transferred mainly from the canyon surfaces to the ambient air, also from the air to the ground in the morning. The effective albedo of the canyon had a daily value of 0.20–0.25, dropped to 0.10 in the afternoon when the ground strongly transformed the direct and reflected solar radiation into sensible heat. Selection of the data has been used to confirm the ability of the thermo-radiative model (SOLENE) for simulating the thermo-radiative behavior of a street. According to Lemonsu and Masson (2002) a numerical simulation strategy TEB (Town Energy Balance) urban scheme and the numerical atmospheric model, Meso-NH were used to investigate the effect of Urban Heat Island in Paris city. Meso-NH is coupled to quantify atmospheric effects of Paris city on the boundary layer, through a comparison with simple simulation. The results showed that UHI above Paris reaches 8 ◦C at night; the UBL presents high instability and turbulence during the daytime. A numerical model was developed by Johnson et al. in 1991 to investigate the cooling of the rural and the urban canyon surfaces on calm, cloudless nights. The model requires the

solution of a system of partial differential equation. This simpler approach of this model is called SHIM which refers to Surface Heat Island Model. It incorporates heat conduction through the vertical and horizontal layers and radiative exchange between the sky and surfaces. The researchers concluded that the simple model of SHIM can be used as a tool for the diagnosis of Urban Heat Island causation under (ideal) conditions. Details of the results are considered the crucial element in selection a model. Swaid and Hoffman (1990) developed the cluster thermal time constant CTTC analytical model for predicting the air temperature variations in urban canopy layer UCL.

3.2 Significance and Characteristics of ENVI-met

ENVI-met simulates the dynamics of the urban microclimate based on the atmospheric physics, and the heat transfer principles (Bruse and Fleer, 1998). 3D wind flow is calculated using the incompressible, non-hydrostatic Navier-Stokes equations with the Bousinessq approximation. Katul et al. (2003) clarified that the minimum turbulence closure model plays an important role to efficiently simulate the mean flow and measures of the second order flow statistics. A logical choice is 1.5 closure models, defined as k- ε models considered as the most popular computational models in engineering applications. Potential temperature and specific humidity distributions are calculated using advection-diffusion equations and are modified by sources and sinks of heat and moisture within the model. Comprehensive accounts of the equations regulating the model are given by Bruse and Fleer (1998). The simulation process in ENVI-met is usually of 24-48 hours. The ideal time to start a simulation is at night or sunrise so that the simulation can comply with the atmospheric processes. ENVI-met requires an input area which defines the 3D geometry of the target area: the buildings, vegetation, soils, and receptors. The main input information of ENVI-met simulation includes weather conditions, the geometry and materials properties of the urban area, and characteristics of vegetation. Huttner et al. (2008) indicated that with ENVI- met it is not possible to simulate the micro-climate of the whole city because the maximum number of grid cells is quite limited. According to Vanessa, (2014) ENVI-met does not have an anthropogenic heat component, which can be a significant source of energy input in areas with high urban metabolism (city centers).

ENVI-met includes a grid-cell structure, with a maximum grid size of (250 x 250 x 30) cells. Horizontal resolution can range from 0.5 m to 10 m, which makes the model suitable for micro-scale to local scale analyses. There are two different type of vertical grid in ENVI-met (http://www.envi-met.com/):

1. An equidistant grid, as depicts in Fig. (3-3), the first cell closest to the surface is split into five equally spaced sub-sections with a height equivalent to 0.2Δz, where z is specified grid cell height. Above this, Δz is constant for the rest of model height
2. A telescoping grid for the vertical resolution. The grid size expands with height, according to a user-specified extension (or telescoping) factor.

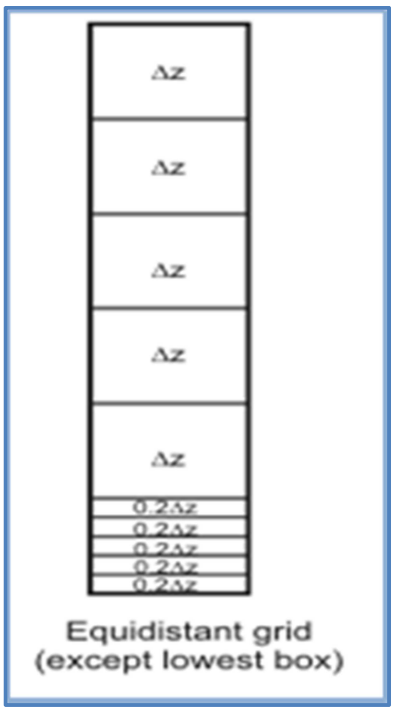

Figure (3-3): Schematic of equidistant vertical grid in ENVI-met (http://www.envi-met.com/).

3.3 General Model Properties

ENVI-met model consists of a one-dimensional boundary model that includes vertical profiles of different meteorological parameters up to a height of 2500 m above the ground level and a three-dimensional core model that includes all atmosphere, soil, buildings and

vegetation processes (Simon, 2016). ENVI-met model consists of several sub-models as shown in Fig. (3-4) that interact with each other (Huttner, 2012):

3.3.1 1D boundary model.

3.3.2 D atmospheric model.

3.3.3 3D/1D soil model.

3.3.4 Vegetation model.

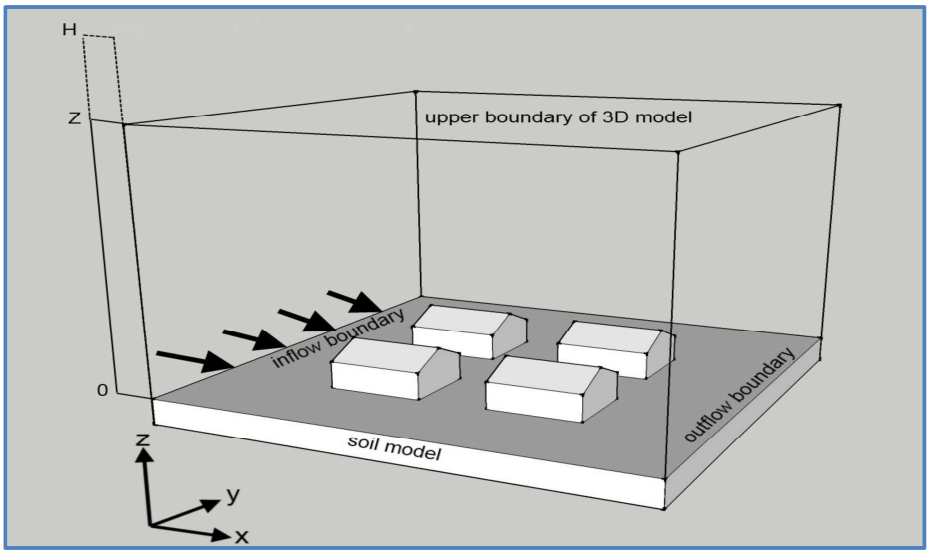

Figure (3-4): Schematic of basic model layout (Huttner, 2012).

3.3.1 1D boundary model

1D boundary model generates one-dimensional profiles for meteorological parameters such as air temperature, specific humidity, wind vectors (horizontal), kinetic energy and turbulent exchange. To ensure stable laminar conditions the boundary model extends to an altitude of 2500 meters (average height of the planetary boundary layer) (Simon, 2016).

3.3.2 3D atmospheric model

The three-dimensional core model consists of three orthogonal orientated axes, which generate a three-dimensional cube. The model area comprises some cells which represent different objects such as buildings, vegetation or atmosphere. The number of cells

depends on the dimensions of model area and its spatial resolution. A cell is defined by its physical properties. A building cell is defined by its material types, and the material type is defined by the specific heat capacity and other parameters. In combination with databases of all the different objects, this structure allows a detailed reconstruction of an urban environment (Simon, 2016).

3.3.3 Soil model

Huttner (2012) explained that the soil model calculates the temperature and humidity of the soil down to a depth of 1.75 m. Each horizontal grid cell has a soil profile with 14 layers that differ in depth. The depth of single layers increases from top to bottom, the top layers have a thickness of 1 cm, and the lowest layer has a thickness of 50 cm. Neglecting horizontal transfer, the soil is treated as a vertical column in which the distribution of temperature T and soil volumetric moisture content η are given by (Bruse and Fleer, 1998):

$$\frac{\partial T}{\partial t} = k_s \frac{\partial^2 T}{\partial z^2} \quad (3\text{-}1)$$

$$\frac{\partial \eta}{\partial t} = D_\eta \frac{\partial^2 \eta}{\partial z^2} + \frac{\partial K_\eta}{\partial z} - S_\eta(z) \quad (3\text{-}2)$$

For the natural soils, the thermal diffusivity ($k_s \; in \; m^2/sec$) is a function of the soil moisture. The hydraulic parameters that are used in Eq. (3-2) as clarified below:

η : is the volumetric water content of the soil ($m^3 m^{-3}$).

K_η: is the hydraulic conductivity.

D_η: is the hydraulic diffusivity.

The water absorbed by the plant roots (S_η) is provided by the vegetation model and treated as an internal sink of moisture (Bruse and Fleer, 1998). According to Bruse and Fleer (1998), the boundary conditions for the surface temperature will provide the upper boundary value.

3.3.4 Vegetation model

Huttner (2012) indicated that the vegetation in ENVI-met interacts with the atmospheric model and the soil model. The interactions between the vegetation and soil can be explained by the direct heat flux $J_{f,h}$ (Kms^{-1}) and the evaporation flux $J_{f,evap}$ (ms^{-1}) and the transpiration flux $J_{f,trans}$ (ms^{-1}). The interactions between the plant leaves and the surrounding air are given as explained in details by (Bruse and Fleer, 1998).

$$J_{f,h} = 1.1\, r_a^{-1}(T_f - T_a) \tag{3-3}$$

$$J_{f,evap} = r_a^{-1}\Delta_q \delta_c f_w + r_a^{-1}(1 - \delta_c)\, \Delta q \tag{3-4}$$

$$J_{f,trans} = \delta_c (r_a + r_s)^{-1}(1 - f_w)\, \Delta q \tag{3-5}$$

Huttner (2012) explained precisely the terms of the Eqs. (3-3), (3-4), and (3-5) as:

T_a (K) is the air temperature, T_f (K) is the foliage temperature, q is the specific humidity of the air ($KgKg^{-1}$) and Δq is the humidity difference. δ_c defines whether the evaporation is possible ($\delta_c = 1$) or not ($\delta_c = 0$). r_a is the aerodynamic resistance (sm^{-1}) that is a function of the leaf diameter and the wind speed.

3.4 Model Physics

The significant prognostic variables computed by ENVI-met are (Bruse and Fleer, 1998):

- Wind speed and direction.
- Air and soil temperature.
- Air and soil humidity.
- Radiative fluxes.
- Gas and particle dispersion.

The computation of these variables needs to use several sub- models that combined with each other. Figure (3-5) illustrates the ENVI-met sub models.

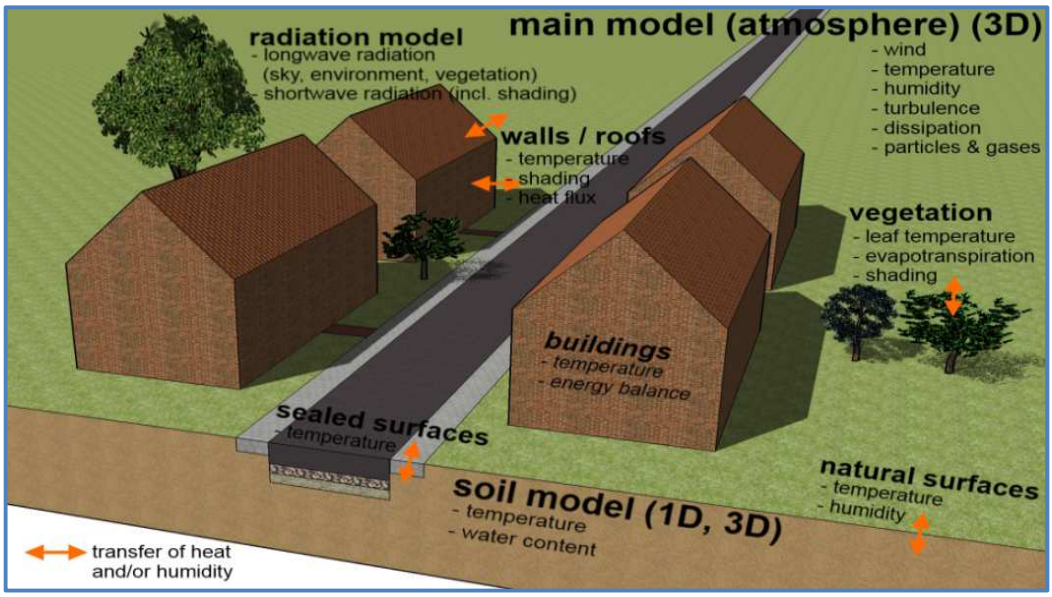

Figure (3-5): Diagram of the sub-models of ENVI-met (Huttner, 2012).

3.5 Physical Properties of the Atmospheric Model

The atmospheric model predicts the wind flow (speed and direction), turbulence, temperature, humidity, and short-wave and long-wave radiations fluxes.

3.5.1 Wind flow equations

Huttner (2012) indicated that the simplification of the Boussinesq-approximation is utilized to eliminate the density ρ from the Navier-Stokes equations which can be composed as:

$$\frac{\partial u}{\partial t} + u_1 \frac{\partial u}{\partial x_i} = -\frac{\partial p'}{\partial x} + K_m \left(\frac{\partial^2 u}{\partial x_i^2}\right) + f\left(v - v_g\right) - S_u \qquad (3\text{-}6)$$

$$\frac{\partial v}{\partial t} + u_2 \frac{\partial v}{\partial x_i} = -\frac{\partial p'}{\partial y} + K_m \left(\frac{\partial^2 v}{\partial x_i^2}\right) + f\left(u - u_g\right) - S_v \qquad (3\text{-}7)$$

$$\frac{\partial w}{\partial t} + u_3 \frac{\partial w}{\partial x_i} = -\frac{\partial p'}{\partial z} + K_m \left(\frac{\partial^2 w}{\partial x_i^2}\right) + g\,\frac{\theta\,(z)}{\theta_{\,ref}(z)} - S_w \qquad (3\text{-}8)$$

u_1 , u_2 and u_3 (ms^{-1}) are the wind speed in x, y and z direction. Air is currently treated as an incompressible fluid. Therefore, the continuity equation is:

$$\frac{\partial u}{\partial x} + \frac{\partial v}{\partial y} + \frac{\partial w}{\partial z} = 0 \qquad (3\text{-}9)$$

According to Bruse and Fleer (1998) p' is the local pressure perturbation (P_a).

The friction force is defined as $\frac{\partial^2 u}{\partial x_i^2}$, and multiplied with K_m which means as the local exchange coefficient in Eqs (3-6), (3-7) and (3-8). Referring to the equations that are used in ENVI-met, local source or sink terms for impulse (ms^{-2}) are ($S_{u,}\, S_{v,}\, and S_w$) represent the loss of the wind speed due to the drag forces from the vegetation elements. θ (K) Symbolizes the potential temperature at z height. The reference temperature θ_{ref} should represent the average mesosacle conditions and is provided by a one-dimensional model running parallel to the main model. The nomenclatures u_i and x_i represent to u, v, w and to x, y, z with i=1, 2, 3 respectively (Ali-Toudert, 2005).

3.5.2 Temperature and humidity

The distribution of the potential temperature θ (K) and specific humidity q ($KgKg^{-1}$) inside the atmosphere is given by the combined advection-diffusion equation with internal source/sinks (Bruse and Fleer, 1998):

$$\frac{\partial \theta}{\partial t} + u_i \frac{\partial \theta}{\partial x_i} = K_h \left(\frac{\partial^2 \theta}{\partial x_i^2}\right) + Q_h \qquad (3\text{-}10)$$

$$\frac{\partial q}{\partial t} + u_i \frac{\partial q}{\partial x_i} = K_q \left(\frac{\partial^2 q}{\partial x_i^2}\right) + Q_q \qquad (3\text{-}11)$$

Q_h and Q_q are used to link the heat and the vapor exchange at the plant surface with the atmospheric model. Huttner (2012) illustrated that Q_h is the term that defines the heat exchange between the air and the vegetation and K_h is the turbulent exchange coefficient for heat. Also, he clarified that Q_q defines the exchange of humidity between air and vegetation, and K_q is the turbulent exchange coefficient for the humidity. Huttner (2012)

indicated that ENVI-met does not simulate the phase change between liquid and vapor, and vice versa.

3.5.3 Turbulence and exchange processes

Under windy conditions, the magnitude of the local turbulence production regularly surpasses its dissipation, so the mean flow transports the turbulent eddies. Based on the work of Mellor and Yamada (1975) two further variables are added namely the turbulent kinetic energy k and its dissipation ε. Two additional equations for the local turbulence k ($m^2\ s^{-2}$) and its dissipation rate ε ($m^2\ s^{-3}$) are added to the model (Bruse and Fleer, 1998).

$$\frac{\partial k}{\partial t} + u_i \frac{\partial k}{\partial x_i} = K_k \left(\frac{\partial^2 k}{\partial x_i^2}\right) + P_r - T_h + Q_k - \varepsilon \qquad (3\text{-}12)$$

$$\frac{\partial \varepsilon}{\partial t} + u_i \frac{\partial \varepsilon}{\partial x_i} = K_\varepsilon \left(\frac{\partial^2 \varepsilon}{\partial x_i^2}\right) + c_1 \frac{\varepsilon}{k} P_r - c_3 \frac{\varepsilon}{k} Th - c_2 \frac{\varepsilon^2}{k} + Q_\varepsilon \qquad (3\text{-}13)$$

The terms P_r and T_h describe respectively the production and the dissipation of turbulent energy due to wind and thermal stratification.Q_k and Q_ε are the local source terms for the turbulence production at vegetation.

3.5.4 Radiative heat fluxes

The atmospheric radiation defines the absorption and the emission of the different atmospheric layers. These coefficients depend on the optical thickness of the atmospheric. Five reduction coefficients are defined to describe the modification of the model (Bruse and Fleer, 1998).

$$\sigma_{sw,dir}(z) = \exp(F.LAI^*(z)) \qquad (3\text{-}14)$$

$$\sigma_{sw,dir}(z) = \exp(F.LAI(z, z_p)) \qquad (3\text{-}15)$$

$$\sigma \downarrow_w (z, z_p) = \exp(F.LAI(z, z_p)) \qquad (3\text{-}16)$$

$$\sigma \uparrow_w (0, z) = \exp(F.LAI(0, z)) \qquad (3\text{-}17)$$

$$\sigma_{svf}(z) = 1/360 \sum_{\pi=0}^{360} cos\lambda\,(\pi) \quad (3\text{-}18)$$

LAI^* is defined as the angle of incidence of the incoming sun rays. If the building is found to lie between the point of interest and the sun, $\sigma_{sw,dir}$ is set to zero immediately. (Bruse and Fleer, 1998).

LAI is the Leaf Area Index defined as the one-dimensional vertical leaf area index of the plant from the level z to the top of the plant at z_p or the ground $z = 0$:

$$LAI(z, z + \Delta z) = \int_{z'}^{z'+\Delta z} LAD(z')dz' \quad (3\text{-}19)$$

The coefficient (σ_svf) in the Eq. (3-18) describes the local obstruction by buildings (sky view factor) and ranges from 1 (free sky) to 0 (no sky visible). λ is the maximum shielding angle found by the ray-tracing model in direction π (Bruse and Fleer, 1998).

The shortwave radiation can be summed up as:

$$Q_{sw}(z) = \sigma_{sw,dir}(z)Q^0_{sw,dir} + \sigma_{sw,dif}(z)\sigma_{svf}(z)Q^0_{sw,dif} + \left(1 - \sigma_{svf}(z)\right)Q^0_{sw,dir}.\bar{a} \quad (3\text{-}20)$$

$Q^0_{sw,dir}$ is the short-wave direct radiationThe term $\bar{a}$ denotes as the average albedo of the walls within the model area.

The long wave radiation fluxes can be expressed as:

$$Q^{\downarrow}_{lw}(z) = Q^{\downarrow}_{lw}(z, z_p)Q^{\downarrow,0}_{l,w} + \left(1 - \sigma^{\downarrow}_{lw(0,z)}\right)\epsilon_f \sigma B\bar{T}^4_f + (1 - \sigma_{svf}(z))Q^{\leftrightarrow}_{lw} \quad (3\text{-}21)$$

$$Q^{\uparrow}_{lw}(z) = \sigma^{\uparrow}_{lw}(0, z)\epsilon_s \sigma BT^4_0 + (1 - \sigma^{\uparrow}_{lw}(0, z))\epsilon_f \sigma f\bar{T}^4_{f-} \quad (3\text{-}22)$$

$\bar{T}^4_{f-}$ and $\bar{T}^4_f$ are the average foliage temperature of the underlying, and overlaying of vegetation.

ϵ_s, ϵ_f are the emissivity of the surface and foliage.

T_0 is the surface temperature.

Q_{lw} is the horizontal long wave radiation flux from surrounding walls.

σ_B is the Stefan-Boltzmann constant , σ_B= 5.67.$10^{-8} Wm^{-2}K^{-4}$.

3.5.5 Ground surfaces

Huttner (2012) indicated that the temperature at the ground surface can be calculated from the energy balance:

$$Q_{sw,net} + R_{lw,net}(T_0) - G(T_0) - H(T_0) - LE(T_0,q_0) = 0 \quad (3\text{-}23)$$

$Q_{sw,net}$ is the net short-wave radiation at the surface, $R_{lw,net}$ is the net long-wave radiation at the surface.

G is the soil heat flux, H is the sensible, and LE is the latent turbulent heat flux.

With $R_{sw,dir}(z = 0)$ and $Q_{sw,dif}(z = 0)$ which are the direct and diffuse radiation of the shortwave, the short-wave net flux can be summed as:

$$Q_{sw,net} = (cos\beta^*.Q_{sw,dir}(z = 0))(1 - a_s) \quad (3\text{-}24)$$

β^* is the angle between the surface normal and the incoming radiation. a_s is the surface albedo.

The turbulent flux H and LE are a function of the turbulent coefficients K_h, $K_q$for temperature and the humidity of the ground surface and the lowest atmospheric grid cell (Huttner, 2012):

$$H(T_0) = \rho c_p K_h^0 \frac{T_0 - \theta_{k=1}}{0.5\Delta z_{k=1}} \quad (3\text{-}25)$$

$$LE(T_0,q_0) = \rho L(T_0) K_q^0 \frac{q_0 - q_{k=1}}{0.5\Delta z_{k=1}} \quad (3\text{-}26)$$

The soil heat flux G calculated as:

$$G(T_0) = \lambda_s(k = 1) \frac{T_0 - T_{k=-1}}{0.5\Delta z_{k=-1}} \quad (3\text{-}27)$$

Bruse and Fleer (1998) illustrated that the long-wave net radiation taken into consideration the impact of vegetation and the long-wave fluxes from the buildings and

the reflection of radiation from the buildings and the surface. The concept of the long-wave varies from the formulation for the leaf energy balance. Huttner (2012) indicated that the long-wave energy balance of the ground surface is split into two parts:

$$Q_{lw,net}(T_0) = \sigma_{svf} Q_{lw,net}^{sky}(T_0) + (1 - \sigma_{svf}) Q_{lw,net}^{screened}(T_0) \quad (3\text{-}28)$$

The sky view factor (σ_{svf}) is calculated for the surface level $z = 0$ (Bruse and Fleer, 1998). $Q_{lw,net}^{sky}$ is the long-wave radiation for the part of the sky with the unhindered view, $Q_{lw,net}^{screened}$ is the long-wave radiation for the screened part (vegetation and buildings are block the view) (Huttner, 2012).

3.6 Initial Conditions

The main model is designed in 3D with two horizontal dimensions (x, y) and one vertical dimension (z). The typical elements of the buildings and vegetation are represented inside this main model. Figure (3-6) depicts the schematic of the ENVI-met model layout.

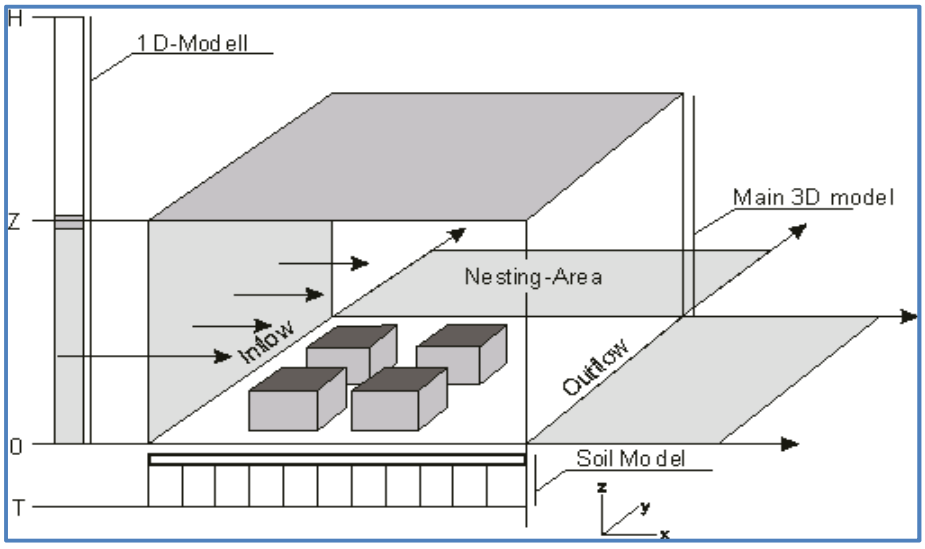

Figure (3-6): The Schematic of the ENVI-met model layout (http://www.envi-met.com/).

The 1D model takes the calculation from the top of the 3D model which is depending on the model layout, normally between 50 and 200 m and the total height of the model at

2500 m. The 1D model provides the vertical profiles of all the model variables (http://www.envi-met.com/).

3.6.1 Initial meteorological conditions

The initial temperature θ_{start} provided as an input parameter at a height 2500 m is set to the whole vertical profile assuming start conditions of neutrality. A vertical gradient forms if the initial surface temperature differs from the initial air temperature. The air humidity profile is linear and is determined by means of input values at 2500 m and the relative humidity at 2 m. Turbulence quantities k and ε are constant at 2500 m and are a function of the local friction velocity u^* (a reference wind velocity applied to motion near the ground where the shearing stress is often assumed to be independent of height and proportional to the square of the mean velocity). The surface temperature and humidity are given by the 3D model as mean values of the nesting area relevant values.

3.6.2 Initial conditions for soil

The surface temperature is calculated to the 1 D model by the soil in the sub-model and is calculated by three input values of soil temperatures and soil humidity. The deep soil temperature (-2.00 m) is kept constant during simulation (http://www.envi-met.com/).

3.7 Nesting Area and the Boundary Conditions

The nesting area is a band of the grid cells surrounding the core of the 3D model as explained in Fig. (3-7). ENVI-met creates an area of the nesting grids around the core model to move the model boundary away from the interested area to minimize undesired boundary effects (http://www.envi-met.com/).

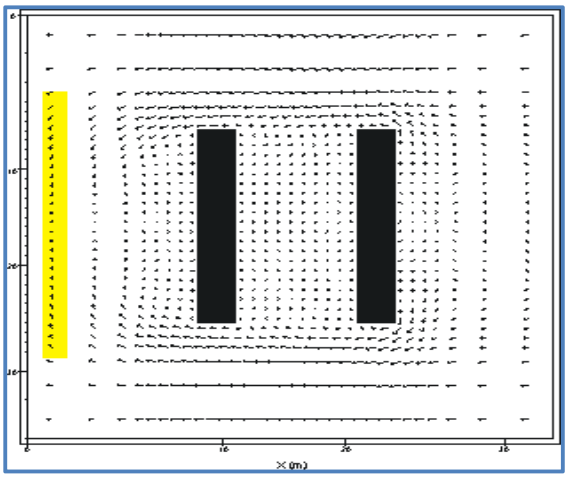

Figure (3-7): Flow around two buildings with 3 nesting grids (http://www.envi-met.com/).

ENVI-met model includes three different types of lateral boundary conditions (Bruse, 2015b):

- Open lateral boundary conditions: The values of the next grid point close to the border are copied to the border each time step.
- Forced lateral boundary conditions: The values of the one-dimensional model are copied to the border.
- Cyclic lateral boundary conditions: The values of the downstream model border are copied to the upstream model border.

The open and the cyclic lateral boundary condition types allow starting the simulations with only a few initial parameters. However, with these lateral conditions it is not possible to recreate specific scenarios, which means it is very difficult to compare the simulation output with a real situation. The forcing method, in contrast, allows reconstructing real scenarios or imaginary scenarios by defining a diurnal cycle of boundary conditions for the various meteorological parameters such as radiation, air temperature or humidity that obtained from measured data or data from the other models (Simon, 2016).

Figure (3-8) illustrates the description of the equations for the boundary conditions. The vertical wind inflow profile up to a height of 2500 m is calculated with the 1 D model by

using a logarithmic law, based on the input values of the horizontal wind (u, v) at 10 m height above ground and the roughness length z_0.

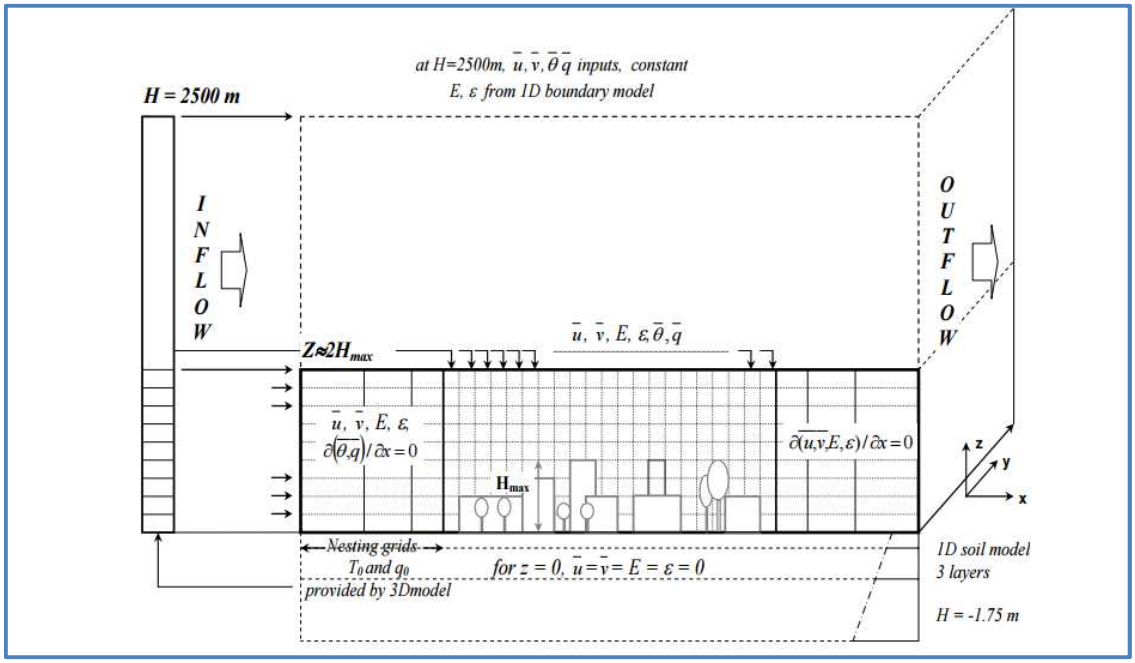

Figure (3-8): General scheme of the ENVI-met model including the boundaries (Ali-Toudert, 2005).

The boundary conditions at the ground surface $z = 0$ and on the walls K and ε are calculated as a function of local friction velocity u^* calculated from the flow components tangential to the surface. The inflow profile and the top boundary are obtained from the one-dimensional model, and a zero-gradient condition is used at outflow boundaries (Bruse and Fleer 1998).

3.8 Reliability of the Simulation Results with ENVI-met

Many researchers attempt to exhibit the precision and the importance of the results of their simulation works with using ENVI-met. Lahme and Bruse (2002) indicated that the results were obtained from the ENVI-met represented the real environment based on a limited set of numerical methods available to describe the magnitude of physical processes in reality. According to Ghaffarianhoseini et al. (2015) they affirmed that the dependability of using ENVI-met for simulating the thermal performance of outdoor

spaces was proved in many studies. These studies indicated that the data measured or observed at local meteorological stations appeared an agreement with the simulated air temperature. Yu and Hien (2006) came to the same conclusion, stating that the ENVI-met simulation endorsed the data generated from the field measurement. Monam and Ruckert (2013) indicated that according to many researchers (Ali-Toudert, 2005), and (Ozkeresteci et al., 2003) ENVI-met results are considered as more precise and reliable compared to other software. According to an investigation study carried out by Ozkeresteci et al. (2003) the descriptive inquiry based on the experimental use of ENVI-met model for linear parks cities in Arizona. The conclusion of this study recommended that ENVI-met can be successfully used insofar as it can become an integrated part of the information system of the city. Also, they concluded that through the adaptive use of such innovative tool like ENVI-met, there is a possibility of progress for urban information systems to serve for sustainable environments.

3.9 UHI Researches with ENVI-met

Many Researchers are using ENVI-met software for developing the models to verify the effect of the Urban Heat Island. Huttner et al. (2008) investigated the effects of global warming on the heat stress by using ENVI-met in central European cities. They recommended that the green spaces consider an important factor to improve the human thermal comfort.

Hedquist et al. (2009) used ENVI-met as well as CFD modeling of CBD to interpret the local flow modifications due to the UHI diurnal cycle. They indicated that ENVI-met model inputs were further improvements and made more accurate by the use of free tools, as well as by identifying the trees, vegetation, and building materials in the particular area. Results from this study explained that the dynamics of the UHI within the built environment also suggested the solutions to mitigate heat and increase outdoor thermal comfort in hot, arid cities. According to Yang et al. (2012) they proposed a method for the quantitative analysis of building energy performance for an urban context by linking the microclimate model ENVI-met to the building energy simulation (BES) program Energy Plus. Figure (3-9) depicts Energy plus model and ENVI-met model. Results

revealed that the method is capable of quantifying the effects of various microclimatic factors on building energy performance under any given urban contexts. The method could be useful for urban planning and building design.

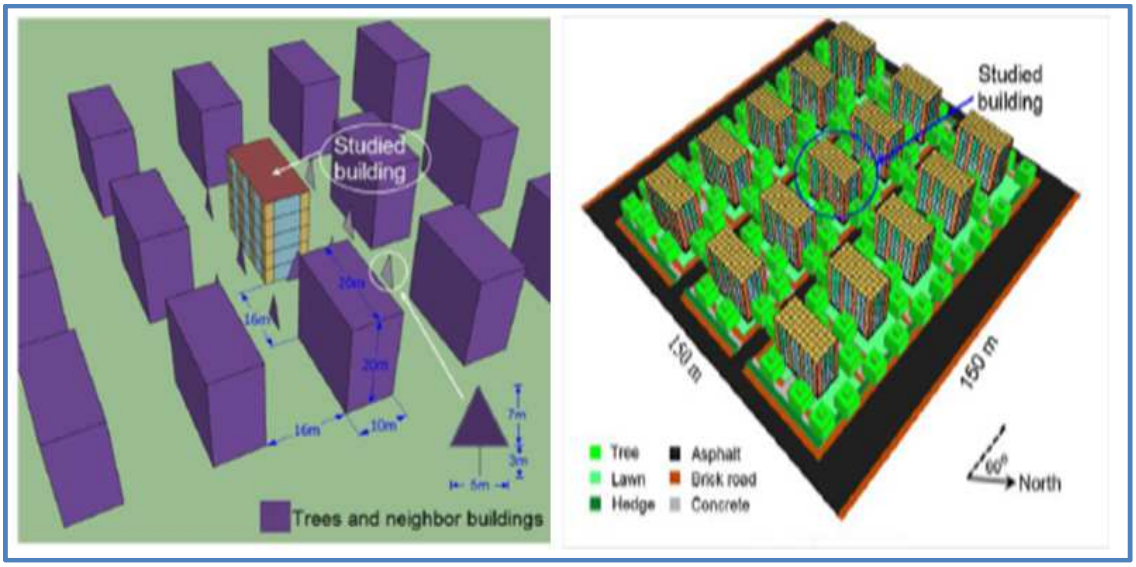

Figure (3-9): Energy plus model and ENVI-met model (Yang et al., 2012).

The aspect ratio was studied by using ENVI-met for two different street orientations in Fortaleza. The results showed that optimal aspect ratio could be higher than 1.5 due to increased shading from buildings (Dardel, 2015). In a recent study presented by Maleki and Mahdavi (2016) they used ENVI-met to simulate microclimate conditions in a part of the city of Vienna. This study focused on investigating the effects of the variation of physical and geometrical properties of the urban area (cool roofs, green lands, and perviousness of paving materials) on the urban micro-climate and outdoor thermal comfort. The results suggested the modifications within the urban canopy were more effective in influencing the microclimate conditions than those implemented to the roof levels. Increasing the amount of vegetation and permeable pavements can cool the air temperature down by up to 3 K.

CHAPTER FOUR

SIMULATION RESULTS FOR TWO DISTRICTS IN BAGHDAD AND THE EFFECT OF THE SHADINGS PATTERN AND GREENERY STRATEGIES ON THE OUTDOOR THERMAL COMFORT

4.1 Introduction

In this chapter we look for a better understanding on how vegetation and shading patterns help reducing the effect of UHI and improving the pedestrians outdoor thermal comfort. The usual approach consists of increasing the city permeability to facilitate heat exchanges and therefore the cooling of city. How does it work in an arid climate? What lessons do we learn from choices consisting in importing Western cities practices to such environment? We intend to observe the impact of architectural choices on the main outdoor comfort indicators. We compare an old district built according to ancestral customs to a typical western-type neighborhood made of several high-rise buildings. Not only is the urban fabric different but also are the material choices. Next, we envisage mitigation strategies to provide more outdoor thermal comfort to pedestrians. The results of this work will be discussed in the form of recommendations design for the urban area in the hot and arid climates which are intended to help in further defining improved UHI mitigation strategies and enhancing the pedestrian comfort.

4.2 Criteria for Selecting the Study Area

We look for a district classified as historical and heritage and another one considered as built as a modern design. The criteria deal with the design, plan, materials, structural and constructional systems, and the ornamentation details which are particularly pertinent to heritage buildings. Some buildings stand out as excellent examples of art and architecture, while others exhibit a particular style or a structural innovation. As far as Baghdad is concerned, the traditional houses are scarce, and these traditional houses are threatened with extinction. Figure (4-1) depicts Al-Rasheed Street which is considered as the most vital and oldest street in Baghdad with heritage houses and traditional buildings. Heritage houses serve to a positive historical legacy, and as such, they are considerably helpful to historians and architectural conservationists. The high rise buildings in Baghdad are concentrated on Haifa Street as shown in Fig. (4-2).

Figure (4-1): Al-Rasheed Street (http://www.google.com).

Figure (4-2): Haifa Street (http://www.google.com).

4.3 The Selected Study Area

Baghdad the capital of Iraq, is located in the central part of the country on both sides of the Tigris River, it lies at latitude 43 East and longitude 34 North as shown in Fig. (4-3). The climate of the Baghdad is defined as a semiarid, subtropical and continental, with dry, hot in summer, and cool winters. The recorded maximum temperature was 50 ℃ in the summer of 2010, which considers the hottest days in summer in the hottest year in Iraq (Hassoon, 2015). The area of Baghdad covers 4555Km^2, which represented 1.047% from the total area of Iraq. The population density of Baghdad city reaches to 5233 (prs) /km^2.

Figure (4-3): Iraq map and the location of Baghdad city (http://www.worldatlas.com/).

Hence, two representative areas in Baghdad will be assessed and used as case studies, Fig. (4-4). These two areas are different in their location, buildings materials, height of buildings, and style design. The two districts occupy the same area.

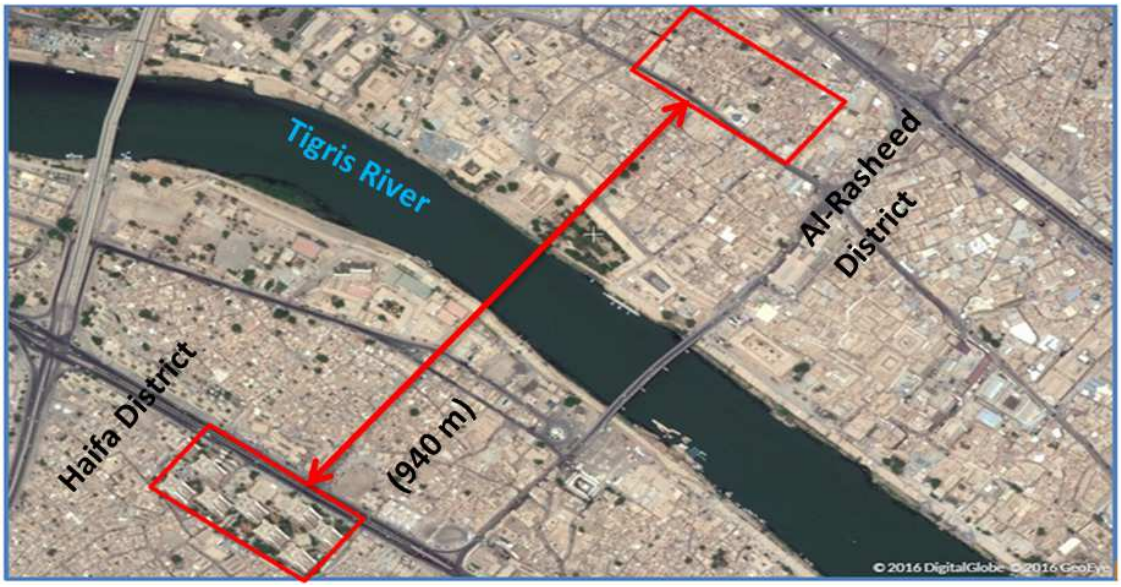

Figure (4-4): Location of the two districts (www.eartflash.com).

4.3.1 Haifa street district

The first selected area is Haifa Street which contains nine buildings constructed in 1984 (Alousi, 1985). The height of the buildings is 60m, distances between the buildings are 30 m, and 35 m in some places. Haifa Street is one of the famous and vitality streets in the Karkh district. The chosen area is 48750 m^2 as shown in Figs. (4-5) and (4-6).

Figure (4-5): Haifa Street District (http://www.google.com).

Figure (4-6): 3D satellite image for Haifa Street District (http://www.flashearth.com).

The material used in construction in Haifa Street is precast concrete. According to an investigation study by Qasim (2015) Haifa Street represents a new urban style for Baghdad.

4.3.2 Al-Rasheed street district

Al-Rasheed Street was established in 1918. The colonnaded pavements and the decorative buildings from 1930 make it the most attractive and exciting street in Baghdad. All the traditional houses in Al-Rasheed Street are planned around an open central courtyard. The courtyard represents the essential element contributing improving the environment of the severely hot climate conditions in summer (Bianca et al., 1984). Bricks were used in construction houses for the walls and roofs. The alleyways are small and narrow (3 m in width) linking the houses each to others. Asphalt pavement was used for these alleyways. Old builders used local materials (bricks, gypsum) they realized that these materials contributed as the main factor to confront the hot, dry weather in summer and coldness in winter. Houses in Al-Rasheed district have an area 150m^2. The width of the courtyard is 5m, and the length is 7m, the width of the house is 15 m, and the length is 10 m, the typical height is 8m. The courtyard represents the focal element, and it has been used over the past several centuries. An over-riding consideration in the design of such houses was privacy. The courtyards provided not only privacy, but it also evolved as a response to the severe hot and dry climatic conditions. In addition to using it as a general working space, and acted as an effective temperature regulator, cooling the house during daytime, Fig. (4-7). Taleghani et al. (2012) indicated that the courtyard building typically contains an open space that is surrounded by rooms or walls, this spatial structure provides an isolated space and often acts as a source of light, fresh air movement, and heat. There is a typical section of a traditional alleyway in the whole system of the traditional houses which is long and highly in the overall proportion which helps to provide almost continuous shade for pedestrians throughout the year. Figure (4-8) depicts the alleyway in the old heritage design houses. We can observe in the same figure Mashrabiya (oriel window) is the continuation of the built area on the first floor along opposite sides of the alleyway, which provides natural lighting and ventilation (Agha, 2015). We also show the corresponding district in Fig. (4-9).

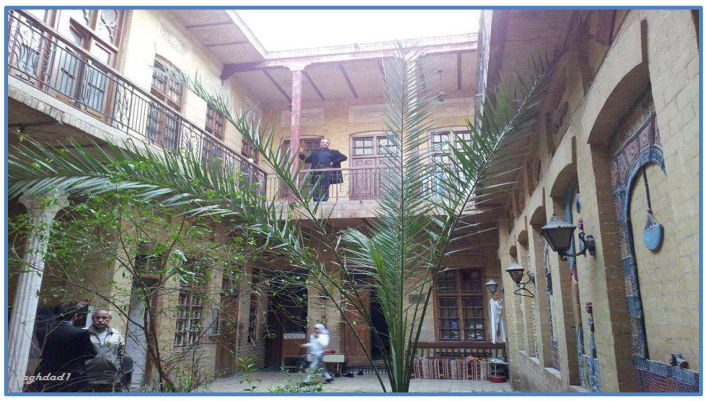

Figure (4-7) The courtyards in the heritage houses in Al-Rasheed Street (Al-Ani, 2011).

Figure (4-8): Sketch of an alleyway in old design houses districts (Al-Ani, 2011).

Figure (4-9): Al-Rasheed Street district area. (http://www.flashearth.com).

Heritage buildings that predate the development of construction typically had some inherent capability to moderate the external influences on interior conditions. In these older structures, the building itself had a ventilation system for the human thermal comfort. The hydrothermal performance of these buildings relied on construction materials, thermal mass, moisture buffering, landscape, interior spaces, and the courtyards (Henry, 2007). Figure (4-10) depicts a section of the heritage house in Baghdad showing the shape and location of courtyards.

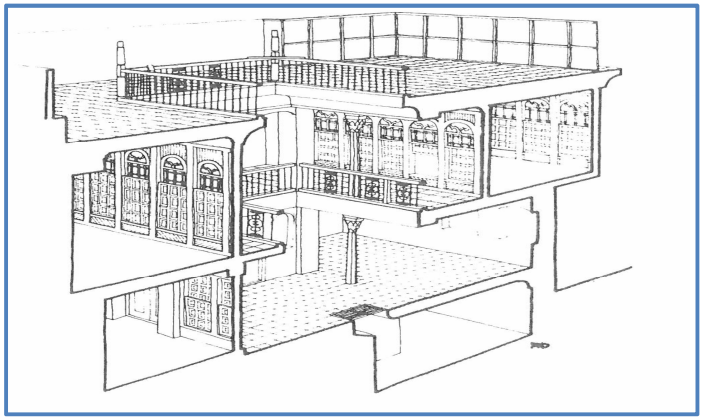

Figure (4 -10): The essential form of the Baghdadi house (Bianca et al., 1984).

4.4 Input Data for the Model

The weather data used to initiate the simulation models were provided by the Iraqi Meteorological Organization and Seismology. The microclimate characteristics represent the air temperature and relative humidity of the hottest summer day in Baghdad city (12th of July 2010, Hassoon, 2015)). The basic meteorology settings for the initial conditions were 5 m/s for the wind velocity and 315 deg. for the wind direction. The simple forcing for the air temperature and the relative humidity are used along one day period, with a minimum air temperature of 35 ℃ at 6 am and a maximum value of 50 ℃ at 4 pm. The relative humidity was minimum (24%) at 4 pm, and it was maximum at 7 am (36%). The total simulation time was 24 hours. The modelled area has the following dimensions: 325×150 m^2. The model area for Haifa Street has been rendered with grid size 130 cells

along the x axis, 60 cells along the y axis and 20 cells along the z axis. The size of a grid cell was: dx= 2.5m, dy =2.5m and dz=5m. The model was rotated of 57° according to the location of the buildings to the main North direction, Fig (4-11). For Al-Rasheed Street, the model area was made of a grid size of 130, 150, and 20 cells respectively along the x, y, and z axis. The size of the cell was: dx= 2.5m, dy =1.0 m and dz=5m. The model was rotated of 45° according to the location of the buildings to the main North direction, Fig. (4-12).

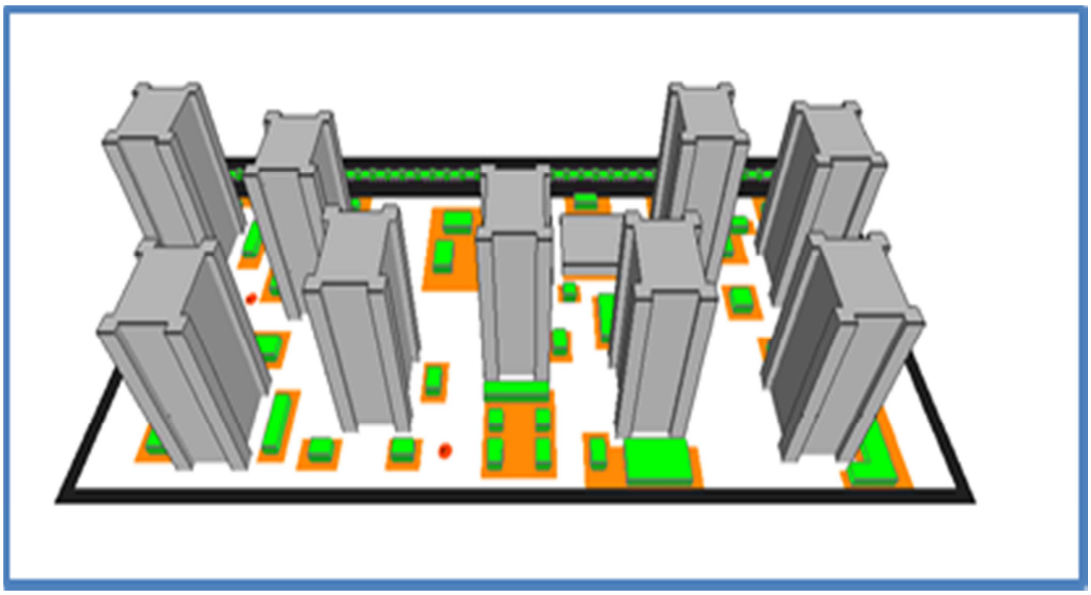

Figure (4-11): Perspective view of the Haifa Street.

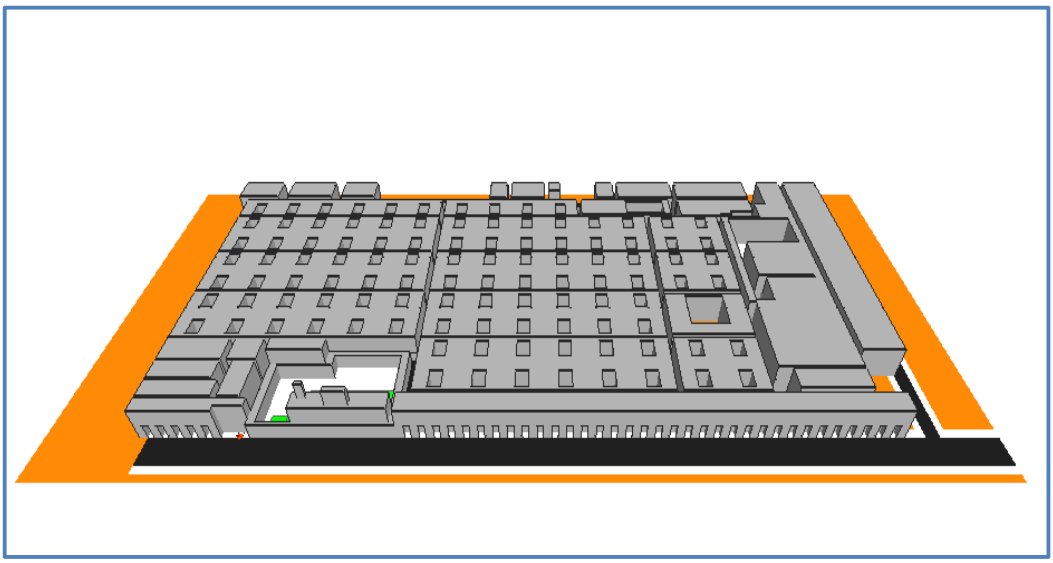

Figure (4-12): Perspective view of the Al-Rasheed Street.

4.5 Analysis of the Simulation Results for the Base Models of the two Districts

4.5.1 Interdependence between ENVI-met results and the data measured

Six receptors were placed in the Haifa Street district as shown in Fig. (4-13), while 8 receptors were located in the Al-Rasheed neighbourhood because Al-Rasheed Street contains more architectural details, Fig. (4-14). Receptors are selected points inside the model area, where atmospheric and soil data can be monitored. Receptors are used to obtain the air temperature, wind speed, mean radiant temperature, relative humidity, specific humidity, and sky view factor.

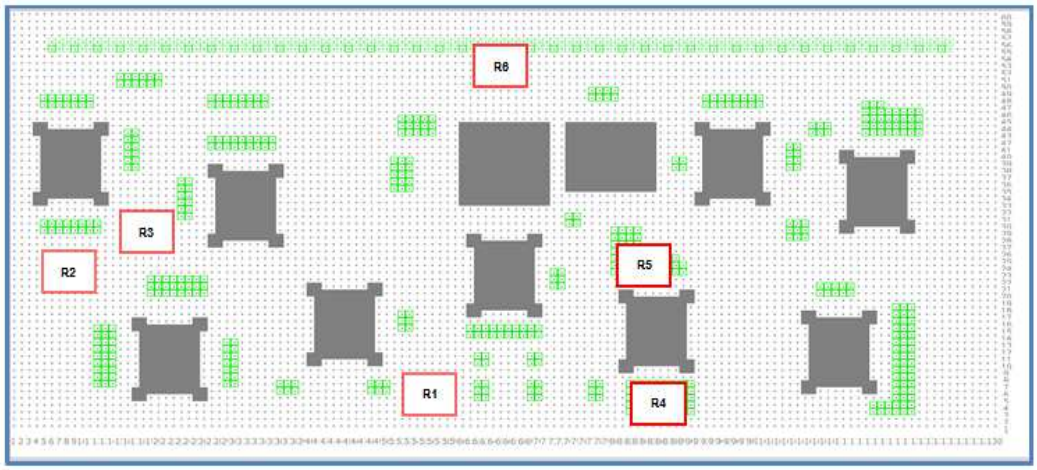

Figure (4-13): Location of the six receptors for Haifa Street.

Figure (4-14): Location of the eight receptors for Al-Rasheed Street.

Figures (4-15) and (4-16) show a comparison between the results of air temperature at 1.5 m above the ground and measures acquired from the Iraqi Meteorological Organization and Seismology. The simulation outputs are quite consistent with the experimental measurements. Note that the temperatures are very similar. According to Wang and Akbari (2014) the simulation of ENVI-met has been done for the cloud-free sky conditions without regard to the actual cloud cover which could lead to lower temperature comparing with the clouded sky.

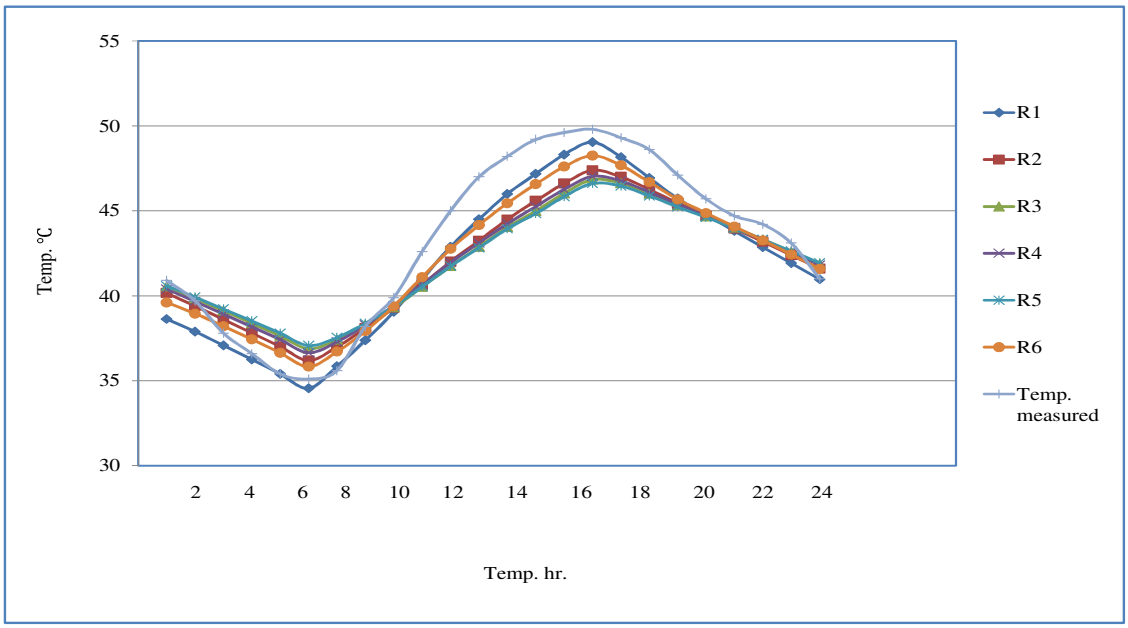

Figure (4-15): Simulation results of air temperature and experimental results for Haifa Street.

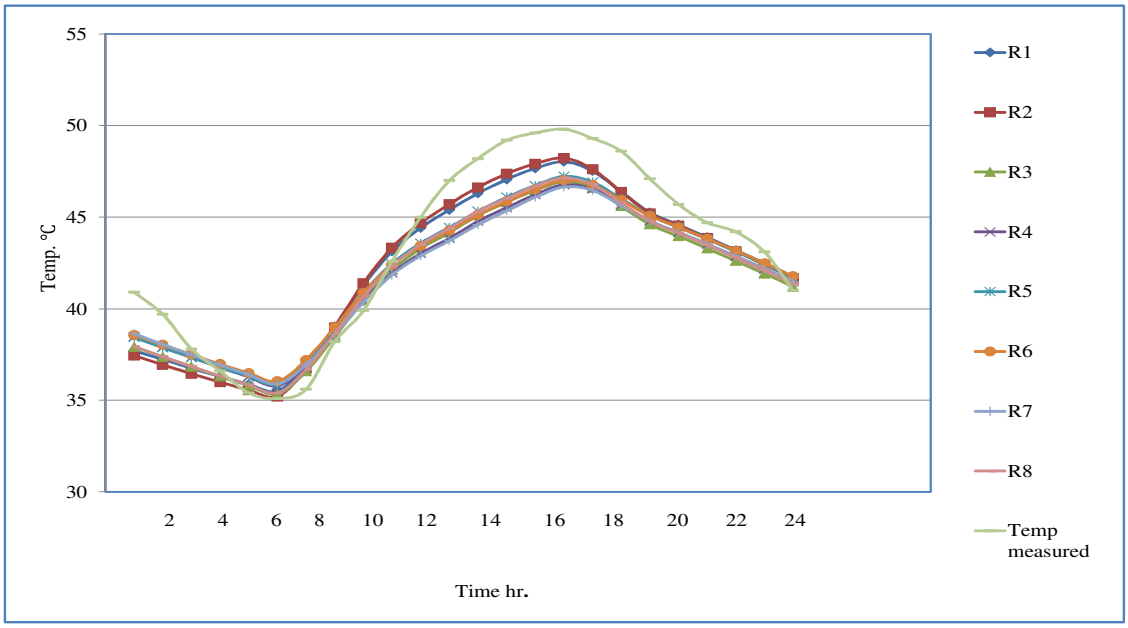

Figure (4-16): Simulation results of air temperature and experimental results for Al-Rasheed Street.

It can be noted that at 6 a.m the measured temperature is equal to 35℃, and almost all the receptors give the same value. It seems that there is a difference between the temperature measured and the modelled temperatures between midday until 10 p.m. The reason can be attributed largely to the shadows in some area because of the effect of tall buildings in Haifa Street, as well as to the existence of the shadings because of the presence of the narrow alleyways in Al- Rasheed district. The highest temperature measured was 50℃ , it be observed that all the receptors were close to approaching this value around 4pm.

4.5.1.1 Air temperature results

The distribution of air temperatures for the two districts was plotted at daytime at noon when the sun is high above the head. The hour to represent the distribution of air temperature at night was picked according to Oke (1981,1987) who indicated that the effect of the Urban Heat Island is the strongest around 3-5 h after sunset. The sunset in Baghdad in July 2010 started from 7:14 p.m. Hence, we selected 10 p.m assuming that the Urban Heat Island phenomenon could occur.

(http://www.timeanddate.com/sun/iraq/baghdad).

The results are presented in Figs (4-17) and (4-18) for the two districts at noon, 1.5 m above the ground. Figures (4-19) and (4-20) depict the air temperature distribution at night, 1.5 m above the ground. The results of air temperatures at noon indicate that the maximum temperatures were 45.33 ℃ for Haifa Street and 45.86 ℃ for Al-Rasheed Street. The minimum temperatures were 43.03 ℃ for Haifa Street and for Al-Rasheed Street 43.31℃.

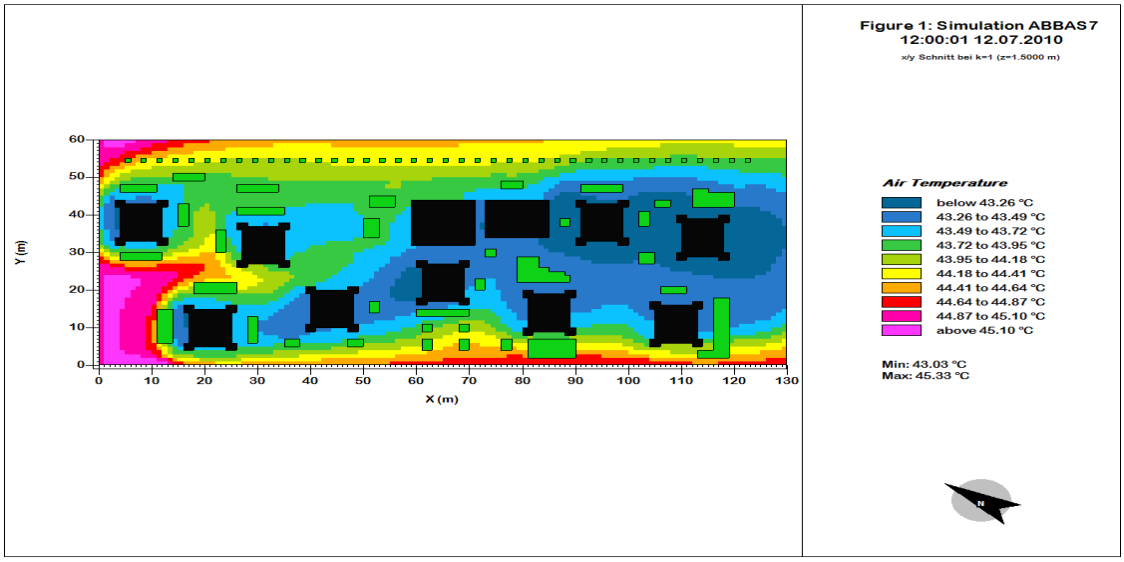

Figure (4-17): Air temperature distribution for Haifa Street at noon, at 1.5 m above the ground.

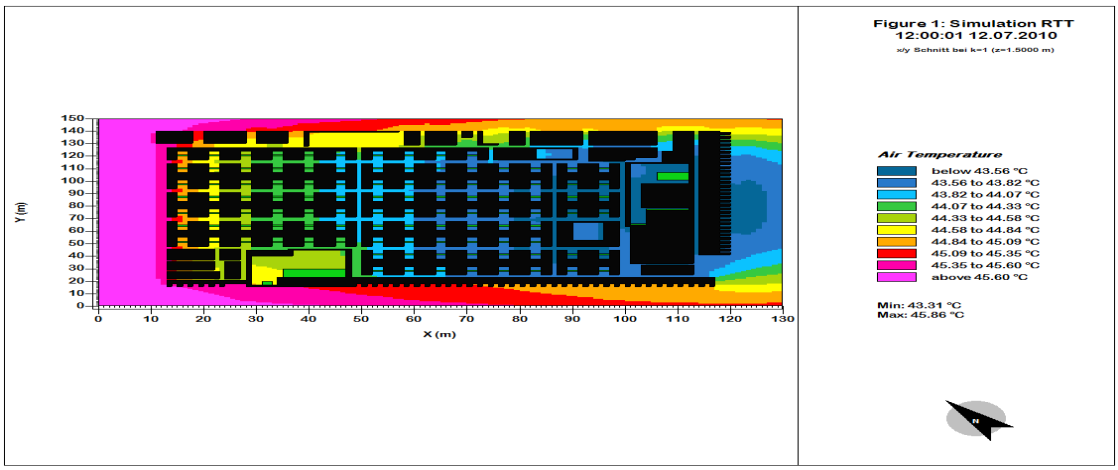

Figure (4-18): Air temperature distribution for Al-Rasheed Street at noon, at 1.5 m above the ground.

The distribution of air temperatures at night for the two districts is shown in Figs (4-19) and (4-20). Figure (4-19) reveals that we have obtained a slight decrease in temperature in Haifa Street compared with the air temperature at daytime. The decrease for Haifa

Street is 1.69℃. Ground surfaces and the buildings surfaces of Haifa Street are composed of a high percentage of non-reflective and water-resistant construction materials. As a consequence, they tend to absorb a significant proportion of the radiation, and release heat at night. Vegetation intercepts radiation and produces shading that contributes to reducing the urban heat release at night. The decrease of vegetated areas in Haifa Street inhibits atmospheric cooling due to the horizontal air circulation generated by the temperature gradient between vegetation and buildings.

Al-Rasheed Street at night experiences a decrease in temperature of 2.55 ℃. We observe that the courtyards in the traditional houses play a vital role in the cooling system. At night the courtyards lose heat by outgoing radiation to the sky, and movement of air during night time (Al-Azzawi, 2010). Also, the Mashrabiya provide shading and obstruct the passage of long-wave radiation between the houses, walls, the ground and the sky, reducing the heat absorption at day time.

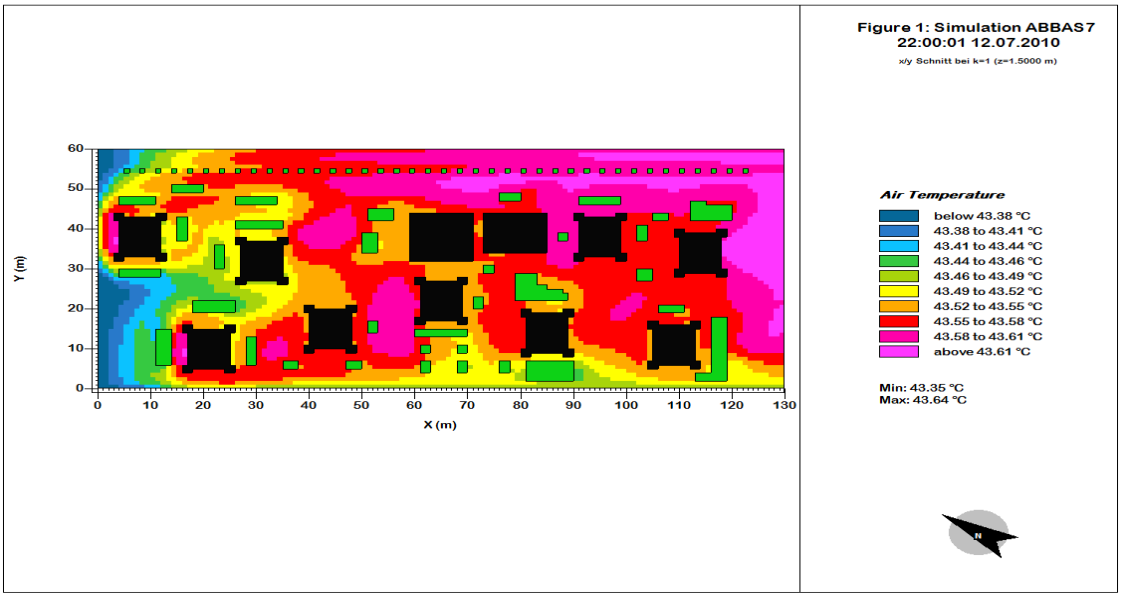

Figure (4-19): Air temperature distribution for Haifa Street at night, at 1.5 m above the ground.

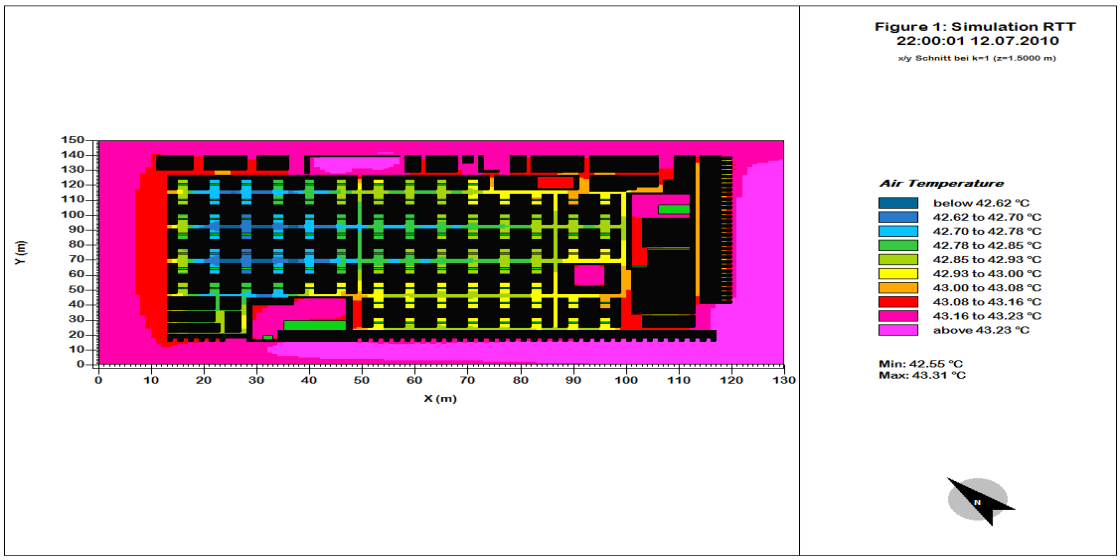

Figure (4-20): Air temperature distribution for Al-Rasheed Street at night, at 1.5 m above the ground.

Figure (4-21) represents the percentage of the district area at 1.5 m above the ground below 43 ℃, between 43 ℃ and 45 ℃, and above 45 ℃. We observe that Al-Rasheed Street is cooler than Haifa Street: the percentage of the temperature less than 43 ℃ for Al-Rasheed Street is more than 40%, while for Haifa Street it ranges to 12%. We indicate from the results in Fig. (4-21) that Haifa Street is hotter than Al-Rasheed Street at noon because the percentage value of air temperature between 43 ℃ and 45 ℃ is more than 80%, while for Al-Rasheed Street it is 33%.

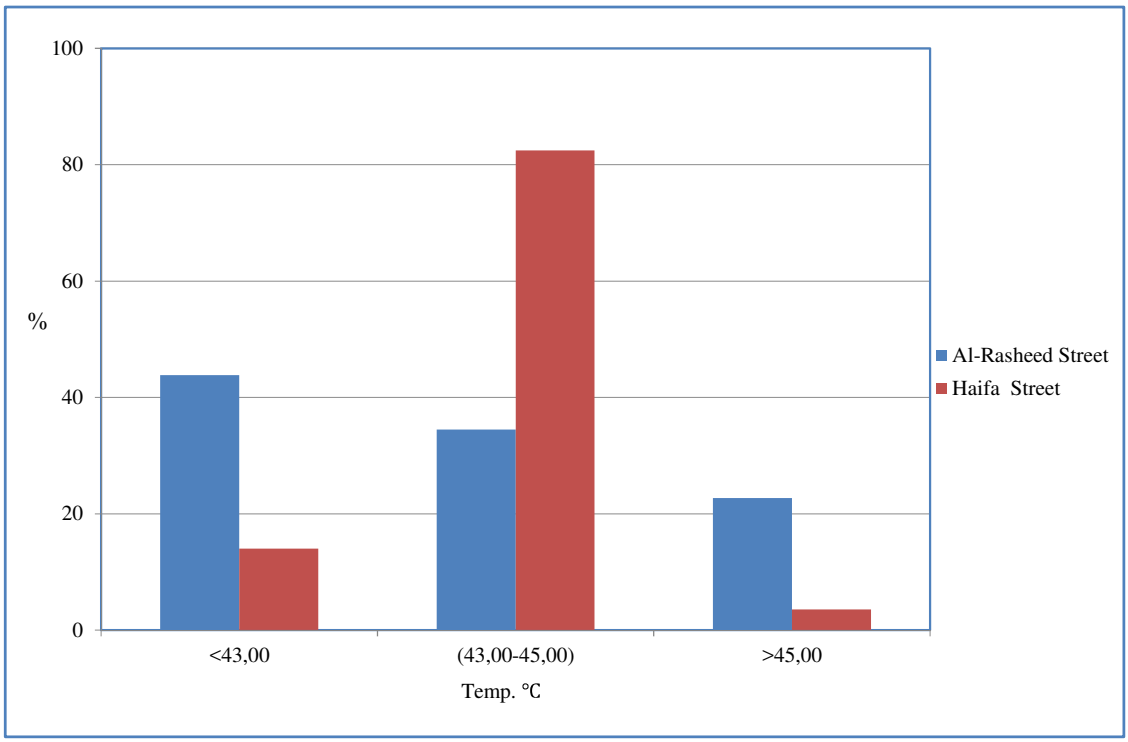

Figure (4-21) Percentage values of air temperature for the two districts at noon, at 1.5 m above the ground.

Figure (4-22) is equivalent to Fig. (4-21) at night. The air temperature in Haifa Street is consistently higher than the air temperature in Al-Rasheed Street. Higher temperatures in Haifa Street occur because of the dense concentrations of materials like asphalt and concrete in buildings. These materials absorb heat during the day and release it slowly at night. It is the contrary for Al-Rasheed Street which construction materials absorb heat slowly and reflect the radiation at day time. According to many researchers, UHI usually reaches its highest intensity after sunset, when the urban surfaces have sufficiently warmed-up. Consequently, the urban area with high rise buildings exhibits temperatures several degrees higher than the surroundings area at night showing the effect of UHI.

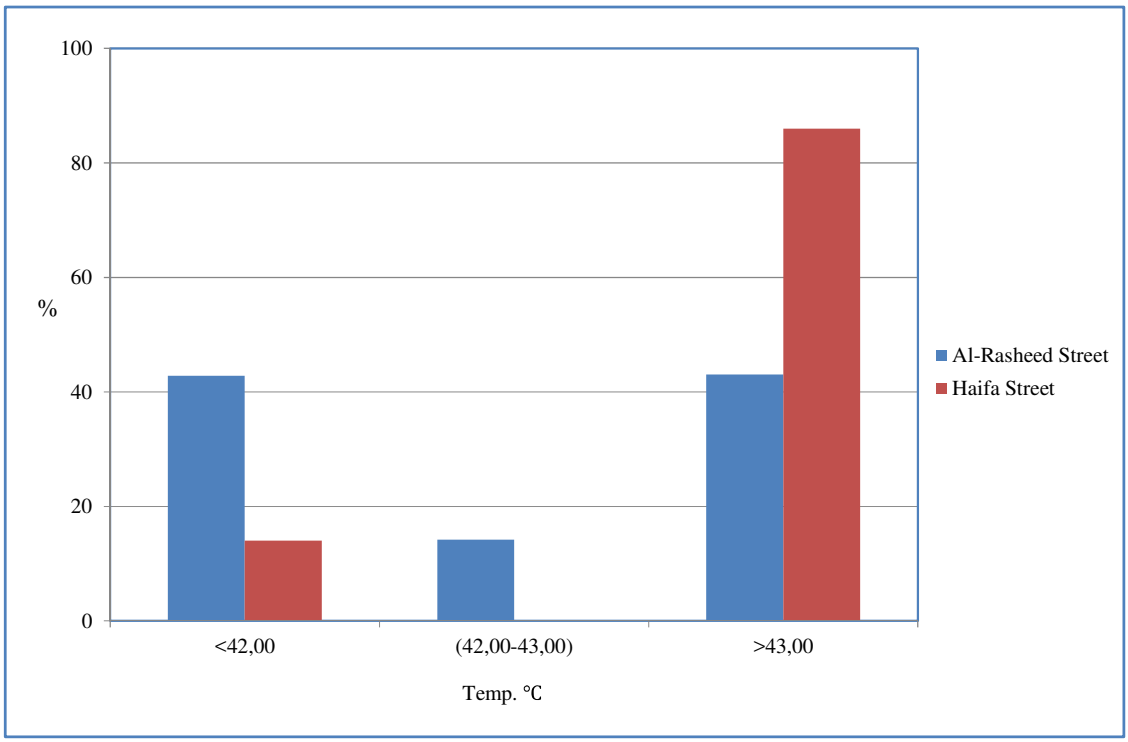

Figure (4-22) Percentage values of air temperature for the two districts at night, at 1.5 m above the ground.

4.5.1.2 Wind speed results

Figure (4-23) presents the results of wind speed obtained from the receptors in Haifa Street. The maximum values of wind speed are recorded by the receptors 3 and 2. According Fig. (4-13) the receptors are located in an open area without any buildings or obstacles that could lead to limiting the air movement, so the velocity is close to the initial value (5 m/s). The lowest value of wind speed was recorded for the receptors 4 and 5, because these receptors have been imposed inside vegetation. Figure (4-24) shows the wind speed values in Al-Rasheed Street area where 8 receptors were placed. We observe that values of wind speed do not exceed 2m/s, due to the existence of narrow alleys.

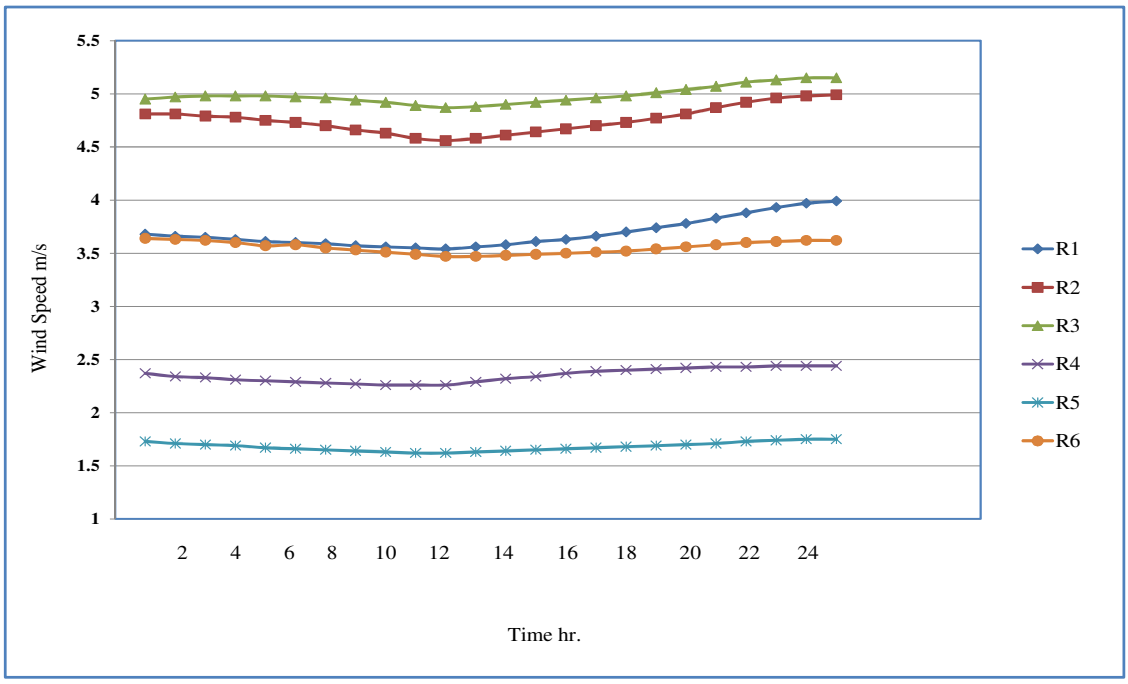

Figure (4-23): Wind speed values for Haifa Street, at 1.5 m above the ground.

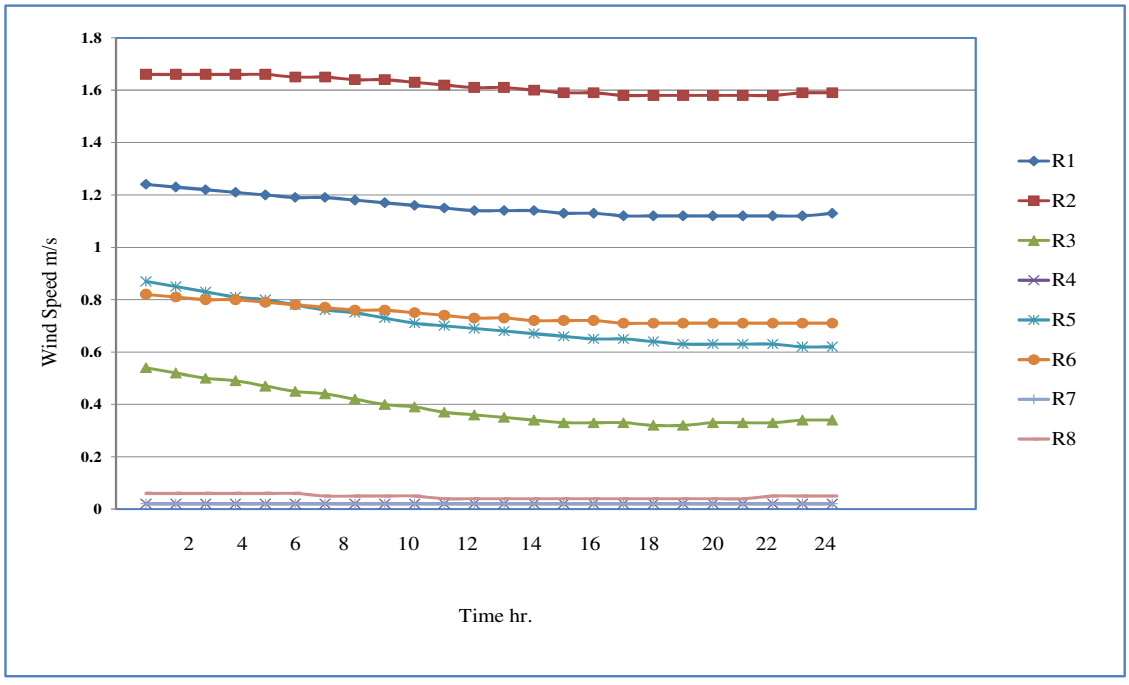

Figure (4-24): Wind speed distribution for Al-Rasheed Street, 1.5m above the ground.

A comprehensive comparison has been conducted on a horizontal plane on the wind speed values for the two districts Figs. (4-25) and (4-26) represent the proportion of wind speed, 1.5 above the ground at day time and night respectively for the two districts. Figure (4-25) reveals that at noon the wind speed less than 0.4 m/s represents 60% of Al-Rasheed Street districts while for Haifa Street it is less than 20%. Higher wind speed can be observed at noon (more than 4 m/s) in Haifa Street. Similar behaviour is observed at night, Fig. (4.26).

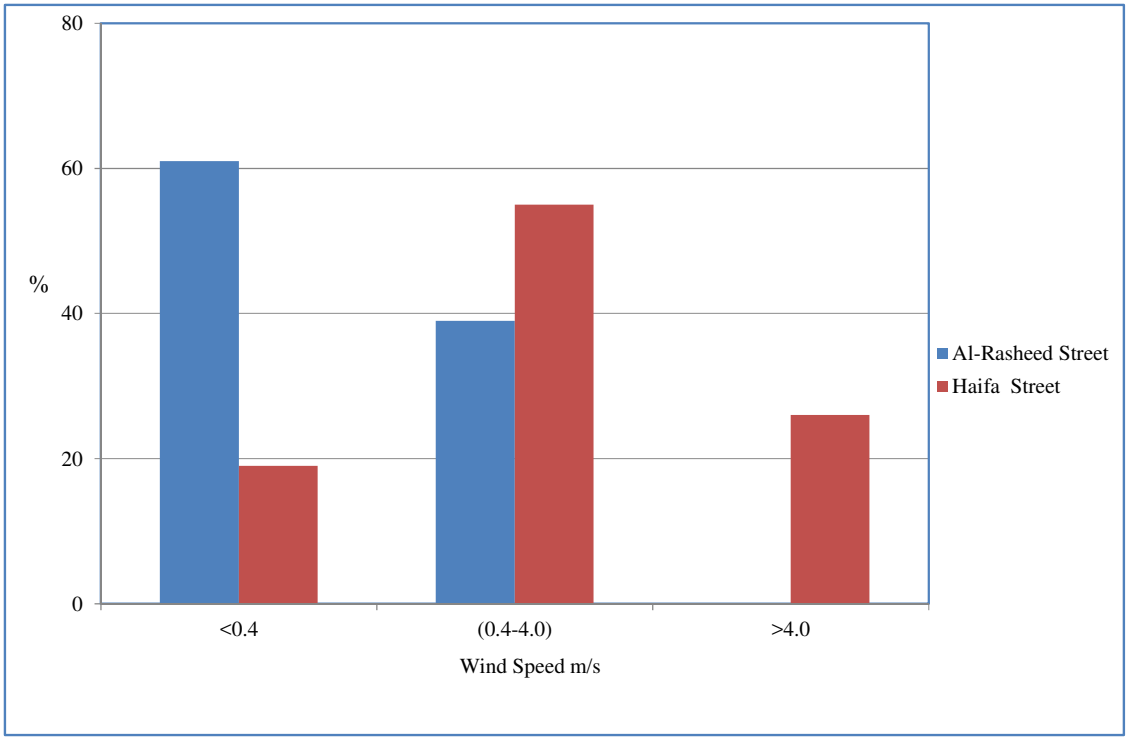

Figure (4-25) Percentage values of wind speed for the two districts at noon, at 1.5 m above the ground.

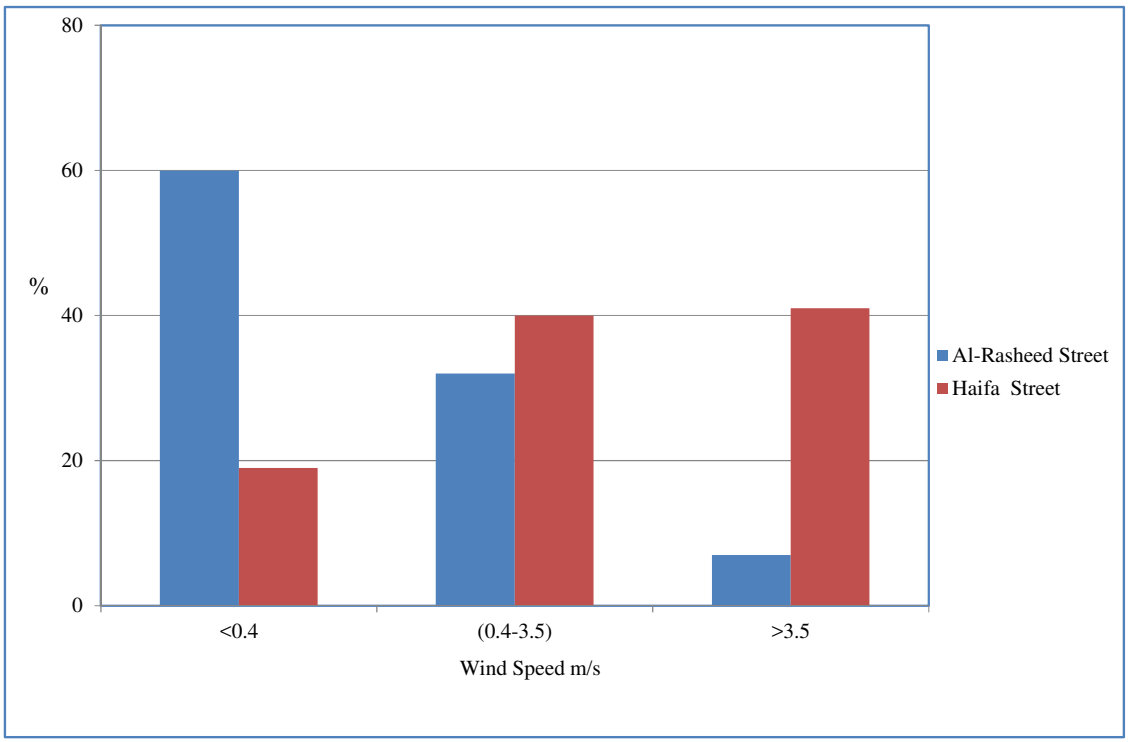

Figure (4-26) Percentage values of wind speed for the two districts at night, at 1.5 m above the ground.

4.5.2 The Results of the outdoor thermal comfort indices

The outdoor thermal comfort indices values that have been calculated in the simulation work are represented at level 1.5 m above the ground. The mean radiant temperature values calculated in ENVI-met take into account the radiation absorbed by a standing human body. We measured the outdoor thermal comfort indices Tmrt, PET, PMV at noon.

4.5.2.1 Mean radiant temperature results

Figures (4-27) and (4-28) show the mean radiant temperature distribution Tmrt at noon in Haifa and Al-Rasheed Street respectively. Shadows from both the buildings and vegetation, is the most effective measure to reduce the maximum values of Tmrt. Regarding Haifa Street we observe that the lack of vegetation and the scarcity of shadow

contribute to increase the values of Tmrt. Concerning Al-Rasheed Street we find that the presence of the oriel window within the narrow alleys creates adequate shadow, which leads to reduce the values of Tmrt. In addition, the courtyards inside the house provide sufficient shading thanks to the trees.

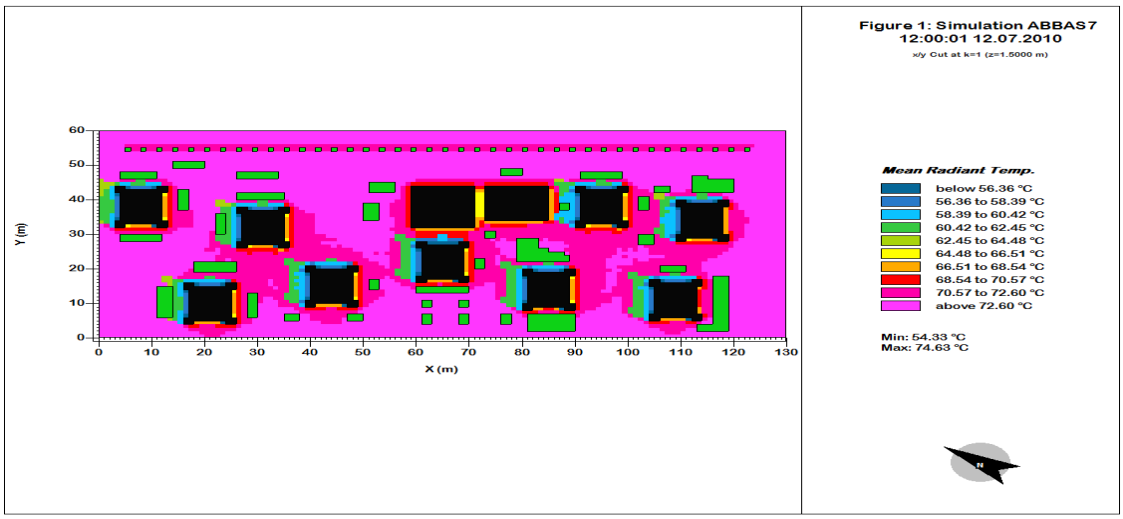

Figure (4-27): Mean radiant temperature distribution for Haifa Street at noon, at 1.5 m above the ground.

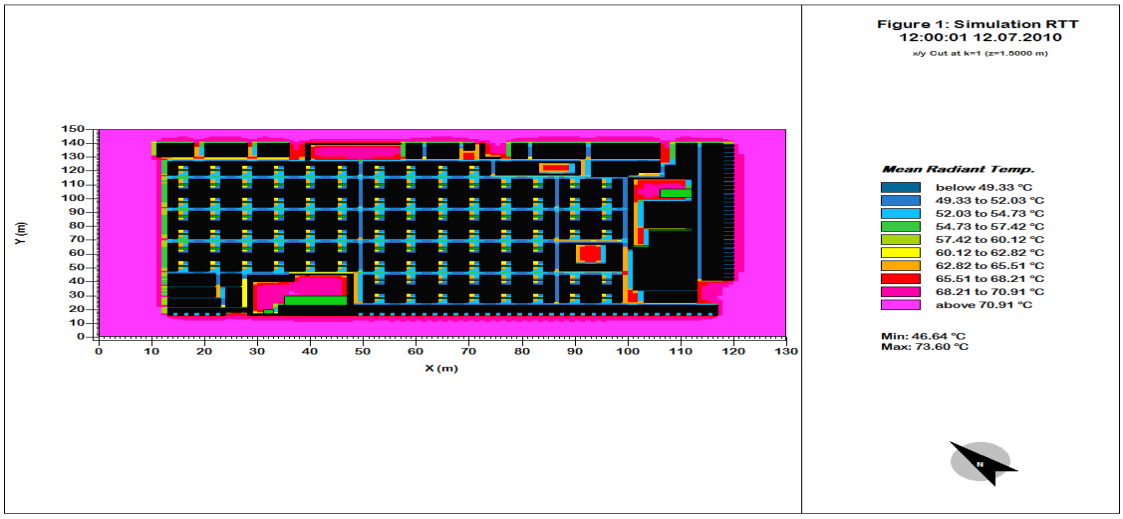

Figure (4-28): Mean radiant temperature distribution for Al-Rasheed Street at noon, at 1.5 m above the ground.

According to Mostafa and Aliriza (2012) there is a relatively strong relationship between the sky view factor and the mean radiant temperature during day time. Shading is one of the restricted factors of thermal stress as it reduces the convective heat transfer from the sunlit building and the ground surfaces (Spronken-Smith and Oke, 1999). Shading also reduces direct shortwave radiation reaching the construction and ground surfaces as well as humans. Figures (4-29) and (4-30) represent the distribution of the sky view factor at noon for the two districts. Table (4-1) compares the sky view factor obtained from ENVI-met and the theoretical formula proposed by Oke (1981). The obtained results are in good agreement.

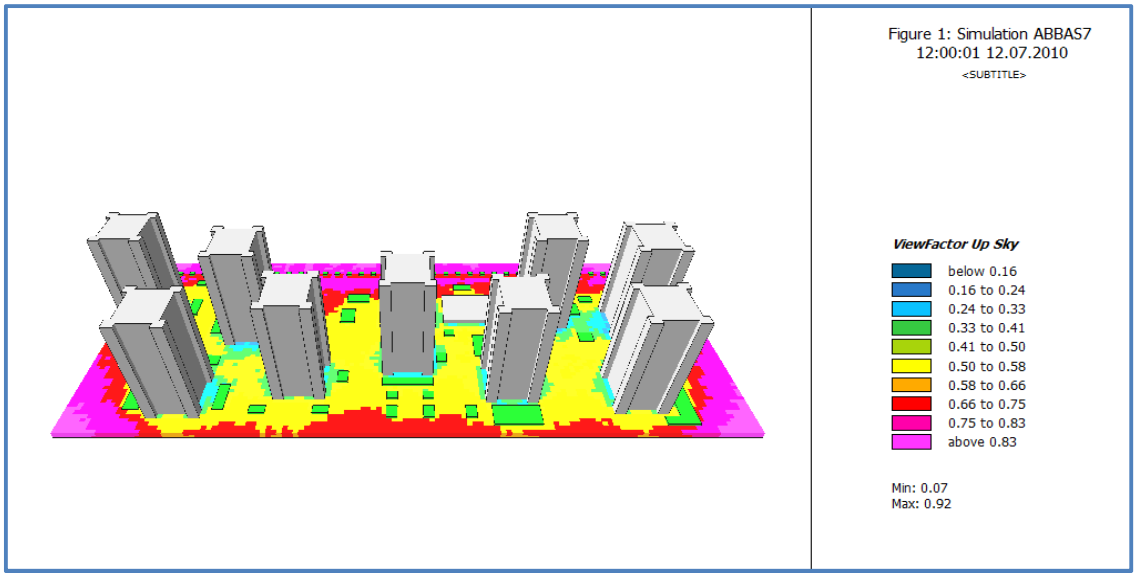

Figure (4-29): Distribution of the sky view factor value for Haifa Street at noon, at 1.5 m above the ground.

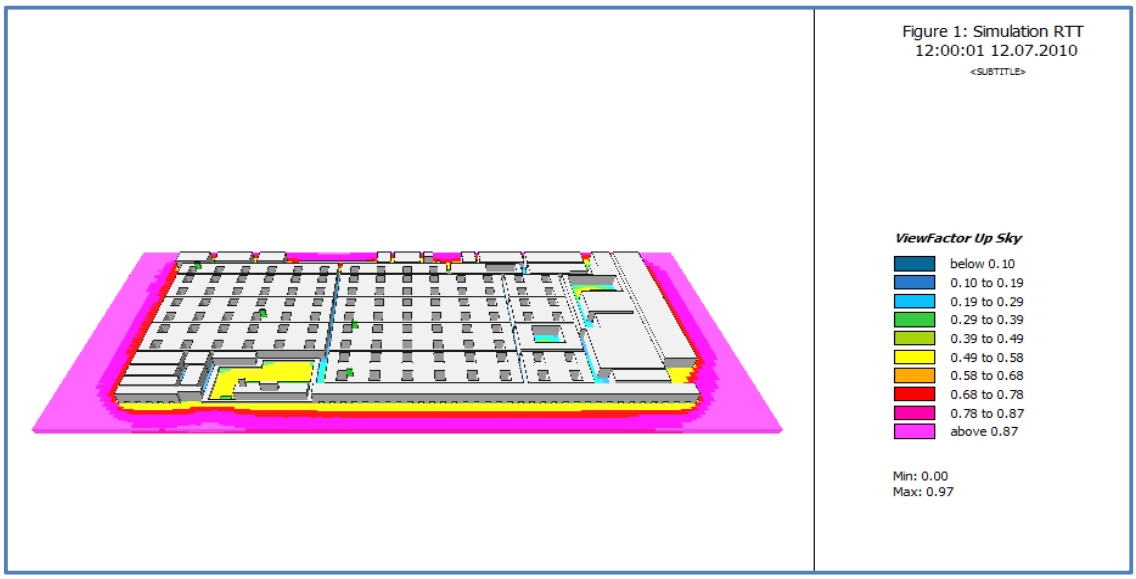

Figure (4-30): Distribution of the sky view factor value for Al-Rasheed Street at noon, at 1.5 m above the ground.

Table (4-1): Comparison of sky view factor values between Oke formula and ENVI-met.

District	H (m)	D(m)	Oke Formula $\psi_{sky} = cos[tan^{-1}(H/D)]$	SVF the simulated value by ENVI-met
Haifa	60	35	0.504	0.50-0.58
Al-Rasheed	8	3	0.351	0.29-0.39

The narrow alleyways and the presence of oriel window contribute to reducing the value of the sky view factor, which leads to decrease the values of Tmrt. In Haifa Street, we find that the sky view factor is about 0.5: the distance between buildings enhances the exposure to sunlight, especially at noon. The highest values of Tmrt were recorded in Haifa Street. That can be explained by the high level of direct and reflected shortwave radiation as well as long wave radiation emitted from the surrounding sunlit surfaces.

4.5.2.2 The Physiological Equivalent Temperature (PET) results

The Physiologically Equivalent Temperature (PET) examines how the changes in the thermal environment can influence the human well-being (Matzarakis and Amelung, 2008). According to ANSI/ASHRAE Standard there are different environmental conditions for human occupancy. In this work we adopted the thermal conditions given below:

Age of the person: 35 years, weight: 75 kg, and height: 1.75 m. Walking at a speed of 1.2 m/s. Clothing insulation (clo) 0.7, Persons Metabolism, internal heat production: 110 W.

Figures (4-31) and (4-32) present the PET for the two districts at noon. In most parts of the two districts, the PET is more than 41℃ , meaning that extreme hot conditions affect people's health and well-being. We conclude that both situations are characterises of extremely thermal stresses. Table (4-2) shows the ranges of PET for different grades of thermal perception by human beings and physiological stress on human beings.

Table (4-2): Ranges of the thermal index physiological equivalent temperature (PET) for different grades of thermal perception by human beings and physiological stress on human beings (Matzarakis and Mayer, 1999).

PET (°C)	Thermal perception	Grade of physiological stress
< 4	Very cold	Extreme cold stress
4,1 - 8,0	Cold	Strong cold stress
8,1 - 13,0	Cool	Moderate cold stress
13,1 - 18,0	Slightly cool	Slight cold stress
18,1 - 23,0	Comfortable	No thermal stress
23,1 - 29,0	Slightly warm	Slight heat stress
29,1 - 35,0	Warm	Moderate heat stress
35,1 - 41,0	Hot	Strong heat stress
>41,0	Very hot	Extreme heat stress

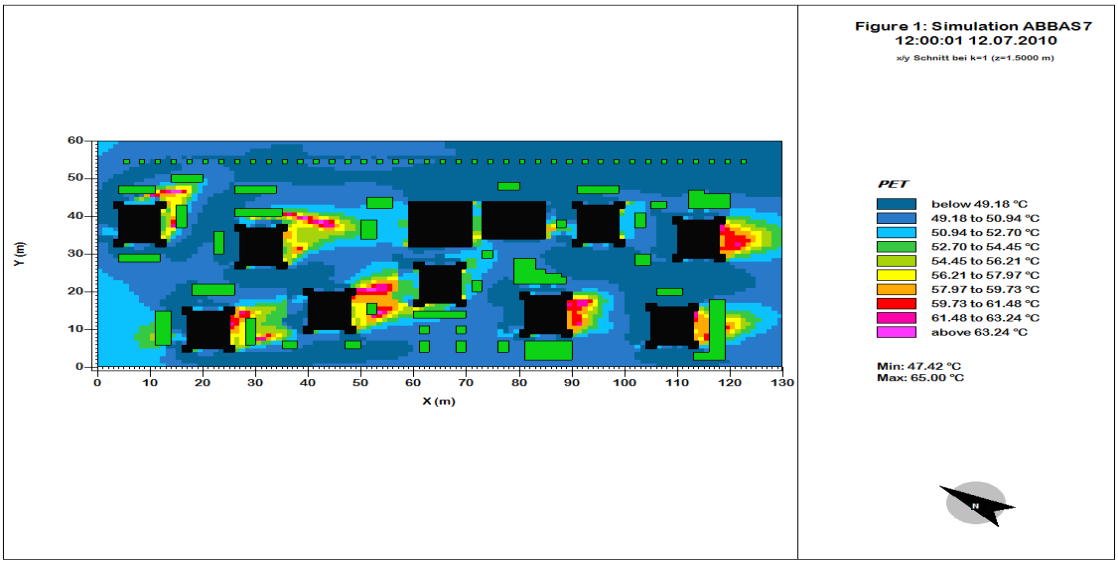

Figure (4-31): Physiological Equivalent Temperature distribution for Haifa Street at noon, at 1.5 m above the ground.

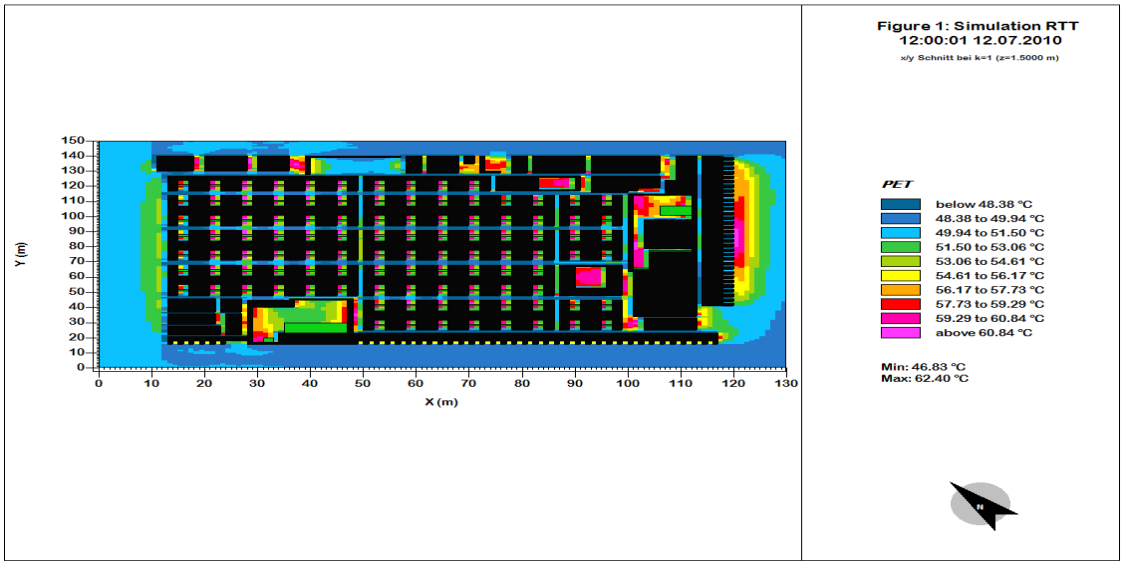

Figure (4- 32): Physiological Equivalent Temperature distribution for Al-Rasheed Street at noon, at 1.5 m above the ground.

4.5.2.3 Predicted Mean Vote (PMV) results

The level of comfort is characterized using the ASHRAE thermal sensation scale, given in Table (4-3). The average thermal sensation response is called the predicted mean vote (PMV).

Table (4-3): ASHRAE Thermal Sensation Scale (ASHRAE Standard, 55-2004).

Value	Sensation
+3	Hot
+2	Warm
+1	Slightly warm
0	Neutral
-1	Slightly cool
-2	Cool
-3	Cold

PMV is a mathematical function of the local climate, in most applications it can also reach above or below [-4], [+4] values, although these are off the scale of the original scale experimental data (http://www.model.envi-met.com/).

Figures (4-33) and (4-34) represent the distribution of Predicted Mean Vote (PMV) at noon for the two districts. The results of Haifa Street, as shown in Fig. (4-33) indicate that the Predicted Mean Vote ranges from 6.50 to 6.78, the maximum value is 7.35.

From Table (4-3) the thermal sensation response of Haifa Street can be classified as hot. In Al-Rasheed Street the Predicted Mean Vote is about 5.12-5.39 meaning that some places especially inside the courtyards and the alleyways it is possible to obtain cooler areas than in Haifa Street. Implementing the PMV equation to outdoor conditions in summer heat stress situations can surely produce PMV values high above +4 (+8 and more). While this result is numerically correct (http://www.model.envi-met.com/).

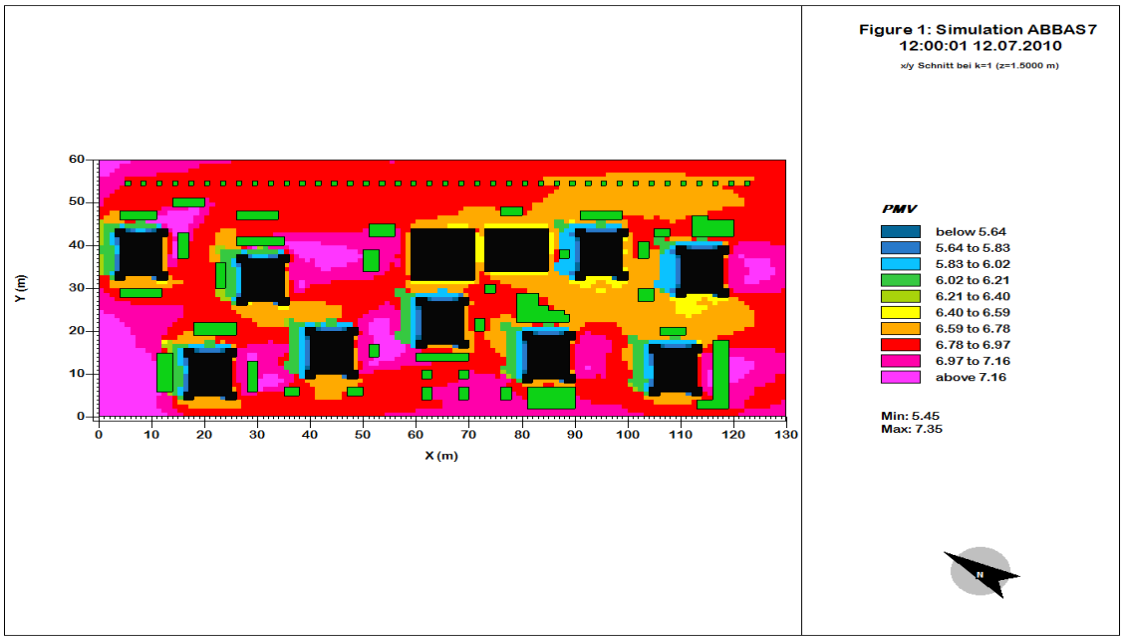

Figure (4- 33): Predicted Mean Vote (PMV) distribution for Haifa Street at noon, at 1.5 m above the ground.

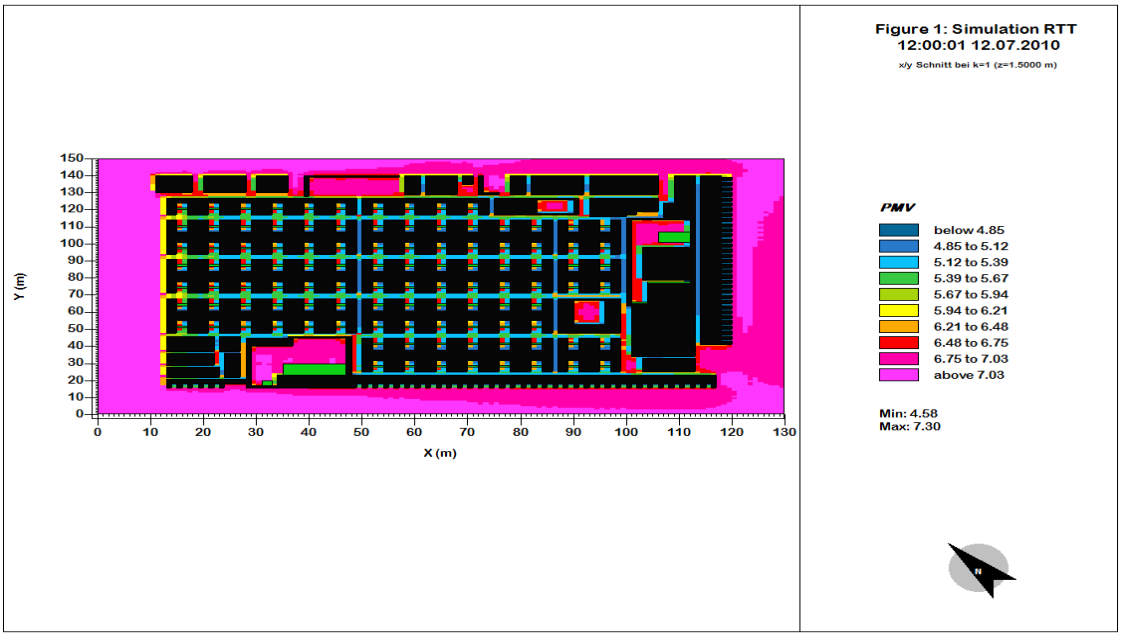

Figure (4-34): Predicted Mean Vote (PMV) distribution for Al-Rasheed Street at noon, at 1.5 m above the ground.

On an average more than 40% of Al-Rasheed district is characterized by a PMV lower than 4, while Haifa Street has only about 10% of its surface, 90% of its territory with a PMV between 4 and 7.

4.5.3 Conclusions

1. According to Santamousris et al. (1999), Nakamura and Oke (1988) there is no apparent correlation between urban geometry and the air temperature. It is different in the present work. Increasing aspect ratio represents the most efficient strategies for decreasing air temperature. Aspect ratio for al-Rasheed Street 2.7 is greater than Haifa Street (1.7-2), the maximum percentage that have been recorded for the air temperature less than 43 ℃ was observed 40% for Al-Rasheed Street at noon.

2. The comparison of the temperatures between the two districts exhibited the presence of the Urban Heat Island at night Fig. (4-22). Through the significant increase in the percentage values of temperature reaches 88% in the Haifa Street for the air temperature more than 43℃ while for Al-Rasheed Street is 44% at night.

3. We found that there is a difference in the wind distribution patterns for the two districts, due to the different district design, and their aspect ratio. Open spaces in Haifa Street contribute to warm air circulation around buildings.

4. According to Walikewitz et al. (2015) during high temperatures or even heat waves the mean radiant temperature is recommended as a mean to calculate thermal indices in heat stress studies. We concluded that the highest values of Tmrt were recorded in Haifa Street, due to the high level of the direct and reflected shortwave radiation and long wave radiation emitted from surrounding sunlit surfaces. Tmrt is lower in Al-Rasheed Street, as more shadow is created by urban configuration. We concluded that the mean radiant temperature in a hot arid climate can be affected significantly by the urban configuration, sky view factor, shadow patterns, and width of the internal passages between buildings. These parameters play an important role for the evaluation of bioclimatic conditions and outdoor thermal comfort.

5. Regarding PET and PMV results, the results revealed that Al-Rasheed Street has thermal conditions better than Haifa Street.

6. The results of this work support the veracity that traditional houses in Baghdad represent the appropriate configuration that serves the extreme climate in Baghdad, especially during the hot, arid summer. The old builders tried since ancient times to adopt the constructions to provide thermal comfort.

In accord with Al-Azzawi (1984) we present the significant points that describe the elements and design features of the traditional houses to mitigate the severe microclimate and internal thermal conditions:

- The courtyard is the focal and separate open space of the house, presents well-proportioned dimensions of length and width to height, these proportions help to provide shade for some of its floor areas even around noon in summer when the sun is nearest to the zenith.
- By being exposed to the clear sky, the floor of the courtyard loses heat to the zenith day and night by long-wave, outgoing radiation. This radiative heat loss helps to reduce the surface temperature of the floor of the courtyard and consequently that of the layer of air in contact with it. The radiative heat loss also helps to reduce the surface temperature of the surrounding habitable rooms and spaces, here the floor of the courtyard, and to some extent, the walls surrounding it, act as intermediary elements in the loss of heat from the surrounding rooms and spaces to the courtyard, then to the clear sky.
- Mashrabiya helps to protect walls from the effect of solar radiation in summer.
- The use of thick brick walls on the ground floor as external walls overlooking the alleyway, and as walls overlooking the courtyard to achieve sufficient time-lag. These walls help to retard and reduce heat gain from the hot exterior to the cooler interior and therefore keep the interior relatively cool during the day in summer.
- The use of traditional porous paving brick as a floor finish in the courtyard: in summer the courtyard floor is washed daily before mid-day and then sprinkled

with water at intervals during the afternoon. The paving brick absorbs and retains some of this water, which helps to reduce the surface temperature of the courtyard floor by evaporative cooling.

- The trees contribute to providing shade in the courtyard which leads to a lower surface temperature of its floor and consequently a lower temperature of the air.
- Using a basic design for the traditional houses rather than articulated and highly-formed configurations. Therefore the three-dimensional area exposed to direct solar radiation is reduced.

4.6 Effect of the Shadings Pattern and Greenery Strategies on the Outdoor Thermal Comfort

In this part, we focus on analysing the human thermal comfort at the pedestrian level in four scenarios characterized by different greenery strategies, such as grass, various types of trees. Two different shadow patterns were created by assuming pergolas around buildings. Other proposals for shading are created with trees on both sides surrounding the pergolas. For evaluating the impact of the shadings pattern and vegetation on the outdoor thermal pedestrian comfort, four different scenarios are represented, only the Haifa Street district is concerned. In addition to the base case plan, other three scenarios were chosen:

- Base Model (BM): is the initial case study of Haifa Street. There are very few trees (Citrus) without vegetation. Figure (4-35) shows the 2D configuration simulated by ENVI-met.
- Vegetation model (GT): Grass and trees were assumed around the buildings, to evaluate the effect of vegetation in the selected area. Sophora Japonica is chosen with a space of grass around the urban area. Sophora Japonica is rounded- headed tree with spreading branches, (4.5-9 m high) Fig. (4-36). Sophora Japonica has long branches and densely twigs (Townsend and Guest, 1974). Figure (4-37) shows 2D view of the model.

- Shadow model (Pergolas around buildings PAB): this model assumes that pergolas are imposed around the buildings with 4 m height. Trees are distributed around theses pergolas (Sophora Japonica), Fig. (4-38).
- The fourth model (SJP) was proposed to solve the problems of the large spacing between the buildings. The objective of this model was to provide continued shadings for the pedestrians by a grid of pergolas Fig. (4-39). Sophora Japonica trees on the both sides surround the pergolas. Figs. (4-40) and (4-41) depict the model before and after trees were distributed around the pergolas.

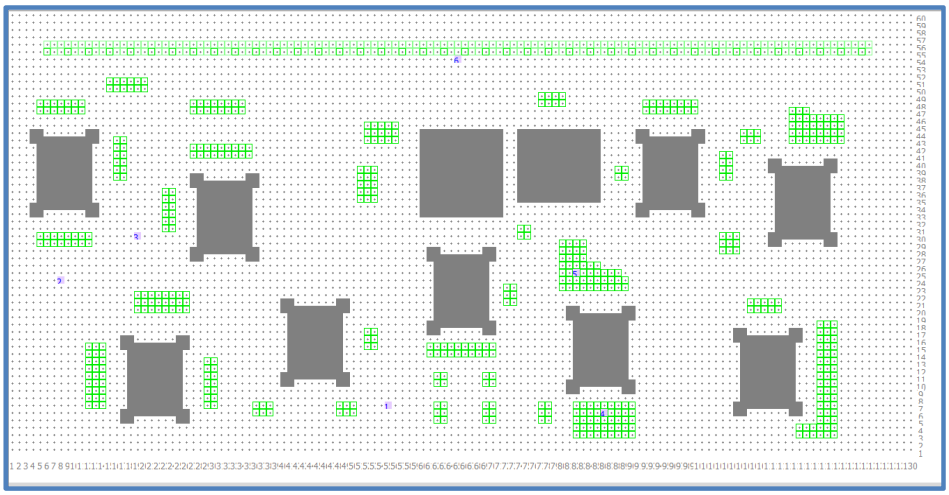

Figure (4-35): Base model (BM) of Haifa Street District.

Figure (40-36) : Sophora japonica tree (https://www.pinterest.com/).

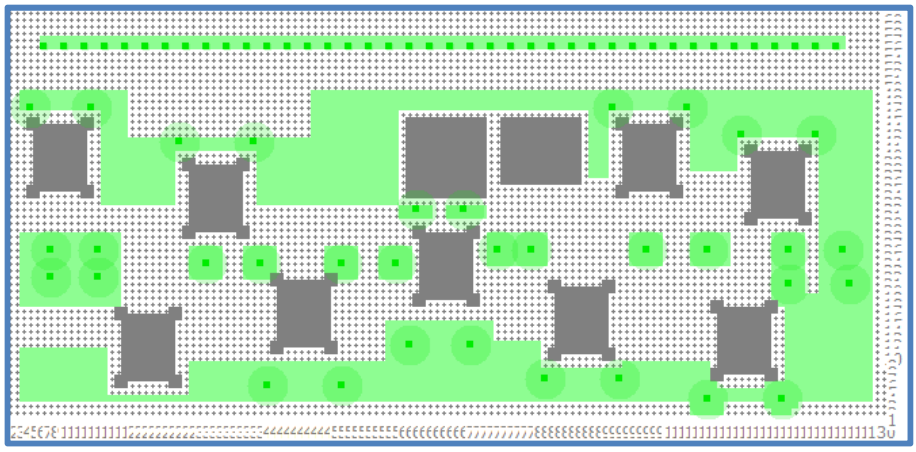

Figure (4-37): Grass and Trees model (GT) of Haifa Street.

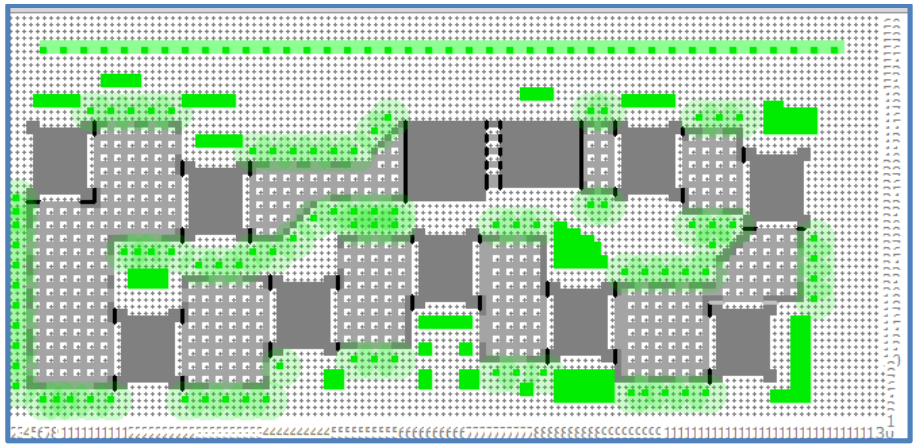

Figure (4-38): Pergolas around the buildings (PAB) of Haifa Street District.

Figure (4-39): The shaded passageway for the pedestrians.

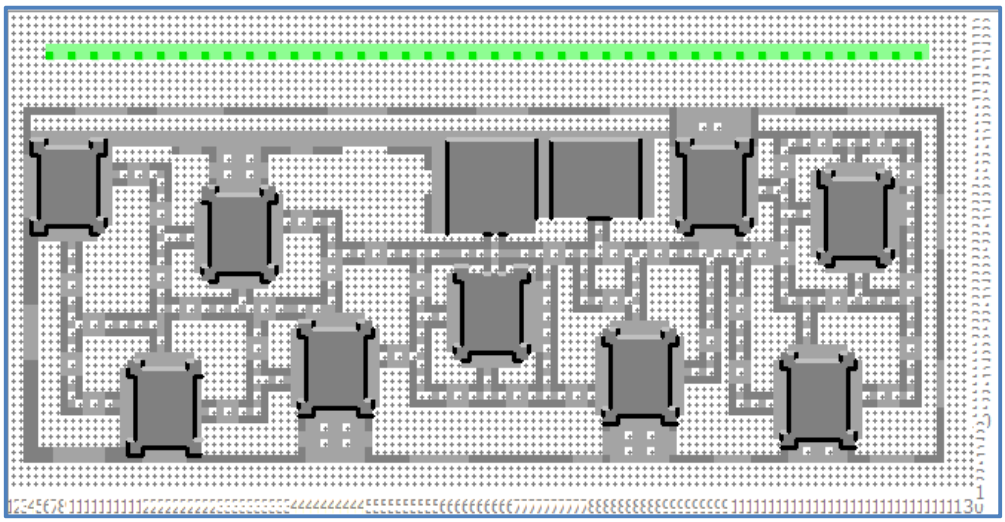

Figure (4-40): SJP model before Sophora Japonica trees were distributed around the pergolas.

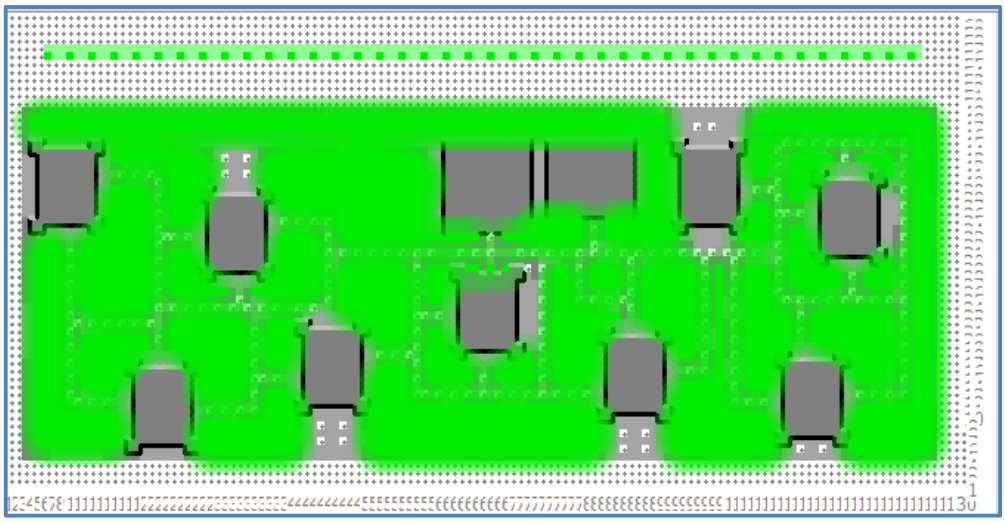

Figure (4-41): SJP model after Sophora Japonica trees were distributed around the pergolas.

4.6.1 Analysis of the results on the outdoor thermal comfort

We analyze the estimated thermal comfort conditions along a proposed pedestrian path linking all the buildings at noon. PET and PMV are measured for pedestrians for the

selected urban area. A scenario of a walkway connecting the buildings is simulated to illustrate the objective. The path (A-B) observed in Fig. (4-42) is about 120m long.

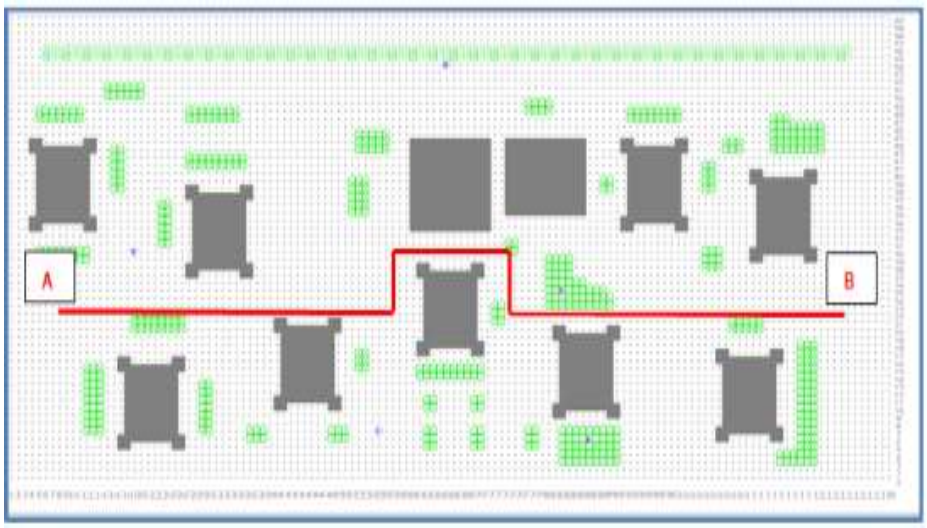

Figure (4-42): The path (A-B) way of the pedestrian in the urban area.

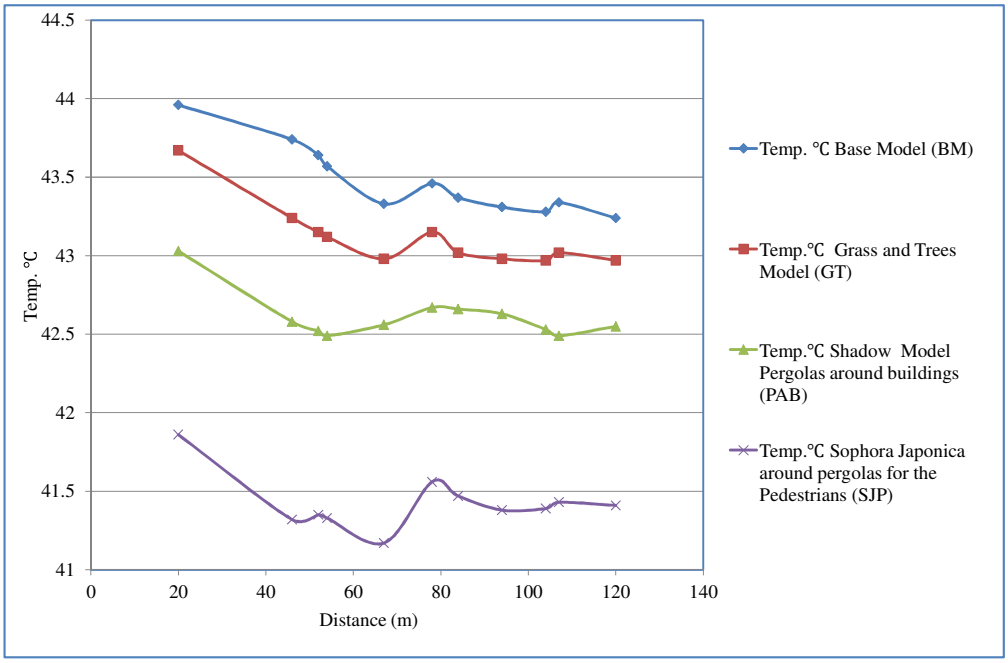

Figure (4-43): Air temperature distribution at noon, at 1.5 m above the ground, along the path (A-B).

The SJP model contributes to minimizing the air temperature along the pedestrians range from 1.83 to 2.42 ℃ as shown in Fig. (4-43). The pergolas reduce the temperature because of the sky view factor decrease, and the effect of sun radiation. Also, trees surrounding the pergolas obstructed the passage of long-wave radiation between the buildings, the ground surfaces and the sky. Higher sky view factor in the base model (BM) leads to higher air temperature in the urban area because the sky view factor increase potentially leads to the increase of the open space and the amount of long wave radiation absorbed by the ground surfaces and buildings façades and roofs. A slight decrease in air temperature is observed for the grass and trees model (GT). This means that the trees cover along the walkways of the pedestrians did not contribute to reducing the temperature at noon, because of the high absorption of long-wave radiation from the ground surfaces. The big space between buildings plays a significant role in absorption and heat storage on the ground. The results for the (PAB) model show that this solution does not contribute to providing enough cover for reducing the sunlight and heat absorption by the surfaces: the decrease in temperature is too insignificant. The grass and trees model (GT) and pergolas around the buildings (PAB) could consist in a good solution to mitigate the high temperatures. Yet they are not ideal. The first one is the high rise buildings. Second, the asymmetric distribution of buildings leads to big open space between the buildings, the shading from the tall buildings to each other is lost. The long distances between the buildings create a big space of ground surface that absorbs heat and keeps it along daytime. The results obtained for the mean radiant temperature indicate that Tmrt minimum can be observed in the SJP model, Fig. (4-44) due to the shadings from the pergolas along the path (A-B) and the effect of the shadow from the trees. Tmrt reaches 35℃ on the path (A-B), for SJP due to the presence of shading, and less long wave radiations from the buildings and grounds surfaces. The surface temperature of urban facades is the primary factor contributing to reducing thermal comfort. The results of grass and trees model are almost equivalent to the Base model due to lack of shading. Shadows, in the PAB model was not enough to improve the results of Tmrt compared to the Base model results.

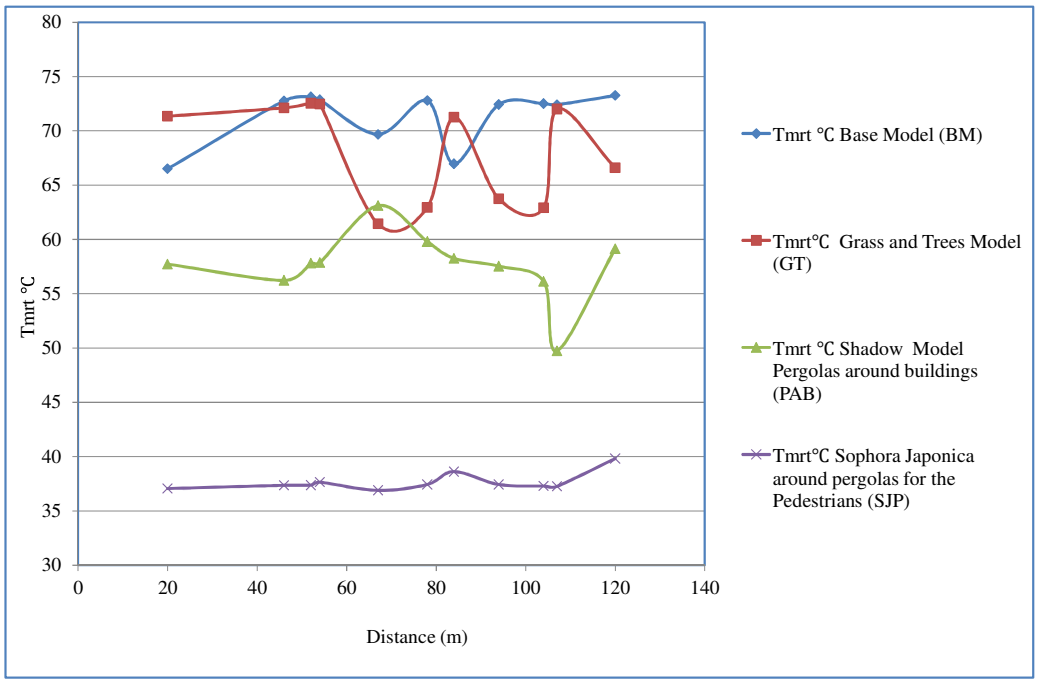

Figure (4-44): The mean radiant temperature at noon, at 1.5 m above the ground along the path (A-B).

Figure (4-45) shows the effect of the vegetation on the specific humidity. Overall, all the tested scenarios lead to similar results as the base model except one SJP allows an increase of 2%.

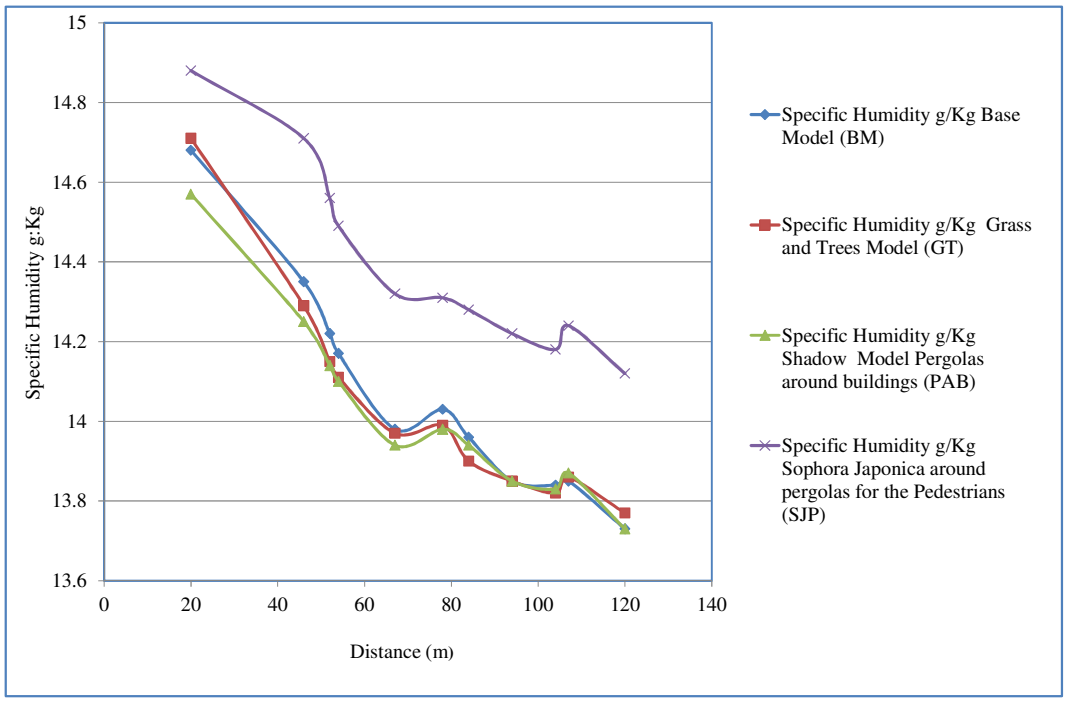

Figure (4-45): Specific Humidity at noon, at 1.5 m above the ground along the path (A-B).

According Figs. (4-46) and (4-47) the shading of trees could impact the human thermal comfort. The Sophora Japonica around pergolas for the pedestrians model (SJP) is the best configuration for improving thermal comfort. We obtained a decrease in PET values of 10℃ from the base model and of 3 in PMV values. Changes in thermal comfort for the other models are barely apparent: the most important factors are the presence of sufficient vegetation and smaller values of the sky view factor.

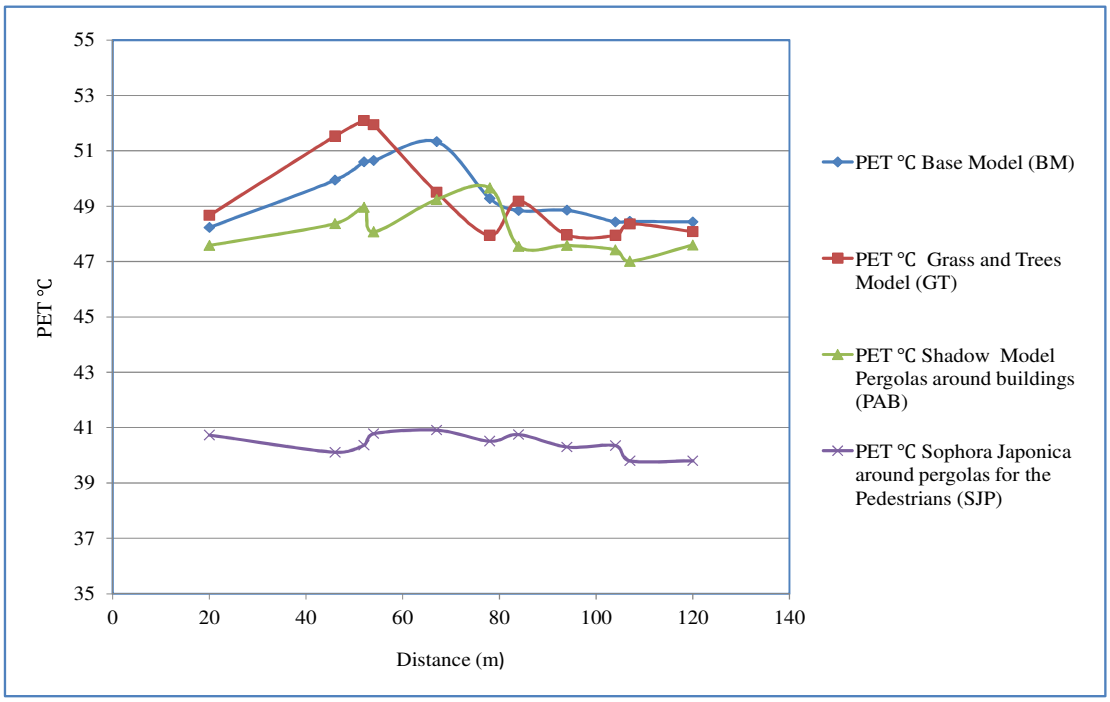

Figure (4-46): PET at noon, at 1.5 m above the ground, along the path (A-B).

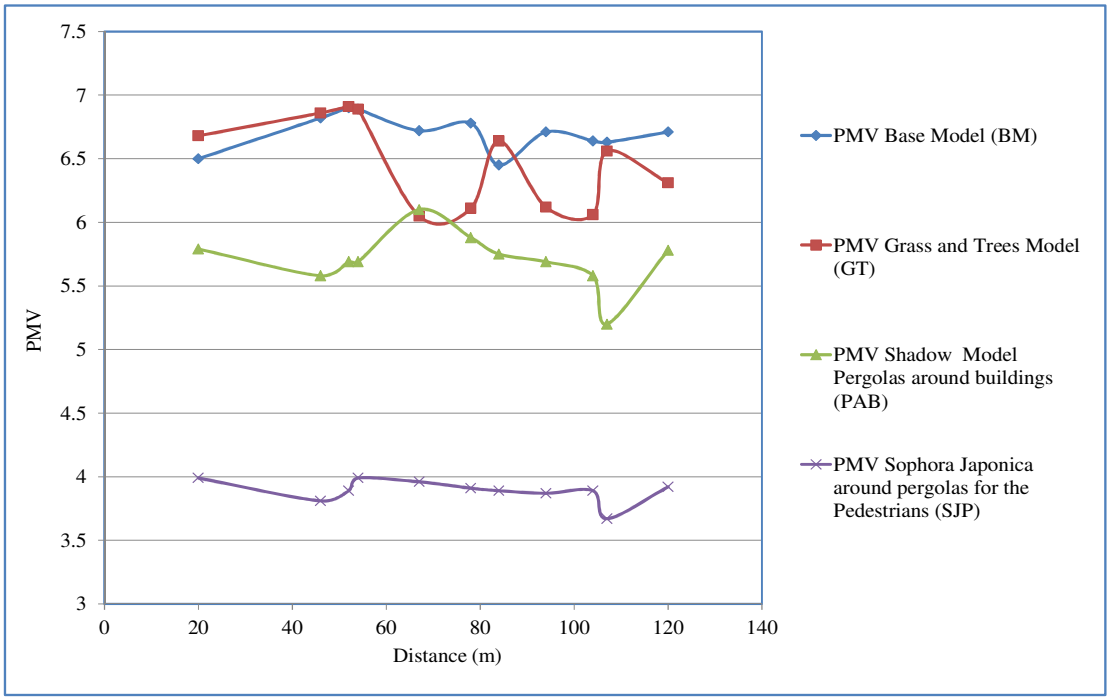

Figure (4-47): PMV at noon, at 1.5 m above the ground, along the path (A-B).

4.6.2 Conclusion

The present study is conducted to assess the perception of thermal comfort for the two indices PMV and PMT. Simulation works are performed on the hottest day in summer (Hassoon, 2010). The results revealed a decrease in temperature of approximately 2.4 ℃ and 10 ℃ in PET index for the SJP model and a decrease in PMV to 3. We highlight the drawbacks of Western design in an arid climate area without taking into consideration the pedestrians thermal comfort. High rise buildings, asymmetrical canyons, large spacing between buildings, lack of vegetation and loss of shading feature play a significant role. The suggestion of the greenery strategies patterns models could take in consideration of the design developments of the urban area. Although plants need some water to grow and live in such an arid climate, this drawback could be solve as the district is near the Tiger River. The properties of trees canopy can affect directly the thermal comfort results as the leaves absorb, reflect and transmit solar radiation, and evapotranspiration contributes to thermal comfort. The final outcomes of the study could lead to urban planning recommendations for municipalities and urban planners.

CHAPTER FIVE

PROPOSAL TO IMPROVE THE THERMAL COMFORT OF PEDESTRIANS IN AN ARID CLIMATE

5.1 Introduction

Designing cities in a hot, arid climate and maintaining an appropriate level of outdoor thermal comfort is one of the most significant challenges for the designers: how to achieve an appropriate climate for pedestrians during the day under the blazing sun, especially in countries with an excessive rise in summer temperatures and for several months, as in Iraq?

5.2 Influence of Aspect Ratio

According to an investigation carried out in the hot and arid city of Riyadh (Saudi Arabia) to evaluate the thermal performance of traditional and modern residential urban canyons, Fig. (5-1), the exposure of urban surfaces to the solar radiation is a function of the aspect ratio (H/W) and orientation of the canyon. They play a dominant role in determining the quantity of received solar radiation by the horizontal and vertical surfaces of canyon and thus affect the ambient temperature inside the canyon. It was observed that the shallow modern canyons with H/W =0.42 experience higher ambient temperatures during daytime when compared to the deep traditional aspect ratio H/W=2.2 (Bakarman and Chang, 2015).

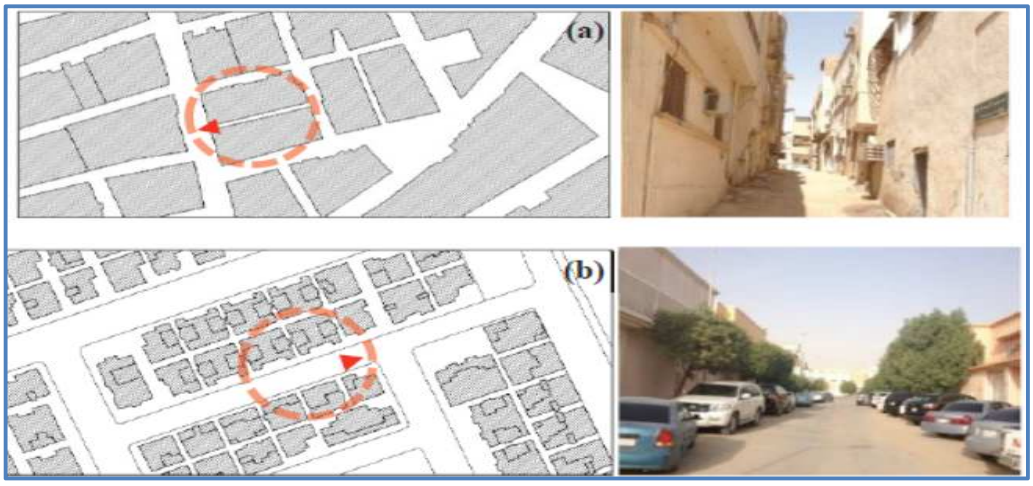

Figure (5-1): Aerial and street view (a) traditional area (b) modern residential area (Bakarman and Chang, 2015).

An investigation study was carried out in Morocco by Alaoui et al. (2016). The aspect ratio (H/W>2) leads to increase the energy cooling demand due to the high thermal recession and the effect of low ventilation. An investigation study was conducted to evaluate the effect of different designs in Cairo, Egypt. Two different urban designs were selected: the renovated and non-renovated part of the alley, Fig. (5-2). The results showed that the non-renovated part of the alley improved pedestrian comfort due to higher aspect ratio and street geometry allowing to stop direct solar radiation in the alley (Mahgoub et al., 2013).

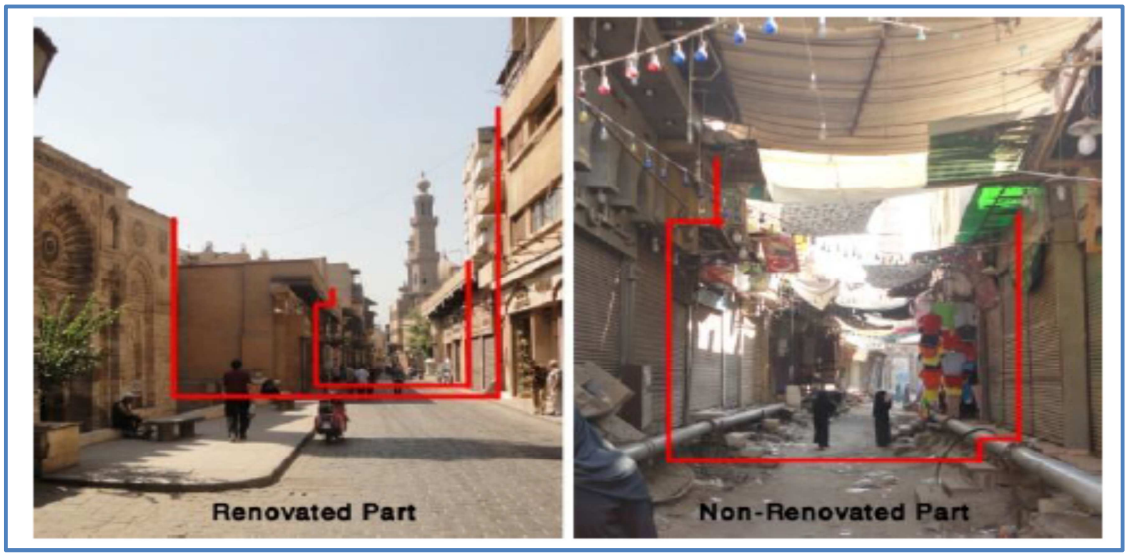

Figure (5-2): Different aspect ratio for two urban area geometries (Mahgoub et al., 2013).

5.3 The Role of Vegetation

It is worth mentioning that the technique of using vegetation in a hot, dry weather was adopted by the Babylonian civilization in Iraq in the 16th-century, as referred by Soomro (2012). Figure (5-3) depicts the hand-colored engraving by Dutch artist Maarten van Heemskerck which represents the Hanging Gardens of Babylon, one of the Seven Wonders of the World. Technically, the gardens did not hang but grew on the roofs and terraces of the royal palace in Babylon.

Figure (5-3): Hanging gardens of Babylon (Soomro, 2012).

Sailor (2006) highlighted that trees shade are a common mitigation strategy by providing a direct shade to buildings and pedestrians at the same time improving the thermal environment through evapotranspiration processes.

5.4 Influence of Street and Buildings Orientation

Street orientation affects the shading geometry and solar irradiance at the canyon surfaces. Consequently, the comfort of pedestrians is also affected. The N-S street orientation is always closer to the comfort level regardless of the canyons aspect ratios. (Swaid et al., 1993). Ali-Toudert and Mayer (2004) concluded that the rotation of the street to (NE-SW) or (NW-SE) in hot, dry climate leads to better comfort conditions because the shading effects on the walls are more efficient than for an E-W orientation, that means a lack of exposure to direct sunlight due to the availability of shade. The ideal street orientation in Hot-Zone must be rotated towards the axis (Northeast- Southwest) and (Northwest - Southeast) to get the best insulation in the winter and less heat and sufficient shading in the summer (Polservice, 1982).

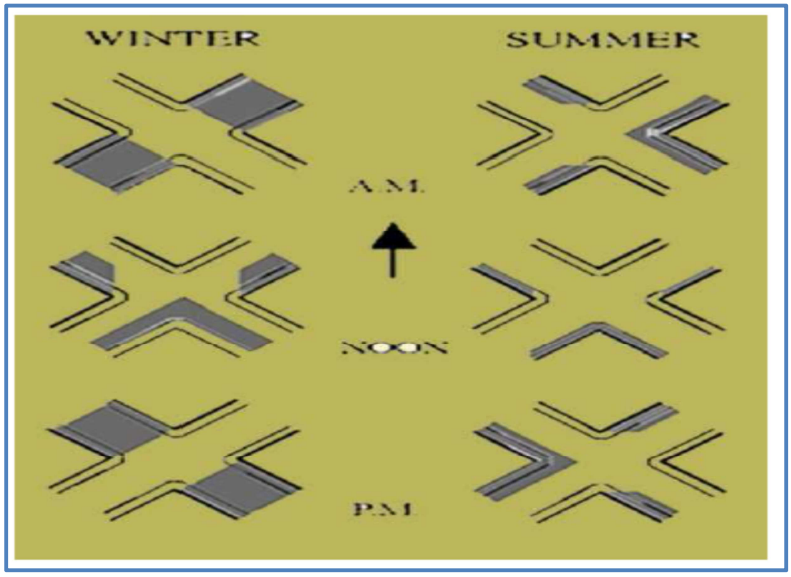

Figure (5-4): Orientation of streets in the hot dry climate (Polservice, 1982).

Al-jumaili (2014) proposed ideal streets and buildings orientations in the hot climate in the case of Baghdad Fig. (5-5).

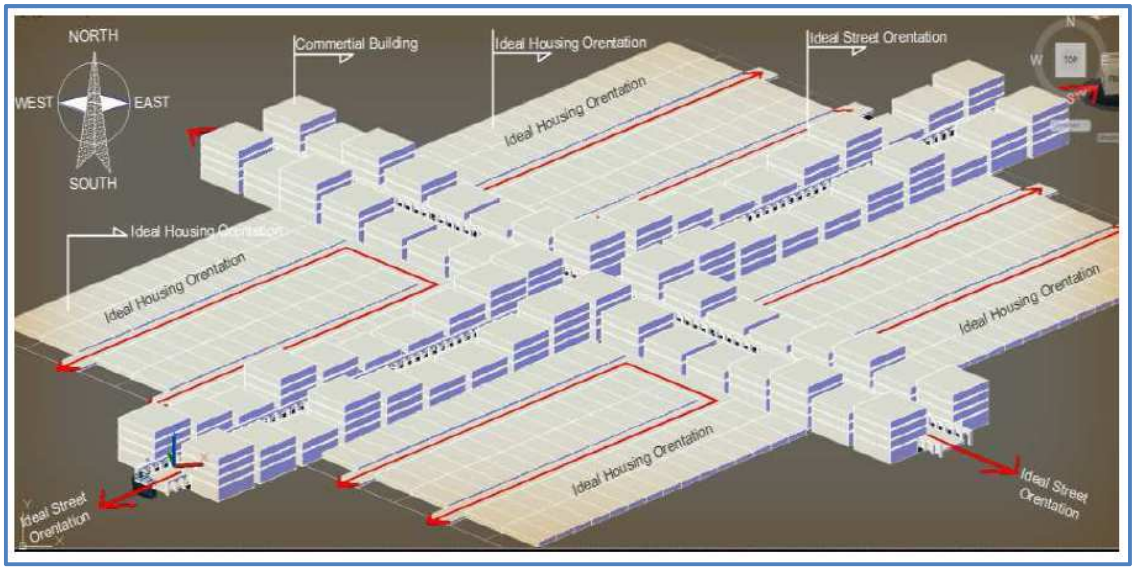

Figure (5-5): Ideal streets and buildings orientations in a hot climate (Al-jumaili, 2014).

The housing Technical Standards and Codes of Practice Report of Iraq, developed by "Polservice" in 1982, recommend that "orientation of buildings in hot- dry zone prefers

within 350 South-East is advisable. However, 250 South-East gives the best balance, and the buildings should be elongated on an East-West axis.

5.5 Sky view factor

A study based on a comparison of the environmental conditions of urban street canyons in traditional and modern neighborhoods of the city of Aleppo, Syria Fig. (5-6), showed that the lowest PET values were noticed in canyons with low SVF (high aspect ratio): the effect of shading on the mean radiant temperature diminishes significantly with the solar radiation decrease. Consequently, wide canyons in the new part of the city are less comfortable with maximum Tmrt and PET, compared to narrow walkways in old Aleppo (Zakhour, 2015).

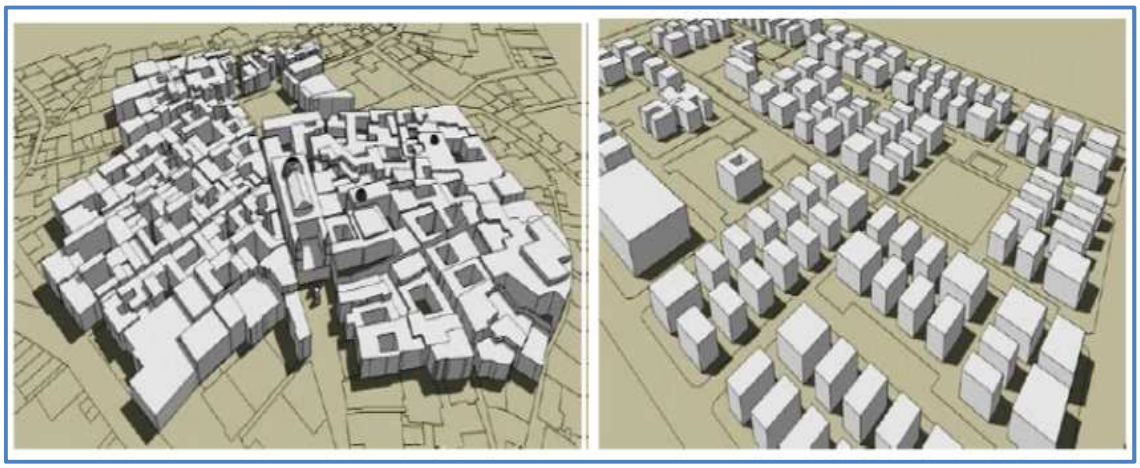

Figure (5-6): Three-dimensional view of new and old Aleppo districts (Zakhour, 2015).

5.6 Influence of Colonnades

Colonnades (arcades) on the ground floor of buildings contribute to improving the comfort conditions, Fig. (5-7). The location of colonnade on the South side of an E-W oriented street means that the colonnades face North, which increases the shaded area in the street and reduces the penetration of solar irradiance to the grounds. (Swaid and Hoffman, 1993).

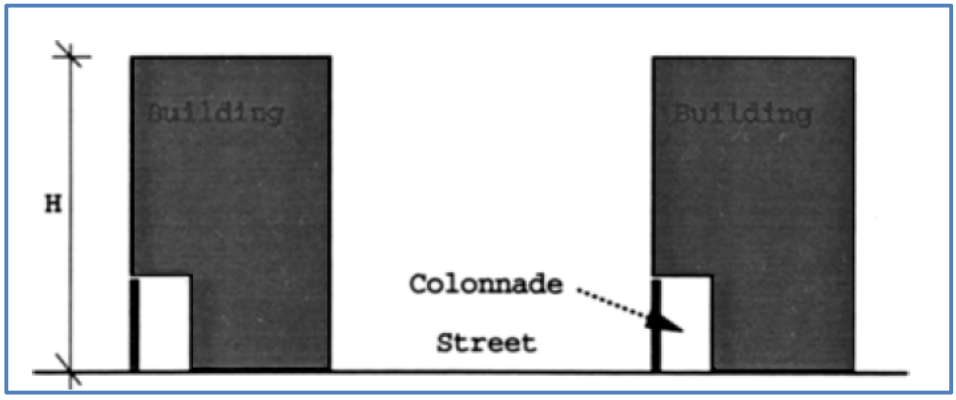

Figure (5-7): Cross-section of an urban street canyon with a colonnade on the South side (exposed to the North) (Swaid and Hoffman, 1993).

Colonnades exist in Baghdad in different locations as one of the essential strategies for improving thermal comfort of pedestrians. The most important ones are Al-Rasheed Street Fig. (5-8a), and the walkways for pedestrians in Al-Salehya Fig. (5-8b).

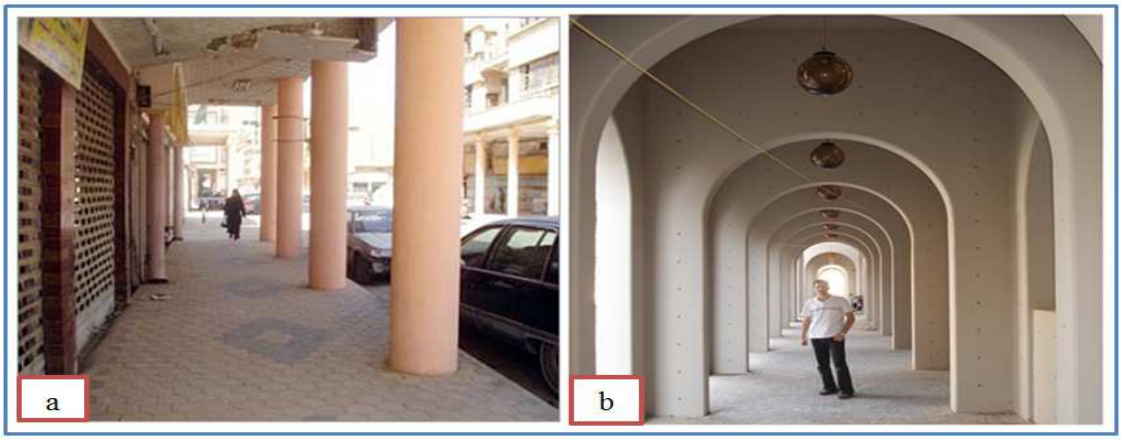

Figure (5-8): (a) Al-Rasheed Street, (b) the walkways for pedestrians in Al-Salehya in Baghdad.

5.7 Influence of Courtyards

Courtyard are the focal and private open space of the traditional houses with well-proportioned ratios of length and width to height; these proportions contribute to providing shade for some of the floor areas even around mid-day in summer (Al-Azzawi, 1984). Typical courtyards are planted with various trees and flowers to improve comfort conditions by modifying the microclimate around the buildings and by enhancing ventilation. According to Ghaffarianhoseini et al. (2015) different archetypes have been adopted for courtyards design through the centuries. Courtyards were principally adopted in traditional buildings in parts of Asia, the Middle East, South America, and the Mediterranean countries. Romans and Arabs often included colonnades, especially in convents. Courtyards are one of the traditional Iranian architecture elements, with significant benefits on thermal performance of indoor spaces in hot and dry climate. An existing traditional courtyard in Kashan city, Iran was used as a case study to analyze the indoor thermal comfort condition, Fig. (5-9). Simulation results revealed that the influence of the internal courtyards on the thermal condition has a high reliance on the envelope openings for air flow (Cho S. and Mohammedzadeh, 2013).

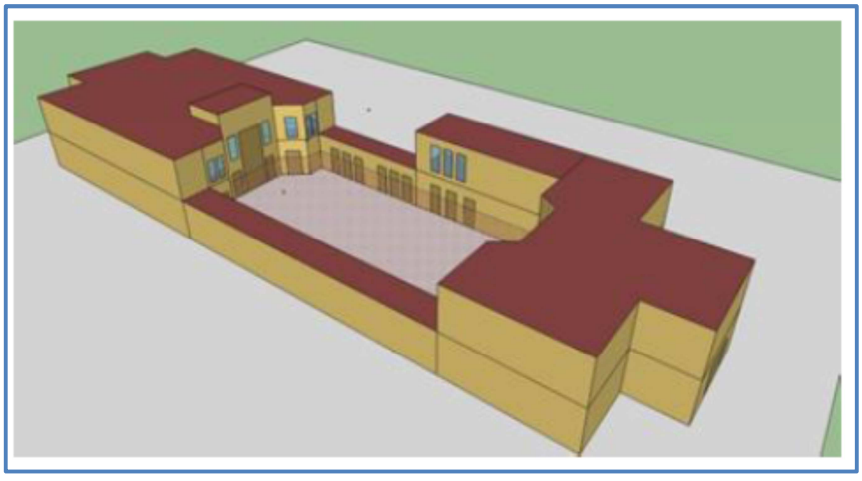

Figure (5-9): Geometry model of case study of courtyards (Cho S. and Mohammedzadeh, 2013).

Another investigation study in Iran carried out by Zamani et al. (2012) showed that courtyards improve natural lighting, heating, cooling and ventilating. Ratti et al. (2003) came to the conclusion that the courtyard configuration allows to improve comfort compared to pavilion, Fig. (5-10).

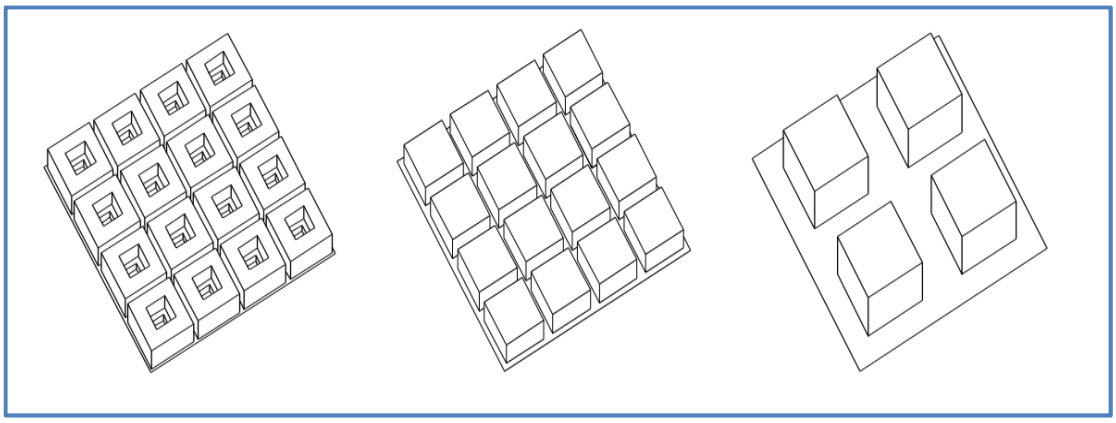

Figure (5-10): The traditional courtyard (left) and two pavilion structures (right), (Ratti et al., 2003).

Figure (5-11) shows (Type 1) comprises courtyards, atriums, and patios. (Type 2) includes attached semi-open spaces which are somewhat covered by a balcony, or a porch, a corridor, a covered street or an arcade. In the third type, the building is entirely enclosed by an open space like pergolas, bus stations, or awnings.

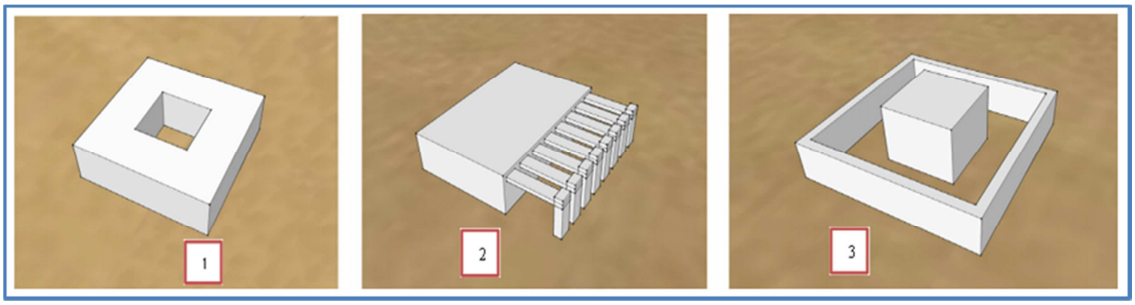

Figure (5-11): Type (1) open space inside the building, type (2) open space attached to the building, and type (3) the open space encloses the building (Taleghani et al., 2012).

Traditional courtyard houses in Baghdad and other parts of Iraq represent indigenous types of houses. They seem to have fulfilled the needs of their inhabitants from the points of view of functional requirements, and internal thermal performance. The traditional courtyard house mainly consists of a centrally-located courtyard, with all rooms and spaces around it. Courtyards receive sunlight, daylight, natural ventilation and have visual as well as physical communication (Al-Azzawi, 1984).

Figure (5-12): View of a courtyard in a traditional house in Baghdad (Al-Ani, 2011).

5.8 Means of shading

The traditional "mashrabiyya" is common in hot-arid regions, it consists mainly of wooden, shading covers over large openings windows which allows ventilation, as well as the passage of daylight. It also maintains family privacy (Skat, 1993). Figure (5-13) depicts a view of mashrabiyya in Cairo, Egypt. Mashrabiyya helps to provide a protection for pedestrians from the solar radiation, Fig. (5-14) shows a view of mashrabiyya in traditional house in Baghdad.

Figure (5-13): View of mashrabiyya in Cairo, Egypt (https://www.flickr.com/photos/).

Figure (5-14): View of mashrabiyya in traditional house in Baghdad (www.google.com).

5.9 The role of the albedo

Roofs and pavements comprise about 60 % of urban surfaces. These surfaces are dark and typically absorb over 80 % of the sunlight and convert that solar energy into heat, which results in more polluted cities, higher energy costs, and impacts global. Replacing

pavements with more reflective materials could modify this warming effect improve pedestrian comfort and lessen the urban heat island effects (Masterbuilder, 2014).

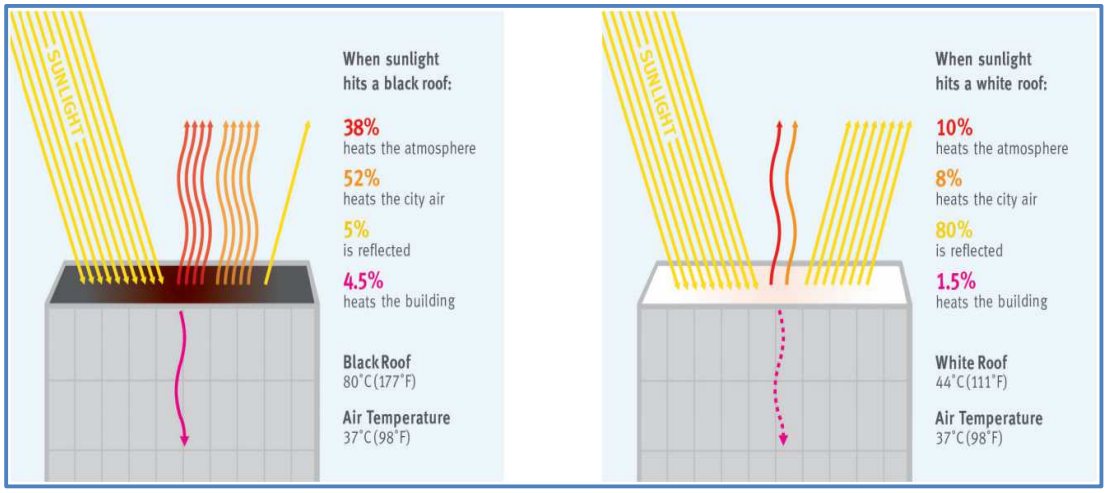

Figure (5-15): The Albedo Effect - Comparison of a black and a white flat roof on a summer afternoon with an air temperature of 37 ℃ (Masterbuilder, 2014).

In the summertime, paving materials can reach peak temperatures of 50 to 65 ℃, contributing to heat the air above them. Using lighter paving materials may create more reflective surfaces (Global Cool Cities Alliance, 2012).

Li (2012) concluded that enhancing the evaporation from pavement helps to reduce the temperature, the mean radiant temperature, and PET. Consequently it improves the thermal comfort in a hot climate.

5.10 Design criteria for the Proposal Model

Here, we adopt the same area, initial meteorological conditions, and date of simulation that were selected previously in this research. We intend to find if an improvement could be obtained by modifying the design of the studied district. The requirements for the adopted design come from the conclusions of the previous review. We also account for the specifications and recommendations from the Ministry of Housing and Construction in Iraq. The criteria used to create the model design are as follows:

1. Height of the residential buildings does not exceed 8 floors, floor height is 3 m. So, we choose the height of the building 25 m.
2. The spacing between buildings depends on the aspect ratio (H/W ≥ 1), we choose H/W=1, so the spacing between the buildings 25 m.
3. According the housing Technical Standards and Codes of Practice Report of Iraq, developed by "Polservice" in 1982, and our conclusions the orientation is (NW-SE).
4. Due to the role of albedo on thermal comfort, we select concrete pavement light for the walkways, and concrete pavement gray for the main street.
5. Providing shading is an essential role in improving thermal comfort, so we use pergolas to protect pedestrians from the direct effect of solar radiation.
6. In order to enhance the role of vegetation on outdoor thermal comfort, we focus on using vegetation, grass and trees. Figure (5-16) shows the proposed model (PM) with buildings, pergolas, and vegetation.

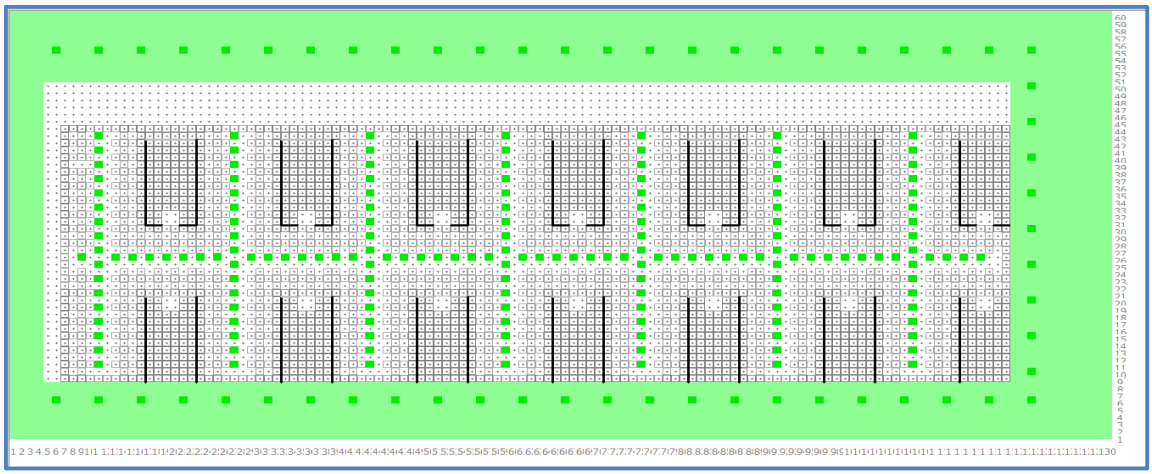

Figure (5-16): Proposed model (PM) with buildings, pergolas, and vegetation.

5.11 Results Analysis

The initial and boundary conditions are indicated to the ones in chapter 4. The results are compared to the results in the current configuration of Haifa Street. Figures (5-17) and (5-18) reveals a significant decrease in temperature in the PM model. For the (PM) the

dominant air temperatures range from 41.5 ℃ to 44.5 ℃ . We obtain a decrease 1.5 ℃ in the air temperature in a proportion of 52% in the PM.

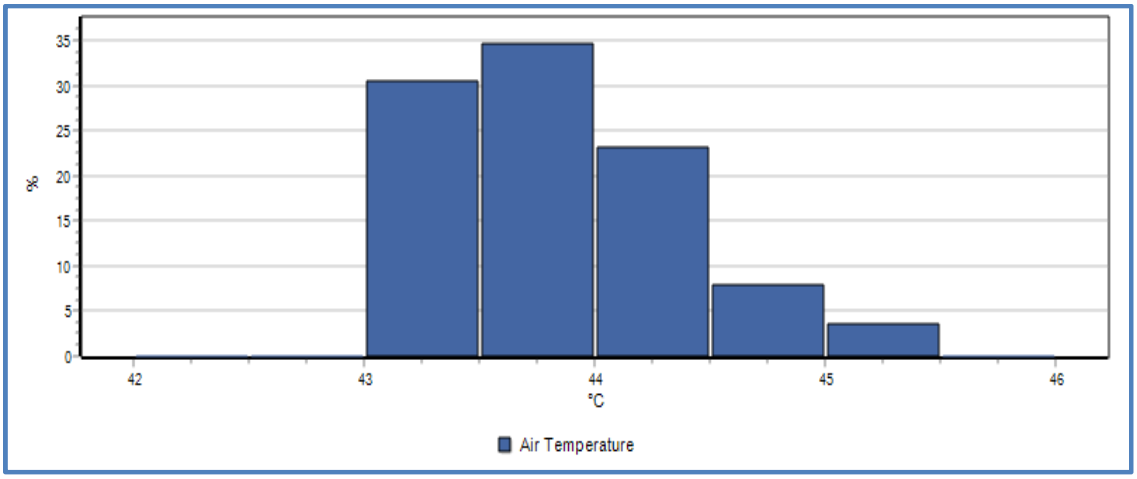

Figure (5-17): Percentage value of air temperature for Haifa Street at noon, at 1.5 m above the ground.

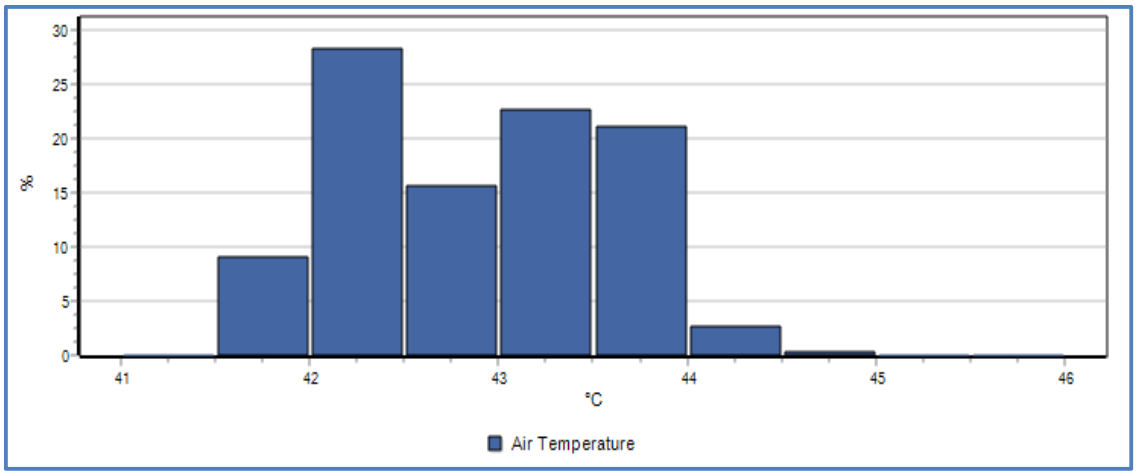

Figure (5-18): Percentage value of air temperature for proposal model at noon, at 1.5 m above the ground.

The results of wind speed in Figs (5-19) and (5-20) reveal that we get a decrease 2 m/s in wind speed for the proposal model due to the presence of pergolas and the presence of vegetation, which leads to obstructing the air movement.

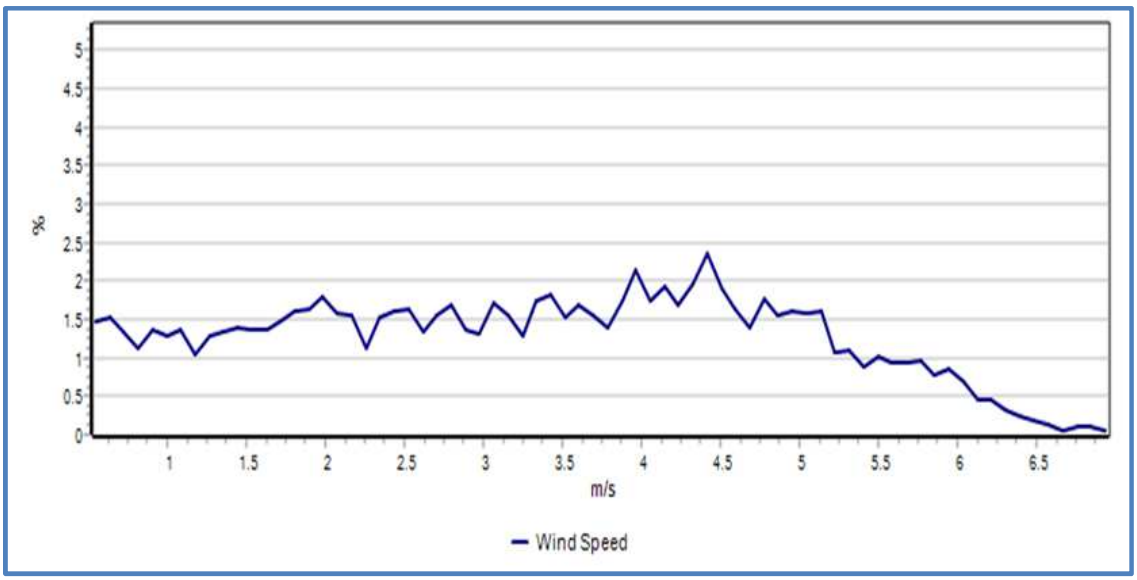

Figure (5-19): Percentage value of wind speed for Haifa Street at noon, at 1.5 m above the ground.

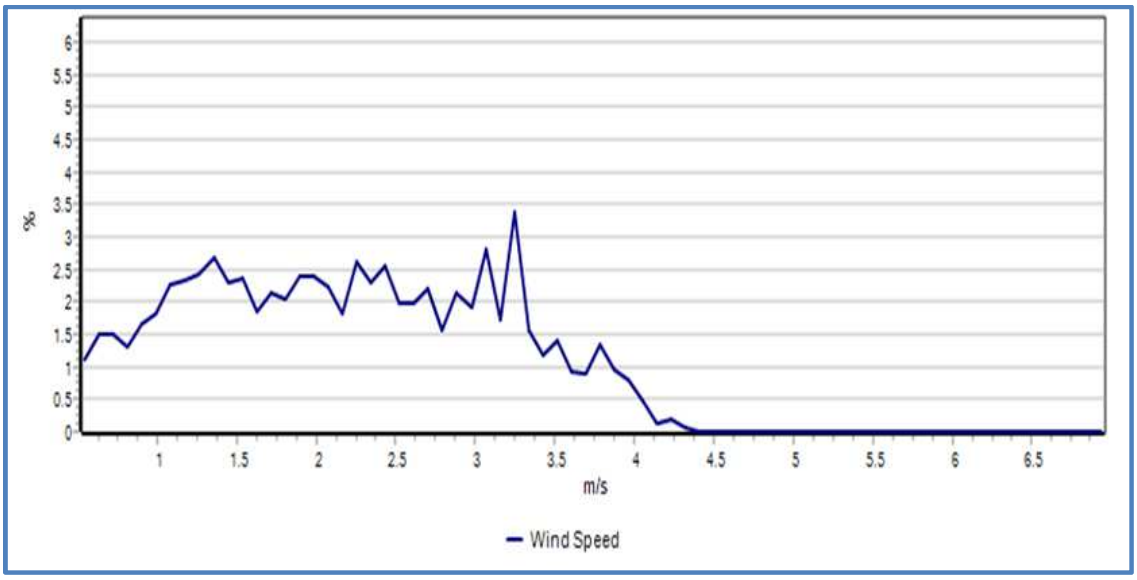

Figure (5-20): Percentage value of wind speed for the proposal model at noon, at 1.5 m above the ground.

The sky view factor decreased also: Haifa Street has more open space than the PM. The existence of pergolas and vegetation minimize the spacing in the urban area, Figs (5-21) and (5-22).

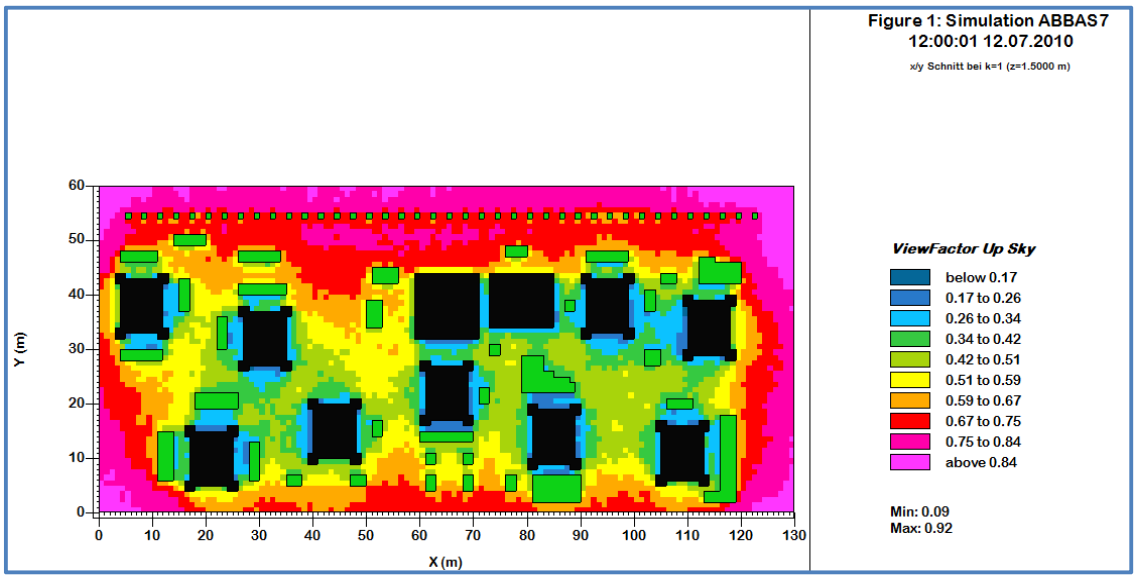

Figure (5-21): Distribution of the sky view factor for Haifa Street at noon, at 1.5 m above the ground.

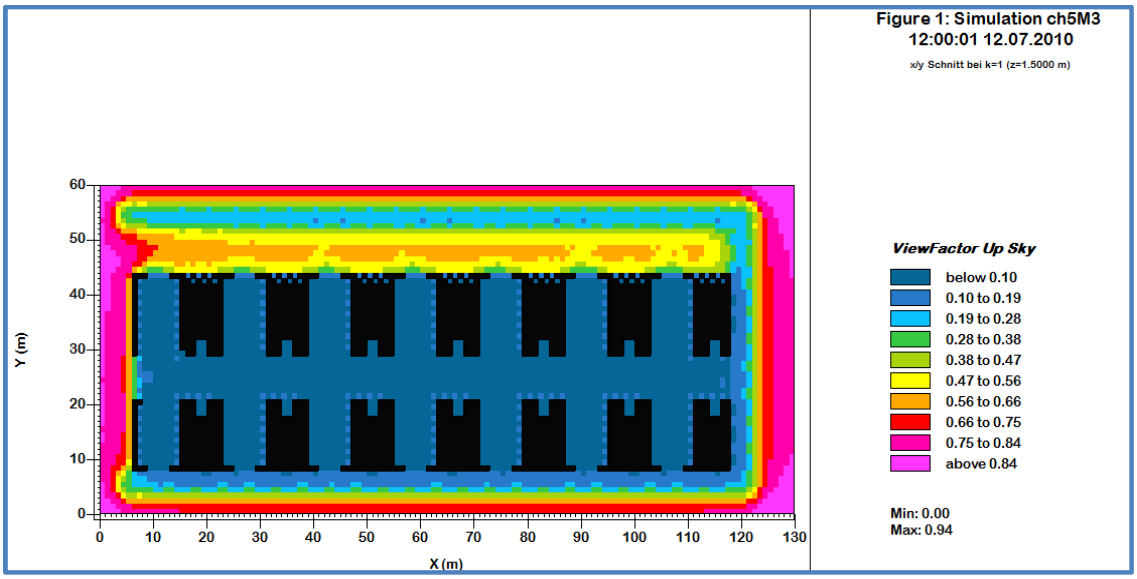

Figure (5-22): Distribution of the sky view factor for the proposal model at noon, at 1.5 m above the ground.

According the results of the mean radiant temperature in Figs (5-23) and (5-24), we observe a decrease in a proportion of 88% in the PM for the mean radiant temperature range from 70 ℃ to 75 ℃, due to the effect of shadows from the vegetation and the pergolas.

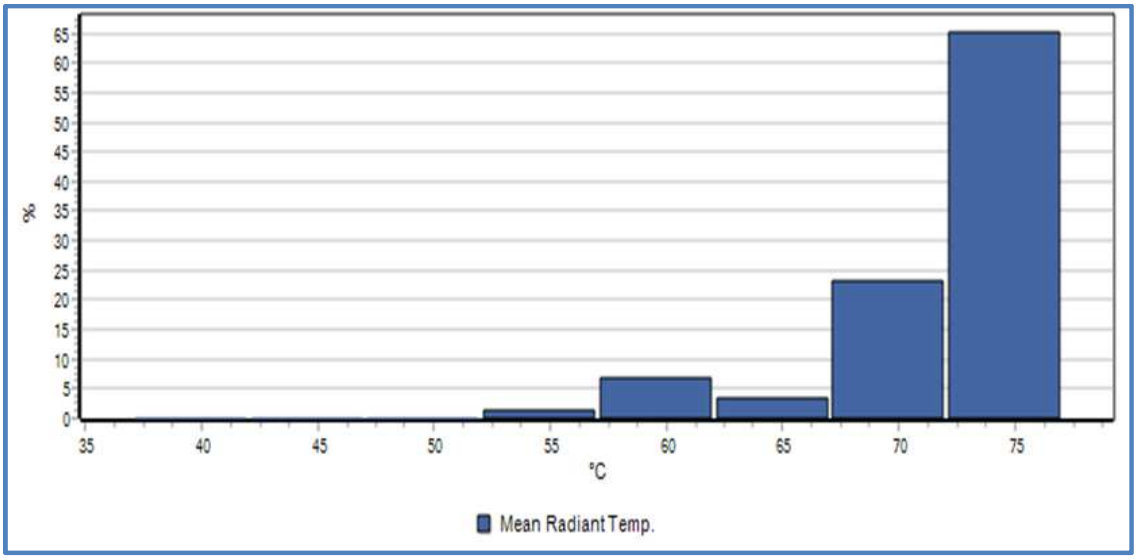

Figure (5-23): Percentage value of the mean radiant temperature for Haifa Street at noon, at 1.5 m above the ground.

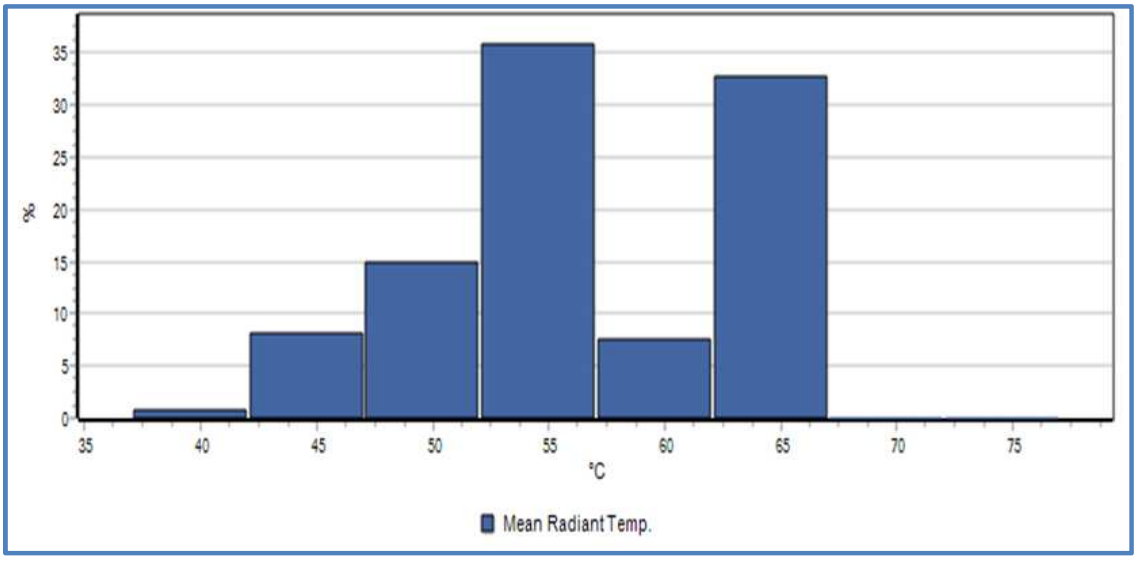

Figure (5-24): Percentage value of the mean radiant temperature for the proposal model at noon, at 1.5 m above the ground.

For PMV results, we observe that an improvement in the thermal comfort could be obtained by modifying the design of the studied district, Fig. (5-25). Haifa Street is considered as hot region, Fig. (5-26).

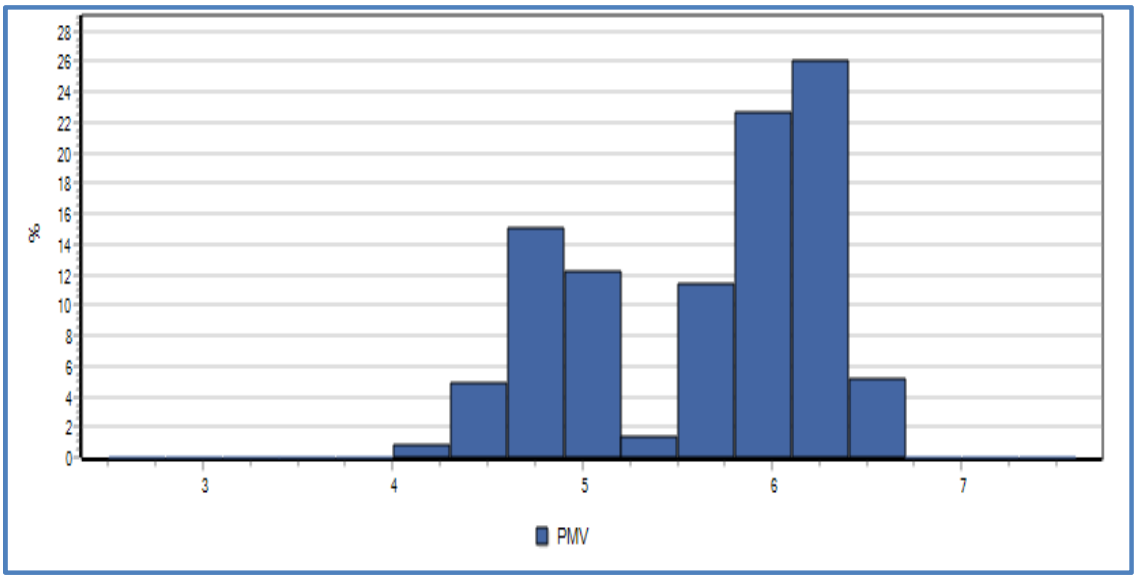

Figure (5-25): Percentage value of PMV for the (PM) at noon, at 1.5 m above the ground.

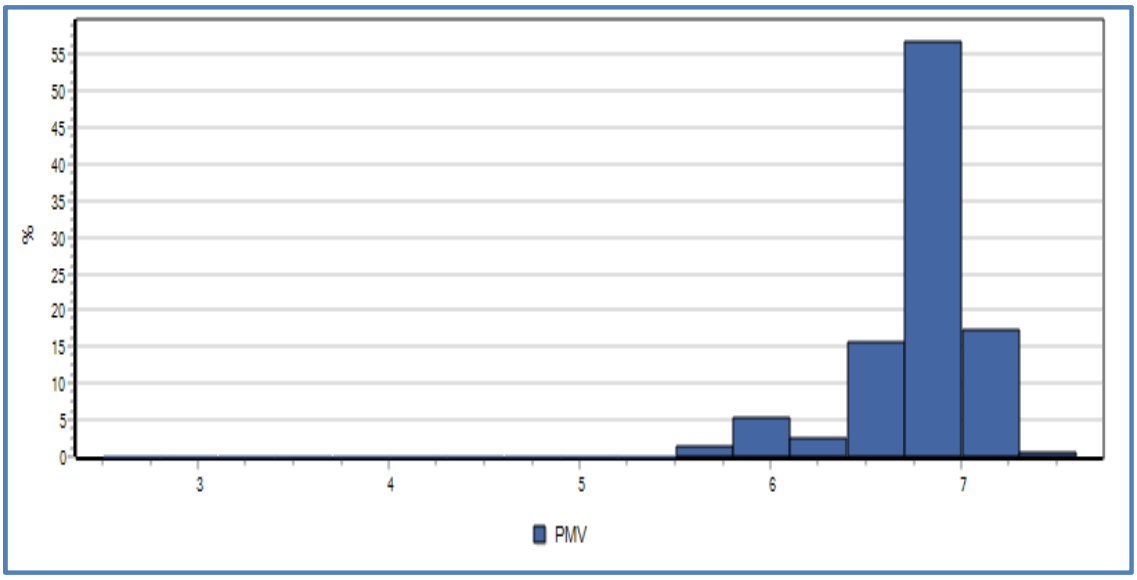

Figure (5-26): Percentage value of PMV for Haifa Street at noon, at 1.5 m above the ground.

On an average, more than 95% of Haifa Street district is characterized by a PMV more than 6, while (PM) has only about 54% of its surface, 46 % of its territory with a PMV between 4 and 6. That means the new design model has better thermal conditions than Haifa Street.

5.12 Evaluating the Results at a Typical Day in Summer

We select 22 June in the same year 2010 to assess thermal comfort in a typical day in summer. The basic meteorology settings for the initial conditions were 2.4 m/s for the wind velocity and 315 deg. for the wind direction. The simple forcing for the air temperature and the relative humidity are used along one day period, with a minimum air temperature of 30 ℃ at 6 am and a maximum value of 40 ℃ at 7 pm. The relative humidity was minimum (25 %) at 2 pm, and it was maximum at 8 am (47%). The total simulation time was 24 hours. We compare the results of air temperature, wind speed, the mean radiant temperature, and PMV between Haifa Street and the proposal model in a typical day in summer. Figures (5-27) and (5-28) depict the percentage value of air temperature for Haifa Street and the (PM) at noon respectively.

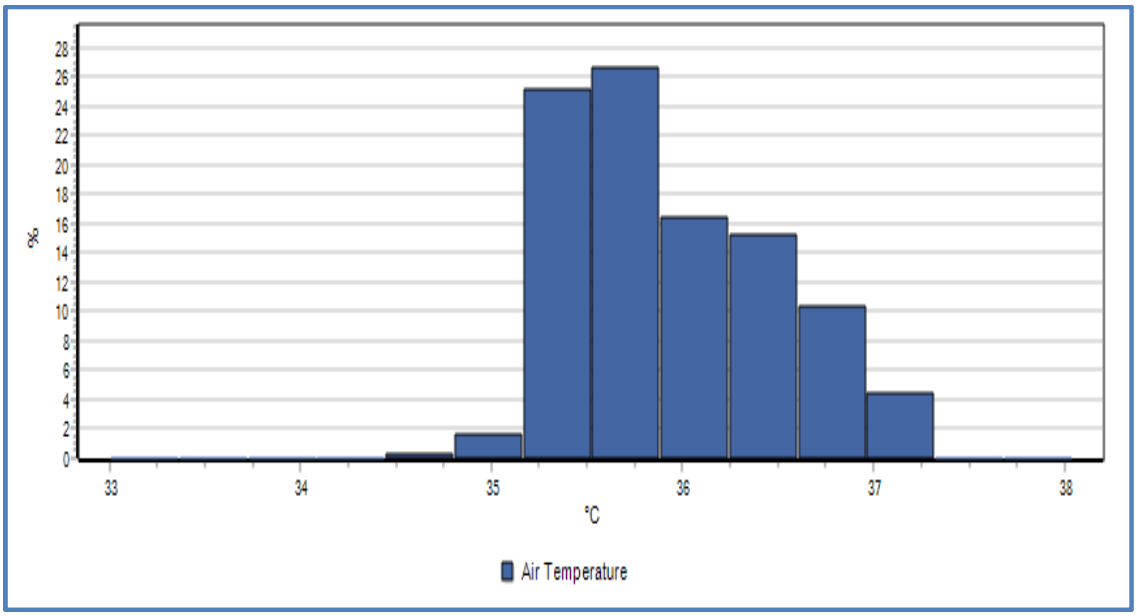

Figure (5-27): Percentage value of air temperature for Haifa Street at noon, at 1.5 m above the ground.

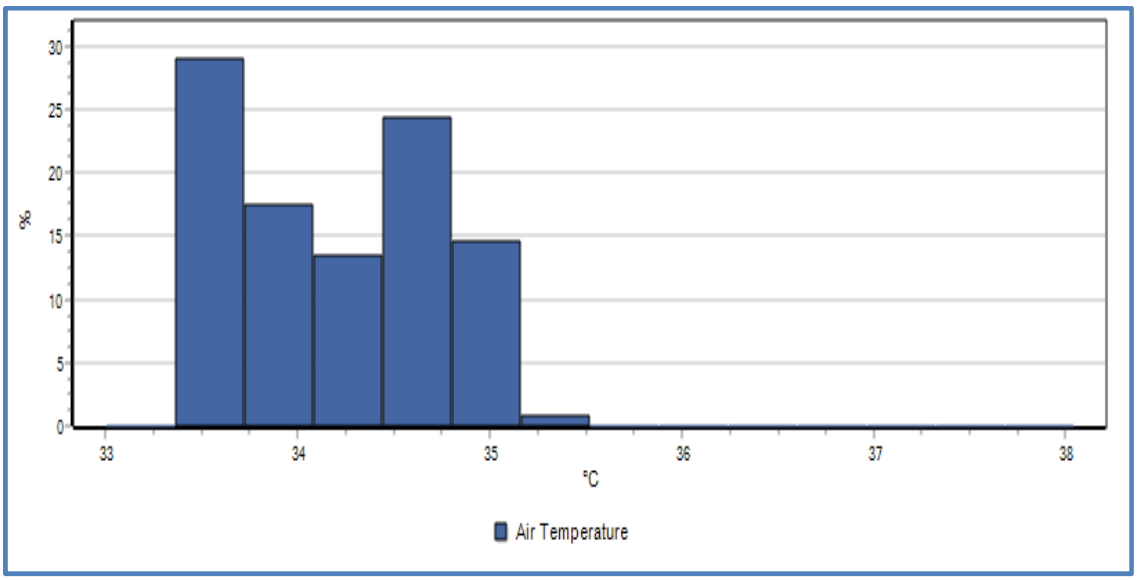

Figure (5-28): Percentage value of air temperature for the (PM) at noon, at 1.5 m above the ground.

Thanks to the new design the temperature went below 35℃.

The results of the mean radiant temperature, Figs (5-29) and (5-30) reveal a decrease of 10.5 ℃ in the (PM) model in a proportion of 90%.

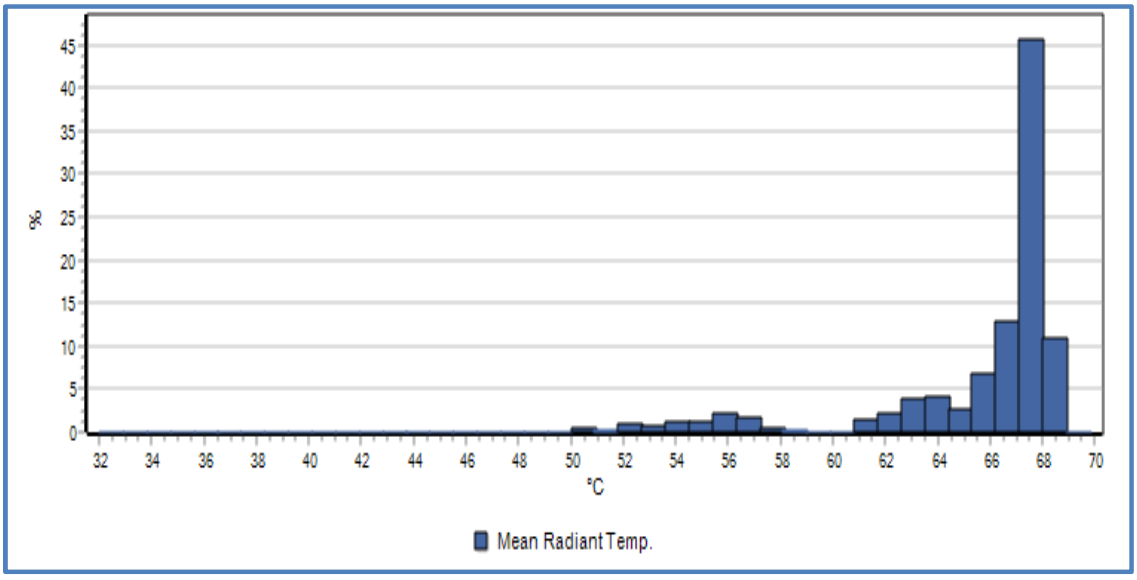

Figure (5-29): Percentage value of the mean radiant temperature for Haifa Street at noon, at 1.5 m above the ground.

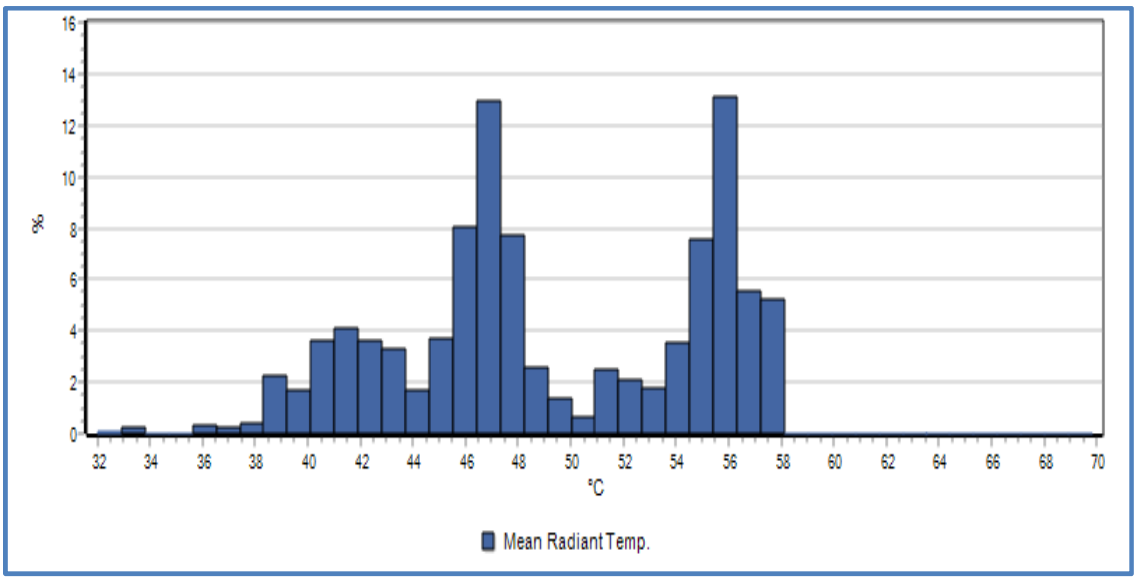

Figure (5-30): Percentage value of the mean radiant temperature for the (PM) at noon, at 1.5 m above the ground.

For PMV results, Figs (5-31) and (5-32) on an average, more than 99% of Haifa Street district is described by a PMV more than 4, while PM has only about 32% of its surface, 68 % of its area with a PMV between 2.5 and 4. That means the new design model has better thermal conditions than Haifa Street at the typical day in summer.

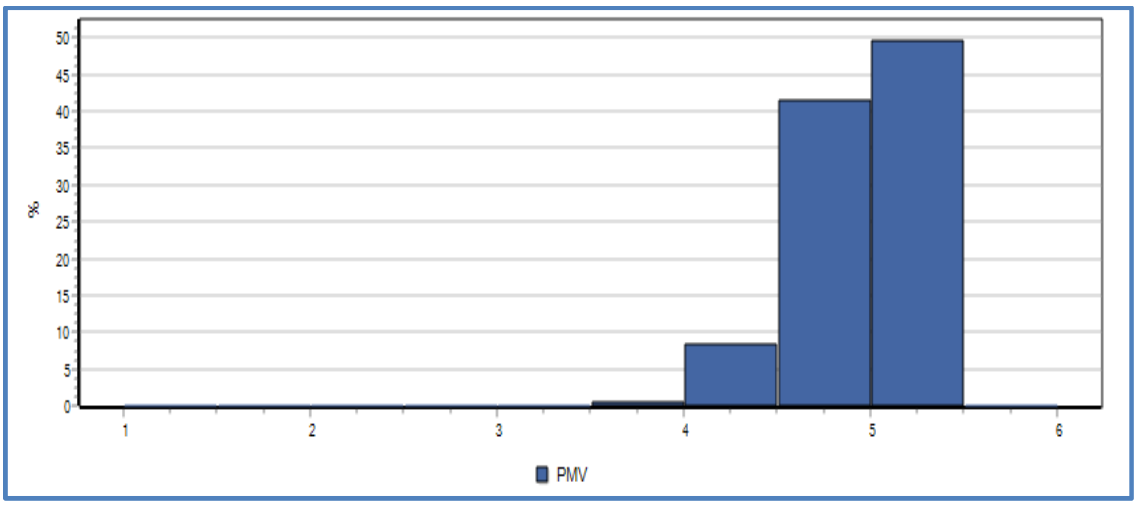

Figure (5-31): Percentage value of PMV for Haifa Street at noon, at 1.5 m above the ground.

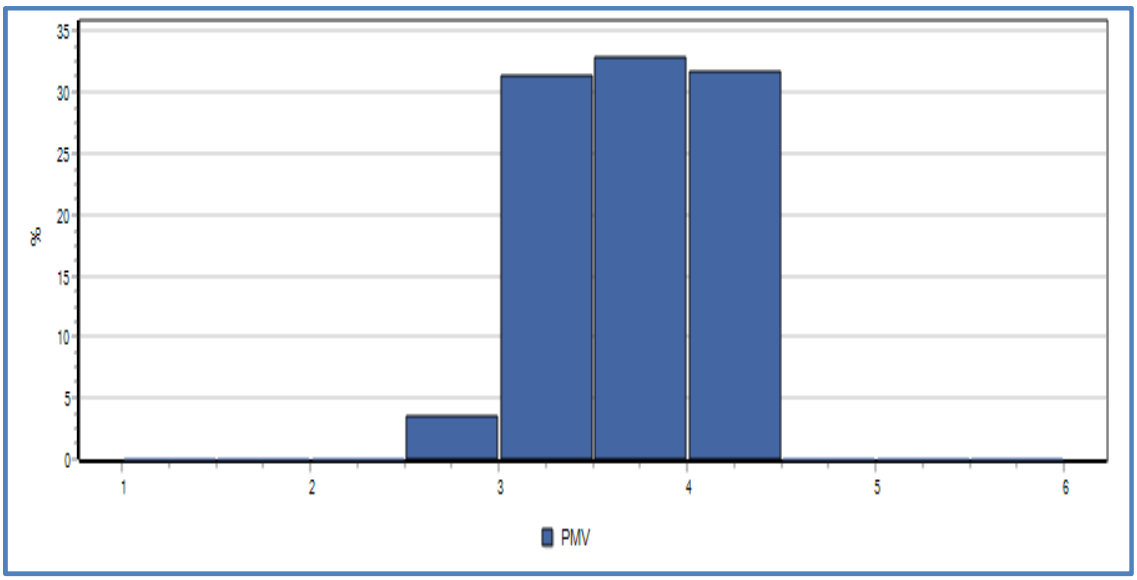

Figure (5-32): Percentage value of PMV the (PM) at noon, at 1.5 m above the ground.

5.13 Conclusions

1. Regarding Tmrt and PMV results in hottest day conditions, the results revealed that the proposal model has better thermal conditions than Haifa Street.

2. The highest values of Tmrt were recorded in Haifa Street, due to the high level of the shortwave and long wave radiation emitted from surrounding surfaces. Tmrt is lower in the proposal model, as more shadow is created by pergolas and vegetation.

3. Vegetation and parasols in the new design play an important role in providing the appropriate shade, which helps to reduce the air temperature, also, to lessen the air movement. We conclude that the maximum effect of vegetation and pergolas is observed in typical day conditions. The effect of shading obtained from vegetation and pergolas play a vital role to moderate the results of the air temperature, Tmrt, and PMV.

4. Regarding the results of the typical day conditions, we notice a significant decrease in the air temperature, Tmrt, and PMV for the PM. The new design model achieved an improvement on the thermal comfort.

5. Large spacing between buildings does not look like appropriate in the design of cities in an arid climate: the aspect ratio (H/W≥1) contributes to increase heat absorbed by buildings and ground surfaces.

6. The design criteria for the PM could be adopted in hot, arid climates that could enhance the outdoor thermal comfort.

CHAPTER SIX

CONCLUSIONS AND PERSPECTIVES

6.1 Conclusions

The main conclusions obtained from this work can be summarized as follows:

1. The ancient homebuilders tried to adopt construction methods to suit the climate conditions and achieve appropriate thermal comfort for the users. The results of this work confirm that traditional houses in Baghdad represent a better solution compared to a Western design in the context of an extreme climate during hot and arid summers.
2. The results of this study proved that Western-type high-rise buildings do not provide the outdoor comfort level expected in the environment of Baghdad, especially in hot and dry weather in summer.
3. In Haifa Street district: the lack of vegetation and shadows, the large distance between buildings lead to an increase in the amount of heat absorbed by the surfaces of buildings and ground during daytime and therefore an increase the amount of heat released at night. All such can lead to the occurrence of the Urban Heat Island.
4. The mean radiant temperature in a hot, arid climate appears to be influenced essentially by the urban configuration, the sky view factor, the shadow patterns, and the width of the internal passages between buildings. These parameters play a significant role in the evaluation of bioclimatic conditions and outdoor thermal comfort.
5. Construction materials play an important role in a hot, arid climate: the use of thick brick walls on the ground floor, and as walls overlooking the courtyard help to delay and reduce the heat gains from the hot exterior to the cooler interior and accordingly keep the interior relatively cool during the day in summer.
6. Shadings pattern reduce the effect of solar radiation on building facades and ground surfaces. Accordingly, enhancing them to improve the thermal comfort is a good idea. The characteristics of shadings should be taken into account by professionals of the urban built environment to improve the thermal comfort outdoors, and lessen the effect of the Urban Heat Island, especially in extreme climate.

7. PET and PMV results, showed that Al-Rasheed Street has thermal conditions better than Haifa Street.
8. Noticeable is that highest value of the mean radiant temperature was recorded in Haifa Street due to the high amount of the short wave and long wave emitted from the surroundings surfaces.
9. The maximum effect of vegetation and pergolas is observed in typical day conditions in summer. Shadings obtained from vegetation and pergolas play a significant role to enhance thermal comfort.
10. Narrow passages contribute to provide shadings at daytime and minimize the amount of heat absorbed by the ground which leads to enhancing thermal comfort.
11. Western - design may not meet the requirements of the urban design in hot, arid climate without taking into consideration the pedestrians thermal comfort.
12. In the hottest day in summer, the new model proposed in the last chapter of the thesis seems to provide better thermal conditions than Haifa Street, due to the effect of shadows and vegetation.
13. In the typical day in summer, the results of Tmrt and PMV showed that the new model proposed in the last chapter of the thesis has thermal conditions better than Haifa Street.

6.2 Perspectives

The evidence and conclusions from this work suggest the following recommendations preferably be taken into account in urban design in the hot, dry climate.

1. In a hot, arid climate, shading patterns and greenery strategies should be adopted for improving thermal comfort. The solar radiation intercepted by twigs and leaves of trees provides a natural protection of outdoor spaces, mitigation of temperatures and reduce energy consumption on cooling indoor spaces.
2. Assessing the effect of mitigation strategies of shadings and vegetation on the thermal comfort and climate change should be evaluated by the thermal indices Tmrt, PET and PMV in hot, arid climate. The use of others indices such as UTCI should be considered.

3. In a hot, arid climate it is advisable to design corridors, arcs, parasols, and colonnades to protect pedestrians and provide the sufficient thermal comfort.
4. The design criteria for the new model proposed in the last chapter of the thesis could be adopted in hot, arid climates that could enhance the outdoor thermal comfort.

Abreu-Harbich L., V., Labaki C., L. Matzarakis A., **Effect of Tree Planting Design and Tree Species on Human Thermal Comfort in the Tropics**, Landspace and Urban Planning 138 (2015) 99-109.

Agha R., **Traditional Environmental Performance: The Impact of Active Systems upon the Courtyard House Type, Iraq,** Journal of Sustainable Development Published by Canadian Center of Science and Education 8 (2015).

Akbari H., Levinson R., and Rainer L., **Monitoring the Energy-use Effects of Cool Roofs on California Commercial Buildings**, Energy and Buildings 37 (2005) 1007-1016.

Akbari H., Matthews H., **Global Cooling Updates: Reflective Roofs and Pavements**, Energy and Buildings 55 (2012) 2-6.

Al-Ani M., **Urban Prediction - Towards a New Generation to Redevelop the Arabic-Islamic City**. PhD Thesis, University of Baghdad, College of Engineering, Department of Architectural Engineering, Iraq (2011).

Alaoui J., and Tahiri M., **Analysis of Canyon Aspect Ratio Impact on Urban Heat Island and Buildings Energy Construction in FEZ Climatic Zone, Morocco,** ARPN Journal of Engineering and Applied Sciences 11 (2016) 3059-3073. .

Al-Azzawi S., **A descriptive, Analytical and Comparative study of Traditional Courtyards Houses and Modern non-Courtyards Houses in Baghdad,** PhD thesis**,** Bartlett School of Architecture and Planning University College, University of London (1984).

Al-Azzawi S., **Analytical study of environmental houses in Kadhimiya,** Baghdad Municipality Conference Traditional city centers, Baghdad Municipality (2010).

Ali-Toudert F. Mayer H., **Numerical Study on the Effects of Aspect Ratio and Orientation of an Urban Street Canyon on Outdoor Thermal Comfort in Hot and Dry Climate**, Building and Environment 41 (2006) 94-108.

Ali-Toudert F. Mayer H., **Thermal Comfort in an East-West Oriented Street Canyon in Freiburg (Germany) Under Hot Summer Conditions**, Theoretical and Applied Climatology. 87 (2007) 223-237.

Ali-Toudert F., **Dependence of Outdoor Thermal Comfort on Street Design in Hot and Dry Climate**, PhD thesis, Freiburg, Germany (2005).

Ali-Toudert F., Mayer H., **Effects of Asymmetry, Galleries, Overhanging Facades and Vegetation on Thermal in Urban Street Canyons**, Solar Energy 81 (2007) 742-754.

Al-jumaili S., **Street orientations: The first step towards a sustainable place.** American Journal of Environmental Protection 3 (2014) 305-317.

Allegrini J., Kämpf J., Dorer V., and Carmeliet J., **Modelling the Urban Microclimate and its influence on Building Energy Demands of an Urban Neighborhood**. CISBAT Lausanne, Switzerland (2013) 4-6.

Al-Mebayedh H., **Climate Changes and Its Effects on the Arab Area.** APCBEE Procedia 4th International Conference on Environmental Science and Development-ICESD 5 (2013) 1-5.

Alousi A., Haifa **Street Development 1981-1985**, Republic of Iraq, Amanat Alasema. Technical studies-Baghdad, Reinicke International Consulting Gmbh-Stuttgart (1985).

Ambronsini D., Galli G., Mancini B., Nardi I., Sfarra S., **Evaluating Mitigation Effects of Urban Heat Island in a Historical Small Center with the Envi-met Climate Model**. Sustainability 6 (2014) 7013-7029.

Arnfield A., J., **Street Design and Urban Canyon Solar Access. Energy and Buildings** 14 (1990) 117-131.

Arnfield A., **Two Decades of Urban Climate Research** : **A review of Turbulence, Exchanges of Energy and water, and the Urban Heat Island**, International Journal of Climatology 23 (2003) 1- 26.

Arthur- Hartranft S., Carlson T., and Clarke K., **Satellite and Ground – Based Microclimate and hydrologic Analysis Coupled with a Regional Urban Growth Model**, Remote Sensing of Environment 86 (2003) 385- 400.

ASHRAE, Standard 55, **Thermal Environmental Conditions for Human Occupancy,** ANSI, American Society of Heating Refrigerating and Air- Conditioning Engineering, INC (2004).

ASHRAE, Standard 55, **Thermal Environmental Conditions for Human Occupancy**, American National Standard (2012).

Attia S., and Duchhart I., **Bioclimatic Landscape Design in Extremely Hot and Arid Climates.** 27th International Conference of Passive and Low Energy Architecture, Louvain La Neuve, Belgium (2011) 13-15.

Auliciems A. Szokolay S., V., **Passive and Low Energy Architecture International Design Tools and Techniques**, PLEA: Passive and Low Energy Architecture International in association with Department of Architecture, The University of Queensland (2007).

Bakarman M. and Chang J., **The Influence of Height/Width Ratio on Urban Heat Island in Hot-Arid Climates.** Procedia Engineering 118 (2015) 101-108.

Bejan A., **Convection Heat Transfer**. 2nd Ed. John Wiley and Sonc, Inc. United States, (1995).

Bennet M. and Ewenz C., **Increased Urban Heat Island Effect due to Building Height Increase.** 20th International Congress on Modelling and Simulation, Adelaide, Australia (2013) 1-6.

Bianca S., Yamada S., Fethi I., and Lombardi G., **Rusafa Study on Conservation and Redevelopment of Historical Centre of Baghdad City**. JCP, Inc., Japan Planners, Architectures and Consulting Engineers (1984).

Blazejezyk K., Epstein Y., **Comparison of UTCI to Selected Thermal Indices**, International Journal Bio-meteorological, 56 (2012) 515-535.

Borbora J., Kumar Das A., **Summertime Urban Heat Island Study for Guwahati City India**, Sustainable Cities and Society 11 (2014) 61- 66.

Bouyer J., Musy M., Huang Y., and Athamena K., **Mitigating Urban Heat Island Effect by Urban Design: Forms and Materials**, Fifth Urban Research Symposium (2009).

Brode P., Fiala D., Blazejczyk K., Epstein Y., Holmer I., Jendritzky G., Kampmann B., Richards M., Rintamaki H., Shitzer A., and Havenith G., **Calculating UTCI Equivalent Temperature,** Poster presentation at the 13th International Conference on Environmental Ergonomic, Boston, Massachusetts, USA (2009) 2-7.

Brown H., Katscherian D., Carter M., and Spickett J., **Cool communities: Urban Trees, Climate and Health.** World Health Organization, workshop held at the Department of Planning Curtin University (2013).

Brown M., J., Grimmond S., and Ratti C.,**Comparison of Methodologies for Computing Sky View Factor in Urban Environments,** International Society of Environnemental Conf. Tempe, AZ (2001).

Bruse M. and Fleer H., **Simulating Surface- Plant – Air Interactions Inside Urban Environments with a Three Dimensional Numerical Model.** Environmental Modeling and Software 13 (1998) 373-384.

Bruse, M. ENVI-met http://www.envi-met.info/hg2e/doku.php?id=lbc-types (2015b).

Busato F., Lazzarin R., M., Noro M., **Three Years of Study of Urban Heat Island in Padua: Experimental Results**, Sustainable Cities and Society 10 (2014) 214- 258.

Carlson T., Arthur S., **The Impact of Land Use - Land Cover Changes due to Urbanization on Surface Microclimate and Hydrology: a Satellite Perspective**, Global and Planetary Change 25 (2000) 49-65

Carlson T., Dodd J., Benjamin S., and Cooper J., **Satellite Estimation of the Surface Energy Balance Moisture Availability and Thermal Inertia,** American Meteorological Society 20 (1981) 67- 87.

Charabi Y., Bakhit A., **Assessment of Canopy Urban Heat Island of a Coastal Arid Tropical City: The Case of Muscat, Oman**, Atmospheric Research 101 (2011) 215-227.

Chen L., and Ng E., A., **Sky View Factor Analysis of Street Canyons and Its Implication for Urban Heat Island Intensity,** 26th Conference on Passive and Low energy Architecture, Quebec City, Canada (2009) 22-24.

Chen L., Ng E., An X., Ren C., Lee M., Wang U., and He Z., **Sky View Factor Analysis of Street Canyons and its Implications for Daytime Intra-Urban Air Temperature Differentials in High-Rise, High-Density Urban Areas of Hong Kong: a GIS-Based Simulation Approach.** International Journal of Climatology 32 (2012) 121-136.

Chen Y., Lin T., Matzarakis A., **Comparison of Mean Radiant Temperature from Field Experiment and Modelling : A Case Study in Freiburg, Germany**, Theoretical and Applied Climatology 118 (2014) 535-551.

Cho S., and Mohammedzadeh N., **Thermal Comfort Analysis of a Traditional Iranian Courtyard for the Design of Sustainable Residential Buildings**. 13th Conference of International Building Performance Simulation Association, Chambéry, France (2013) 26-28.

Chun B., Guldmann J., M., **Spatial Statistical Analysis and Simulation of the Urban Heat Island in High- Density Center Cities,** Landscape and Urban planning 125 (2014) 74- 88.

Corgnati S.,P., Gameiro da Silva M., Ansaldi R., Asadi E., Costa J.,J., Filippi M,, Kaczmarczyk J., Melikov A.,K,, Olesen B.,W., Popiolek Z., Wargocki P., **Indoor Climate Quality Assessment-Evaluation of Indoor Thermal and Indoor Air Quality**. Guide Book 14. Federation of European Heating, Ventilation and Air-conditioning Associations Rehva, Brussels (2011).

Coseo P., Larsen L., **How Factors of Land Use /Land Cover, Building Configuration, and Adjacent Heat Sources and Sinks Explain Urban Heat Islands in Chicago**, Landscape and Urban Planning 125 (2014) 117-129.

Cui Y., Xu X., Dong J., and Qin Y., **Influence of Urbanization Factors on Surface Urban Heat Island Intensity: A Comparison of Countries at Different Developmental Phases,** Sustainability 8 (2016) 706-720.

Dai Q., and Schnabel A., **Relationship between Mean Radiant Temperature and Building Type for pedestrians in Rotterdam,** Spriner-Verlag Berlin Heidlberg (2013).

Dardel S., **Climate Smart Fortaleza**. Thesis for a diploma in Environmental Engineering, Department of Engineering, Faculty of Engineering, Lund University (2015).

Dorer V., Allegrini J., Orehounig K., Moonen P., Upadhyay G., Kämpf J., and Carmeliet J., **Modelling the Urban Microclimate Impact on the Energy Demand of Building and Building Clustres.** 13th Conference of International Building Performance Simulation Association, Chambéry, France (2013) 26-28.

Elnabawi M., Hamza N., Dudek S., **Urban morphology impact on microclimate of the Fatimid city, Cairo, Egypt.** International Conference on "Changing Cities": Spatial, morphological, formal and socio-economic dimensions Skiathos island, Greece (2013).

Elsayed I., **Mitigation of the Urban Heat Island of the City of Kuala Lumpur**, Malaysia. Middle-East Journal of Scientific Research 11 (2012) 1602-1613.

Erell E., Pearlmutter D., Williamson T., **Urban Microclimate Designing the Spaces between Buildings**, New York (2011).

Fabbri K., **Indoor Thermal Comfort Perception**, Springer (2015).

Fahmy M., A., R., **Interactive Urban Form Design of Local Climate Scale in Hot Semi-Arid Zone,** PhD thesis, The University of Sheffield School of architecture, UK (2010).

Fahmy M., and Sharples S., **On the Development of an Urban Passive Thermal Comfort System in Cairo, Egypt**, Building and Environment 44 (2009) 1907-1916.

Fanger P., O., **Assessment of Man's Thermal Comfort in Practice**, British Journal of Industrial Medicine 30 (1973) 313-324.

Figuerola P., I., Mazzeo N., A., **Urban – Rural Temperature Differences in Buenos Aires**, International Journal of Climatology 18 (1998) 1709-1723.

Gago E., Roldan J., Pacheco-Torres R., Ordonez J., **The City and Urban Heat Island : A review of Strategies to Mitigate Adverse Effects**, Renewable and Sustainable Energy Reviews 25 (2013) 749-758.

Ghaffarianhoseini A., Berardi U., and Ghaffarianhoseini A., **Thermal Performance Characteristics of Unshaded Courtyards in Hot and Humid Climates.** Building and Environment 87 (2015) 154-168.

Giannopoulou K., Livada I., Santamouris M., Saliari M., Assimakopoulos M., and Caouris Y., **On the Characteristics of the Summer Urban Heat Island in Athens, Greece**, Sustainable Cities and Society 1 (2011) 16-28.

Giguère M., **Urban Heat Island Mitigation Strategies**, Direction de la santé environnementale et de la toxicologie, The Institut national de santé publique du Québec (2009).

Givoni, B., **Climate Consideration in Urban and Building Design**, New York, Van Nostrand Reinhold (1998).

Global Cool Cities Alliance, **A Practical Guide to Cool Roofs and Cool Pavements** (2012).

Gray K., A., and Finster M., E., **The Urban Heat Island, Photochemical Smog, and Chicago: Local Features of the Problem and Solution,** Department of Civil Engineering North-western, University Evanston (1999).

Guneralp B., Seto K., C**., Environmental Impacts of Urban Growth from an Integrated Dynamic Perspective: A Case Study of Shenzhen, South China.** Global Environmental Change 18 (2008) 720-735.

Hassoon, A., F., **Assessment of Air pollution Elements Concentrations in Baghdad City from Periods (May-December) 2010**, International Journal of Energy and Environment 6 (2015) 191-200.

Hathway E. A., Sharples S., T**he Interaction of Rivers and Urban form in Mitigation the Urban Heat Island Effect**: **A UK Case Study**, Building Environment 58 (2012) 14-22.

Hedquist B., Sabatino S., Fernado H., Leo L., Brazel A., **Results from the Phoenix Arizona Urban Heat Island Experiment**. The Seventh International conference on Urban climate Yokohama, Japan (2009).

Heidari S., **Thermal Comfort in Iranian Courtyard Housing a Field Study of Thermal Environments in Western Iran.** PhD thesis, School of Architecture, The University of Sheffield, UK (2000).

Henry M., C., **The Heritage Building Envelope as a Passive and Active Climate Moderator: Opportunities and Issues in Reducing Dependency on Air-Conditioning,** Contribution to the Experts' Roundtable on Sustainable Climate Management Strategies, Tenerife, Spain (2007).

Herbert J., Johnson G., Arnfield A, **Modeling the Thermal Climate in City Canyons.** Environmental Modelling and Software 13 (1998) 267-277.

Hove L., Steeneveld G., Jacobs C., Heusinkveld B., Elbers J., Moors E., and Holtslag A., **Exploring the Urban Heat Island Intensity of Dutch cities**, Alterra part of Wageningen UR Wageningen (2011).

Howard L., **The Climate of London,** Gerald Mills, I-III, London (1833).

Huttner S., and Bruse M., **Numerical Modelling of the urban Climate a Preview on ENVI-met 4.0** ,The Seventh International Conference on Urban Climate Yokohama, Japan (2009).

Huttner S., Bruse M., Dostal P., **Numerical Modelling of the Urban Climate-A Preview on Envi-met 4.0**.. Environmental Modelling Group EMG, Johannes-Gutenberg University Mainz Johann-Joachim-Becher-Weg 21, D-55099 Mainz, Germany (2009).

Huttner S., Bruse M., Dostal P., **Using ENVI-met to simulate the Impact of Global Warming on the Microclimate in Central European Cities.** 5th Japanese-German Meeting on Urban Climatology (2008) 307-312.

Huttner S., **Further Development and Application of the 3D Microclimate Simulation Envi-met**. PhD Thesis, Mainz, Germany (2012).

Idczak M., Groleau D., Mestayer P., Michel Rosant J., and François Sini J., **An Application of the Thermo-Radiative Model SOLENE for the Evaluation of Street Canyon Energy Balance.** Building and Environment 45 (2010) 1262-1275.

Jamei E., Rajagopalan P., **Urban Growth and Pedestrian Thermal comfort**, 49th International Conference of the Architecture Science Association, the Architecture Association and the University of Melbourne (2015) 907-918.

Johnson G., Oke T., Lyons T., Steyn D., Watson I., and Voogt J., **Simulation of Surface Urban Heat Islands Under Ideal Conditions Journal at Night Part 1: Theory and Tests Against Field Data**. Boundary-Layer Meteorology 56 (1991) 275-294.

Johnsson G. and Hunter L., A **numerical Study of Dispersion of Passive Scalars in City Canyons:** Boundary-Layer Meteorology 75 (1995) 235-262.

Kalz D., and Pfafferott J., **Thermal Comfort and Energy-Efficient Cooling of Non-residential Buildings** (2014).

Katul G., Mahrt L., Poggi D., and Sanz C., **One and Two Equation Models for Canopy Turbulence.** Nicholas School of the Environment and Earth Sciences, Duke University, Durham (2003).

Katzschner L., Burghardt R., Campe S., **Microclimatic Analysis of Arnhem. Future Cities,** Urban Networks to Face Climate Change. Department of Envirnmental

Meteorology Institute for architecture, urban Planning and Landscpace Design. University of Kassel, Germany (2012).

Kenawy I., Afifi M., Mahmoud A., **The Effect of Planting Design on Thermal Comfort in Outdoor Spaces.** First International Conference on Sustainability and Future. The British University in Egypt. Loughborough University, FISC (2010).

Ketterer C., Matazarakis A., **Comparison of Different Methods for the Assessment of the Urban Heat Island in Stuttgart, Germany**, International Journal Bio-meteorological 59 (2015) 1299-1309.

Kolokotroni M., Ren X., Davies M., and Mavrogianni M., **London's Urban Heat Island: Impact on Current and Future Energy Consumption in Office Buildings**, Energy and Buildings 47 (2012) 302- 311.

Lahme E. and Bruse M., **Microclimatic effects of a small urban park in densely built–up areas: Measurements and model simulations**. The European Commission in the 5th Framework Program under the contract (2002).

Landsberg, E., **The Urban Climate**, Maryland, Academic Press (1981).

Landsberg, H.,**The Meteorologically Utopian City**, Bulletin of the American Meteorological Society 54 (1973) 86–89.

Lemonsu A., Masson V., **Simulation of a Summer Urban Breeze over Paris**. Boundary-Layer Meteorology 104 (2002) 463-490.

Li H., **Evaluation of Cool Pavement Strategies for Heat Island Mitigation Improving Outdoor Thermal Environment in Hot Climates through Cool Pavement Design Strategies,** PhD Thesis, Civil and Environmental Engineering, University of California (2012).

Mahgoub M., Hamza N., Dudek S., **Microclimatic Investigation of Two Different Urban Forms in Cairo , Egypt: Measurements and Model Simulations**. Building Simulation Cairo 2013 - Towards Sustainable and Green Built Environment, Cairo, Egypt (2013).

Makaremi N., Salleh E., Jaffar M., Z., Hosein A., Hoseini G.,**Thermal Comfort Conditions of Shaded Spaces in Hot and Humid Climate of Malaysia**., Building and Environmental 48 (2012) 7-14.

Maleki A., Mahdavi A., **Evaluation of Urban Heat Islands Mitigation Strategies Using 3-Dimensional urban Micro-Climate Model ENVI-met.** Asian Journals of civil Engineering (BHRC) 17 (2016) 357-371.

Malekzadeh M., **Positioning of Outdoor Space in House Design - An Energy Efficiency and Thermal Comfort Perspective**. PhD thesis, Loughborough, Leicestershire, United Kingdom (2009).

Martinelli L., Lin T., Matzarakis. **A., Assessment of the Influence of Daily Shading Pattern on Human Thermal Comfort and Attendance in Rome during Summer Period,** Building and Environment 92 (2015) 30-38.

Masson V., **A Physically-Based Scheme for the Urban Energy Budget in Atmospheric Models**. Boundary-Layer Meteorology 94 (2000) 357-397.

Matzarakis A., and Amelung B., **Physiological Equivalent Temperature as Indicator for Impacts of Climate Change on Thermal Comfort of Humans.** Seasonal Forecasts, Climatic Change and Human Health. Springer (2008).

Matzarakis A., and Mayer H., **Applications of a universal thermal index: physiological equivalent temperature.** International Journal Biometeorology 43 (1999) 76-84.

Matzarakis A., Rutz F., and Mayer H., **Modelling Radiation Fluxes in Simple and complex Environment-Application of the Ray Man Model**, International Journal Biometeorology 51 (2007) 323-334.

Matzarakis A., Rutz F., and Mayer H., **Modelling Radiation Fluxes in Simple and Complex Environment: Basis of the Ray Man Model,** International Journal Biometeorology 54 (2010) 131-139.

Medany M., **Impact of Climate Change on Arab Countries. In: Arab Environment Future Challenges,** Eds Mostafa k. Tolba and Najib w. Saab, Report of the Arab Forum for Environment and Development (2008) 127-136.

Mobaraki A., **Strategies for Mitigating Urban Heat Island Effects in Cities: Case of Shiraz City Center.** Master of Science in Urban Design, Eastern Mediterranean University North Cyprus (2012).

Monam A., Ruckert K., **The Dependence of Outdoor Thermal Comfort on Urban Layouts,** German-Iranian Research Project. Young Cities. Developing Energy-Efficient Urban Fabric in the Tehran-Karaji Region. 10623 Berlin-Germany (2013).

Mont´avez P., Gonz´alez-Rouco F., and Valero F., **A Simple Model for Estimating the Maximum Intensity of Nocturnal Urban Heat Island**, International Journal of Climatology 28 (2008) 235- 242.

Morris C., Simmonds I., **Associations Between Varying Magnitudes of the Urban Heat Island and the Synoptic Climatology in Melbourne**, Australia, International Journal of Climtology 20 (2000) 1931- 1957.

Mostafa B., and Alireza M., **The Impact of Sky View Factor on Outdoor Thermal Comfort; Case Study: Tehran Urban Parks**. Journal ARMANSHAHR 3 (2012) 23-34.

Murakami, S., **Environmental Design of Outdoor Climate Based on CFD**, Fluid Dynamics Research 38 (2006) 108-126.

Nakamura Y., and Oke T., Wind, Temperture and stability Conditions in an East-West Oriented Urban Canyon. Atmospheric Environment 22 (1988) 2691-2700.

Nasrallah H., A., **Analysis of the Kuwait City Urban Heat Island,** International Journal of Climatology 10 (1990) 401-405.

Nichol J., **High-Resolution Surface Temperature Patterns Related to Urban Morphology in Tropical City**: **A satellite-Based Study**, American Meteorological (1996) 135-146.

Norton, B. A., Coutts, A. M., Livesley, S. J., Harris, R. J., Hunter, A. M., and Williams, N. S. G. **Planning for Cooler Cities: A Framework to Prioritise Green Infrastructure to Mitigate High Temperatures in Urban Landscapes**. Landscape and Urban Planning 134 (2015) 127-138.

Nuruzzaman M., **Urban Heat Island: Causes, Effects and Mitigation Measures - A Review**, International Journal of Environmental Monitoring and Analysis 3 (2015) 67-73.

Oke T., **Canyon Geometry and the Nocturnal Urban Heat Island: Comparison of Scale Model and Field Observations**, Journal of Climatology 1 (1981) 237- 254.

Oke T., **City Size and the Urban Heat Island**, Atmospheric Environment 7 (1973) 769-779.

Oke T., Johnson G., T., Steyn D., G., Watson I., D., **Simulation of Surface Urban Heat Islands Under Ideal Conditions at Night Part 2** Diagnosis of Causation 56 (1991) 275- 294.

Oke T., **Street Design and Urban Canopy Layer Climate**. Energy and Buildings 11 (1998) 103-113.

Oke T., **The energetic Basis of the Urban Heat Island**, Quarterly Journal of the Royal Meteorological Society 108 (1982) 1-24.

Oke, T., **Boundary Layer Climates**, Second Edition, Taylor and Francis group, London and New York (1987).

Oke, T., **Initail Guidance to Obtain Representative Meteorological Observations at Urban Sites. Instruments and observing Methods**, World Meteorological Organization, instruments and observing methods, report No. 81 Canada (2006).

Oke, T., **Street Design and Urban Canopy Layer Climate**, Energy and Buildings 11(1988) 103-113.

Oke, T., **The Distinction Between Canopy and Boundary-Layer Urban Heat Islands**, Atmosphere 14 (1976) 277- 268.

Olàh A., **The possibilities of Decreasing the Urban Heat Island**, Applied Ecology and Environmental Research 10 (2012) 173-183.

Ozkeresteci I., Crewe K. and Bruse M., **Use and Evaluation of the ENVI-met Model for Environmental Design and Planning: an Experiment on Linear Parks**. The 21st International Conference (ICC). Durban, South Africa (2003) 10-16.

Panariti A., T., Maliqari A., Tashi P., **The Impact of Urban Texture in Outdoor Thermal Comfort,** International Journal of Science and Research 4 (2014) 1629-1633.

Paramita B., and Fukuda H., **Heat Intensity of Urban Built Environment in Hot Humid Climate Region,** American Journal of Environmental Science 10 (2014) 210-219.

Paramita B., Fukuda H**., Study on the Effect of Aspect Building Form and layout Case Study,** Honjo Nishi Danchi, Yahatanishi, Kitakyushu, Fukuka. Procedia Environmental Science. SuSTAIN (2012).

Pearlmutter, D., Berliner P., and Shaviv E**., Physical Modelling of Pedestrian Energy Exchange within the Urban Canopy**, Building and Environment 41 (2006) 783-795.

Peng S., Piao S., Ciais P., **Surface Urban Heat Island Across 419 Global Big Cities**, Environmental Science Technology 46 (2011) 696-703.

Perrineau H., **Development of a Tool Based on the Thermal Dynamic Simulation Software TRNSYS Which Runs Parameters Studies to Assess Outdoor Comfort with the Perceived Temperature**, INSA, Strasbourg. End-of-Studies Project carried out at TRANSSOLAR in Stuttgart (2013).

Pisello L., A., Santamouris M., Cotanta F., **Active Cool Roof Effect: Impact of Cool Roofs on Cooling System Efficiency**, Advances in Building Energy Research 2 (2013) 209-221.

Polservice, **Housing Technical Standards and Codes of Practice**. Report Two, printed by design office MIASTOPROJEKT-KRAKOW; Ministry of Housing and Construction-State Organization for Housing, Baghdad, Iraq (1982).

Poumanyvong P., Kaneko Sh., **Does Urbanization Lead to Less Energy Use and Lower CO2 Emissions, A cross – Country Analysis**, Ecological Economics 70 (2010) 434-444.

Qasim M., **Continuity Urban Development of Baghdad Historical City Centre between Academic and Practice.** Al-Nahrain University, College of Engineering Architecture Department, Baghdad Consulting Architect and Urban Designer (2015).

Radhi H., Fikry F., Sharples S., **Impacts of Urbanization on the Thermal Behavior of New Built Up Environments: A scoping Study of the Urban Heat Island in Bahrain**, Landscape and Urban Planning 113 (2013) 47- 61.

Radhi H., Sharples S., Assem E., **Impact of Urban Heat Island on the Thermal Comfort and Cooling Energy Demand of Artificial Island-A Case Study of AMWAJ Islands in Bahrain,** Sustainable Cities and Society 19 (2015) 310-318.

Rajabi T., and Abu-Hijleh B., **The Study of Vegetation Effects on Reduction of Urban Heat Island in Dubai, World SB4,** Sustainable Building Conference Series, Barcelona (2014).

Ratti C., Raydan D., and Steemers K., **Building Form and Environmental Performance: Archetypes, Analysis and an Arid climate.** Energy and Buildings 35 (2003) 49-59.

Reifsnyder W., **Radiation Geometry in the Measurement and Interpretation of Radiation Balance,** Agricultural Meteorology 4 (1967) 255-265.

Rizwan A., Dennis Y., Lui Ch., **A review on the Generation, Determination and Mitigation of Urban Heat Island,** Journal of Environmental Sciences 20 (2008) 120-128.

Rosheidat A., **Optimizing the Effect of Vegetation for Pedestrian Thermal Comfort and urban Heat Island Mitigation in a Hot Arid Urban Environment**, PhD thesis, Arizona State University (2014).

Sailor D., **Mitigation of Urban Heat Island - Recent Progress and Future Prospects.** America Meteorological Society 6th Symposium on the Urban Environment and Forum on Managing our Physical and Natural Resources, Portland State University, Portland, USA (2006).

Sailor J., D., **Simulated Urban Climate Response to Modifications in Surface Albedo and Vegetation Cover**, Journal of Applied Meteorology 34 (1995) 1694-1704.

Saiz A., Susana A., **Urban Greenery: Increasing Resilience to Climate change Through Green Roofs and Urban Forestry.** World SB4, Sustainable Building Conference Series, Barcelona (2014).

Salata F., Gllasi I., Vollaro E., L., Bisegna F., Nardecchia F., Coppi M., Gugliermetti F., Vollaro A., L., **Evaluation of Different Urban Microclimate Mitigation Strategies through a PMV Analysis**, Sustainability 7 (2015) 9012-9030.

Santamouris M., Adnot J., AlvarezS., Klitsikas N., Orphelin M., Lopes C., and Sanchez F., **Cooling the Cities : Rafraîchir Les Villes**, École des Mines de Paris (2004).

Santamouris M., **Cooling the Cities-A review of Reflective and Green Roof Mitigation Technology to Fight Heat Island and Improve Comfort in Urban Environment,** Solar Energy (2012) 1-22.

Santamouris M., Papanikolaou N., Koronakis I., Livada I., and Asimakopoulos D., **Thermal and air Flow Characteristics in a Deep Pedestrian Canyon Under Hot Weather Conditions,** Atmospheric Environment 33 (1999) 4503-4521.

Santamouris M., **Using Cool Pavements as a Mitigation Strategy to Fight Urban Heat Island-A review of the Actual Developments.** Renewable and Sustainable Energy Reviews 26 (2013) 224-240.

Setaih K., Hamza N., and Townshend T., **Assessment of Outdoor Thermal Comfort in Urban Microclimate in Hot Arid Areas.** 13th Conference of International Building Performance Simulation Association, Chambéry, France (2013) 26-28.

Shahmohamadi P., Che-Ani A., I., Ramly A., Maulud K., N., A., and Mohd- NorM., F., I., **Reducing Urban Heat Island Effects: A systematic Review to Achieve Energy Consumption Balance,** International Journal of Physical Science 5 (2010) 626-636.

Shahmohamadia P., A.I Che-Ania A.I, Etessamb I., Mauludc K., N., A., and Tawila N., M., **Healthy Environment: The Need to Mitigate Urban Heat Island Effects on Human Health,** Procedia Engineering 20 (2011) 61-70.

Shashua-Bar L., and Hoffman M. E., **Vegetation as a Climatic Component in the Design of an Urban Street an Empirical Model for Predicting the Cooling Effect of Urban Green Areas with Trees**, Energy and Buildings 31 (2000) 221-235.

Shashua-Bar L., Pearlmutter D., and Erell E., **The Influence of Trees and Grass on Outdoor Thermal Comfort in a Hot-Arid Environment,** International Journal of Climatology 31 (2011) 1498-1506.

Shishegar N., **Street Design and Urban Microclimate: Analyzing the Effects of Street Geometry and Orientation on Airflow and Solar Access in Urban Canyons.** Journal of Clean Energy Technologies 1 (2013) 52-56.

Simon H., **Modeling Urban Microclimate Development, Implementation and Evaluation of New and Improved Calculation Methods for the Urban Microclimate Model ENVI-met,** PhD Thesis, Mainz, Germany,2016.

Simone Queiroz da Silveira H., Eleonora Sad de A., and Marialena A., **Daytime thermal comfort in urban spaces: A field study in Brazil.** Building and Environment 107 (2016) 245-253.

Skat, **Climate Responsive Building-Appropriate Building Construction in Tropical and Subtropical Regions.** Fislisbach and Zollikon, First edition, Swiss Centre for Development Cooperation in Technology and Management (1993).

Smith R., K., Roebber J., P., **Green Roof Mitigation Potential for a Proxy Future Climate Scenario in Chicago**, Illinois, Smith and Reobber (2011).

Soomro A., **Eco- Town Planning Design Guidelines for Hot and Dry Climate Regions from Architectural Perspective.** Review and Planning Workshop on Eco Town, Dept. of Architecture Kulliyyah of Architecture and Environmental Design, IIUM, Kuala Lumpur (2012).

Spronken-Smith R.A., and Oke T., **Scale modelling of nocturnal cooling in urban parks.** Boundary-Layer Meteorology 93 (1999) 287-312.

Swadin H., Hoffman M., **Prediction of Urban Air Temperature Variations Using the Analytical CTTC Model.** Energy and Buildings 14 (1990) 313-324.

Swaid H., Bar-El M., and Hoffman M., **A Bioclimatic Design Methodology for Urban Outdoor Spaces.** Theoretical and Applied Climatology 48 (1993) 49-61.

Taeghani M., Tenpierik M., Kurvers S., and Dobbelsteen A., **A Review into Thermal Comfort in Buildings,** Renewable and Sustainable Energy Reviews 26 (2013) 201-215.

Taha H., Konopacki St., Gabersek S., **Impact of Large – Scale Surface Modifications on Meteorological Conditions and Energy Use**, A 10 – Region Modeling Study, Theoretical and Applied Climatology 62 (1999) 175-185.

Taha, H., **Urban Climates and Heat Islands: Albedo, Evapotranspiration, and Anthropogenic Heat**, Energy and Buildings 25 (1997) 99-103.

Taleb D., Abu- Hijleh B., **Urban Heat Island: Potential Effect of Organic and Structured Urban Configurations on Temperature Variations in Dubai**, Renewable Energy 50 (2013) 747-762.

Taleghani M., Tenpierik M., and Dobbelsteen A., V., D., **Environmental Impact of Courtyards-A review and Comparison of residential Courtyards buildings in Different Climates.** Journal of Green Building 7 (2012) 113-136.

Taleghani M., **Dwelling on Courtyards Exploring the Energy Efficiency and Comfort Potential of Courtyards for Dwellings in the Netherlands.** Delft University of Technology, Faculty of Architecture and the Built Environment, Department of Architectural Engineering and Technology (2014).

Tan Z., Lun Lau K., and Ng E., **Urban Tree Design Approaches for Mitigating Daytime Urban Heat Island Effects in a High-Density Urban Environment**. Energy and Buildings 114 (2016) 265-274.

Terjung W., O'Rourke P., **Simulating the Causal Elements of Urban Heat Islands**. Boundary-Layer Meteorology 19 (1980) 93-118.

Thapar H., and Yannas S., **Microclimate and Urban Form in Dubai**. PLEA 2008 – 25th Conference on Passive and Low Energy Architecture, Dublin (2008).

The Masterbuilder (2014) www.masterbuilder.co.in.

Thorsson S., Rocklöv J., Konarska J., Lindberg F., Holmer B., Dousset B., and Rayner D., **Mean Radiant Temperature a Predictor of Heat Related Mortality**, Urban Climate 10 (2014) 332-345.

Townsend C., C., and Guest E., **Flora of IRAQ**. Ministry of Agriculture and Agrarian Reform, Iraq (1974).

Vanessa L., **Measuring and Modelling Spatial Variation of Temperature and thermal Comfort in a Low-Density Neighbourhood in Singapore.** Msc. Thesis Department of Geography National University of Singapore (2014).

Varquez A., **Analyses of Multiple Urban Heat Islands from Global Surface Temperature Datasets,** (Washington State Convention Center), American Meteorological Society (2017).

Voogt J., A. and Oke T., R., **Thermal Remote Sensing of Urban Climates**, Journal of Remote Sensing of Environment 86 (2003) 370-384.

Voogt, J. A., **Urban Heat Islands: Hotter Cities**, Actionbioscience E-Newsletter, (2004).

Walikewitz N., Janicke B., Langner M., and Meier F., **The difference between the mean radiant temperature and the air temperature within indoor environments: A case study during summer conditions.** Building and Environment 84 (2015) 151-161.

Wang Y. and Akbari **H., The Effect of Street Tree Planting on Urban Heat Island Mitigation in Montreal**. Sustainable Cities and Society 27 (2016) 122-128.

Wang Y., and Akbari H., **Effect of Sky View Factor on Outdoor Temperature and Comfort in Montreal**, Environmental Engineering Science 31 (2014) 272-287.

Wang Y., Beradi U., Akbari H., **Comparing the Effects of Urban Heat Island Mitigation Strategies for Tornoto, Canada.** Energy and Building 114 (2015) 2-19.

Wong H., N., Yu Ch**., Study of Green Areas and Urban Heat Island in a Tropical City**, Journal of Habitat International 29 (2005) 547-558.

Yamada T and Mellor G., **A Simulation of Wangara Atmospheric Boundary Layer Data**. Journal of Atmospheric sciences 32 (1975) 2309-2329.

Yamashita S., Sekine K., Shoda M., Yamashita K., and Hara Y., **On Relationships Between Heat Island and Sky View Factor in the Cities of Tama River Basin, Japan**, Atmospheric Environments 20 (1986) 681-686.

Yang F., Lau S., S., Y., and Qian F., **Summertime Heat Island Intensities in Three High –Rise Housing Quarters in Inner-City Shanghai China**, Building Layout, density and Greenery, Building and Environment 45 (2010) 115-134.

Yang J., Wong M., S., Menenti M., and Nichol J., **Modeling the Effective Emissive of the Urban Canopy Using Sky View Factor,** ISPRS Journal of Photogrammetry and Remote Sensing 105 (2015) 211-219.

Yang X., Zhao L., Bruse M., Meng Q., **An integrated Simulation Method for Building Energy Performance Assessment in Urban Environments.** Energy and Buildings 54 (2012) 243-251.

Younsi S., A., and Kharrat F., **Outdoor Thermal Comfort: Impact of the Geometry of an Urban Street Canyon in a Mediterranean Subtropical Climate- Case Study Tunis, Tunisia,** Procedia-Social and Behavioral Sciences 216 (2016) 689-700.

Yu Ch., Hien w., **Thermal benefits of city parks.** Energy and Buildings 38 (2006) 105-120.

Yuan Ch., Chen L., **Mitigating Urban Heat Island Effects in High Density Cities Based on Sky View Factor and Urban Morphological Understanding: a Study of Hong Kong**, Architectural Science Review 54 (2011) 305-315.

Zakhour S., **The Impact of Urban Geometry on Outdoor Thermal Comfort Conditions in Hot-Arid Region**. Journal of Civil Engineering and Architecture Research 2 (2015) 862-875.

Zamani Z., Taleghani M., and Hoseini S., **Courtyards as Solutions in Green Architecture to Reduce Environmental Pollution.** Energy Education Science and Technology Part A: Energy Science and Research 30 (2012) 385-396.